

**MECHANISTIC CHARACTERIZATION OF
BNIP-H FUNCTION IN NEURON THROUGH
ITS BINDING WITH ATP CITRATE LYASE**

SUN JICHAO

(B.Sc, Sichuan University)

**A THESIS SUBMITTED FOR
THE DEGREE OF DOCTOR OF PHILOSOPHY
DEPARTMENT OF BIOLOGICAL SCIENCES
NATIONAL UNIVERSITY OF SINGAPORE**

2014

Declaration

I hereby declare that this thesis is my original work and it has been written by me in its entirety. I have duly acknowledged all the sources of information which have been used in the thesis.

This thesis has also not been submitted for any degree in any university previously.

Sun Jichao

23 Jan, 2014.

Acknowledgement

First of all, I would like to express my deepest gratitude to my supervisor Associate Professor LOW Boon Chuan, for giving me the opportunity to work on this challenging project. I am truly indebted for his constant support, encouraging advice and guidance, which always are the motivations support me throughout these four years of research. At many stages of this research project, I have benefitted from his profound and in-depth scientific knowledge, precise professionalism, constructive criticism, and passion in research. Without his open-mindedness, this work would not have been done.

It was exciting to work with colleagues in Cell Signaling and Developmental Biology Laboratory and Mechanobiology Institute. All past and current lab members have been very friendly and supportive from the day I joined this lab. Their help and friendship make my Ph.D journey much easier and with loads of fun. I want to show my great appreciation and gratitude to Dr. PAN Qiurong Catherine, Dr. CHEW Li li, Dr. ZHOU Yiting, Dr. CHEW Ti Weng, Dr. Aarthi RAVICHANDRAN, Dr. HUANG Lu, Dr. Jennifer James SHARMY, Dr. CHIN Fei Li Jasmine, Dr. LIM Gim Keat Kenny, Dr. Anjali Bansal GUPTA, Archana RAVI, Shelly KAUSHIK, Guo Kunyao Alvin, Akila SURENDRAN, JIANG Tingting, LI Jiawei, PAN Meng, ZHOU Haoyu, LIU Xuan, LIN Bocheng Lester, ZHAO Zhihai for all interesting discussion and their help in various molecular biology, cell biology and imaging works. I would also like to thank our lab manager Mr. TAN Jee Hian, Allan for all his kind help.

My deepest thanks go to my parents, who have been a continuous source of love, encouragement and understanding and taught me how to face the challenge of life and be an independent person. My heartfelt thanks also go to my dear friends CHEN Mo, XU Peng, JIN Jingjing, SHAO Xiaowei, LE Shimin and many more who have always wished good for me.

I thank National University of Singapore for offering me this precious opportunity to

pursue my Ph.D in Singapore.

I offer profound thanks to everyone who have supported and helped me to complete my study.

Table of contents

Declaration	i
Acknowledgement	ii
Table of contents	iv
Summary	x
List of figures	xii
List of tables	xvi
List of abbreviations	xvii
1. Introduction	1
1.1 Genetic mental disorder, Cayman ataxia	1
1.1.1 Ataxia	1
1.1.2 Cayman ataxia	3
1.2 BNIP-H protein	7
1.2.1 BCH domain	7
1.2.2 Members of BCH family	9
1.2.3 Physiological studies on BNIP-H	16
1.2.4 Cellular binding partners of BNIP-H	18
1.3 Neurite outgrowth	22
1.3.1 Signals regulating neurite outgrowth	23

1.3.2 Acetylcholine and neurite outgrowth.....	27
1.4 A novel BNIP-H binding partner of BNIP-H, ATP citrate lyase.....	30
1.5 Gaps in understanding the functional mechanism of BNIP-H	32
1.6 Objectives of this study.....	32
2. Materials and methods	34
2.1 DNA cloning techniques.....	34
2.1.1 Polymerase Chain Reaction (PCR).....	34
2.1.2 Agarose gel electrophoresis.....	34
2.1.3 Gel extraction.....	34
2.1.4 Restriction endonuclease (RE) digestion	35
2.1.5 Ligation.....	35
2.1.6 Transformation.....	35
2.1.8 Plasmid isolation	36
2.1.9 DNA sequencing.....	37
2.1.10 Plasmids	37
2.2 Cell culture	39

2.2.1 PC12 cell culture	39
2.2.2 PC12 cells transfection	40
2.2.3 Chemical treatment on PC12 cells	40
2.2.4 Neuro2A cell culture and transfection	41
2.2.5 HEK293T cell culture and transfection	41
2.2.6 Cell number quantification	42
2.2.7 Cryopreservation and recovery of cell lines.....	42
2.3 Immunoassays.....	42
2.3.1 Antibodies	42
2.3.2 Cell lysis	43
2.3.3 Identify the binding partner of BNIP-H.....	43
2.3.3 Co-immunoprecipitation (Co-IP).....	44
2.3.4 Western blotting	44
2.3.5 Immunostaining	46
2.4 Imaging and image processing.....	46
2.4.1 Fixed sample imaging and image processing.....	46

2.4.2 Live cell imaging and image processing	47
2.4.3 Fluorescence recovery after photobleaching (FRAP) assay	47
2.5 ACL enzyme assay	47
2.6 Quantification of ACh by mass spectrometry	48
2.7 Statistical analysis	48
3. RESULTS.....	49
3.1 BNIP-H binds ACL to promote neurite outgrowth	49
3.1.1 BNIP-H promotes neurite outgrowth.....	49
3.1.2 ACL is identified as a novel BNIP-H binding partner	51
3.1.3 BNIP-H and ACL both promote neurite outgrowth.....	53
3.1.4 BNIP-H and ACL require each other for neurite outgrowth	57
3.2 BNIP-H transports ACL via kinesin-1	61
3.2.1 BNIP-H and ACL co-traffic along the neurite.....	61
3.2.2 BNIP-H binds with KLC1 through “WQ-WED” motif	63
3.2.3 BNIP-H functions as a scaffold to traffic ACL	65
3.2.4 BNIP-H regulates ACL accumulation and dynamics at neurite terminal.....	69

3.3 BNIP-H requires ACL enzymatic activity for neurite outgrowth	72
3.3.1 ACL enzyme dead mutant blocks BNIP-H function in neurite outgrowth ..	72
3.3.2 BNIP-H requires ACh synthesis for neurite outgrowth	75
3.4 BNIP-H enhances ACh release.....	77
3.4.1 BNIP-H and ACL synergically recruits ChAT at neurite terminal.....	77
3.4.2 BNIP-H localizes to synaptic vesicle	80
3.4.3 BNIP-H promotes ACh release	82
3.5 BNIP-H promotes neurite outgrowth through ACh autocrine/paracrine-induced MEK/ERK pathway.....	83
3.5.1 BNIP-H promotes neurite outgrowth through ACh secretion	83
3.5.2 BNIP-H promotes neurite outgrowth through ACh autocrine/paracrine loop	84
3.5.3 BNIP-H promotes neurite outgrowth through ACh-activated mAChRs and MEK/ERK pathway.....	90
4. DISCUSSION	98
4.1 Concerted spatiotemporal regulation of ACh synthesis and release.....	98
4.2 An ACh autocrine/paracrine feedback loop for neurite outgrowth	100

4.3 The role of BNIP-H in neurite outgrowth.....	101
4.4 A cholinergic link in ataxia and dystonia	104
4.5 BNIP-H as a kinesin-dependent p(l)acemaker in metabolic and cell signalling	106
4.6 Conclusion.....	107
4.7 Future perspectives.....	110
Bibliography	113

Summary

BNIP-H, also known as Caytaxin, is a brain-specific member of BNIP-2 family protein. Mutations at the *ATCAY/Atcay* allele that encodes BNIP-H, are linked to Cayman ataxia in humans and to ataxia and dystonia in mice and rats. Cayman ataxia is characterized by prominent psychomotor retardation, and non-progressive cerebellar dysfunction. These symptoms are caused by the deficiency of functional BNIP-H protein level in patient's brain, suggesting that BNIP-H is crucial for higher brain functions such as motor coordination. The cerebellum is considered as the most compelling region involved in this disease, as its removal alleviates symptoms in *dystonic (dt)* rats. However, the pathological mechanism of Cayman ataxia and the cellular function of BNIP-H remain unknown, and so far no effective therapies are available to cure this disease. These factors have led to intense investigations on biochemical disturbance which may cause this disease, and on the cellular and molecular functions of BNIP-H in neurons.

To better understand the function of BNIP-H, proteomics pull down assay was performed and ATP citrate lyase (ACL) was identified as a novel binding partner of BNIP-H. BNIP-H and ACL required each other to promote neurite outgrowth. ACL and BNIP-H co-localized in the granules along the microtubule and co-trafficked along the neurite. Biochemical and cellular imaging studies showed that BNIP-H functioned as a scaffold to link ACL and kinesin motor protein, and facilitated ACL trafficking from the cell body to the neurite terminal. A null mutation in the ACL enzyme partially blocked BNIP-H function on neurite outgrowth. These studies thereby suggest that BNIP-H promotes neurite outgrowth through trafficking ACL. To further investigate the cellular mechanism of the neurite outgrowth induced by BNIP-H, the downstream signaling pathway regulated by BNIP-H and ACL was identified. BNIP-H binding to ACL promoted their assembly with acetylcholine transferase and its transporter into the vesicles. BNIP-H and ACL up-regulated acetylcholine secretion in PC12 cells. The neurite outgrowth induced by BNIP-H was abrogated by preventing

acetylcholine secretion or blocking acetylcholine binding to muscarinic receptors, indicating that BNIP-H enhances neurite outgrowth through acetylcholine autocrine. This acetylcholine autocrine process in turn activated MAPK pathway. BNIP-H therefore functions as a dynamic regulatory scaffold protein that promotes cholinergic neurotransmission and MAPK signaling necessary for neuronal differentiation.

In summary, this thesis reveals that BNIP-H interacts and localizes acetylcholine synthesis enzymes at neurite terminal to facilitate acetylcholine release. This process in turn activates MAPK pathway through the muscarinic receptors and enhances neurite outgrowth. The current investigation of the regulatory effects of BNIP-H in acetylcholine release may extend our understanding on how scaffold proteins regulate the transportation of the metabolism enzymes in neurons, and provide novel therapeutic strategies for Cayman ataxia disease.

List of figures

Figure 1-1 The clinical signs of the mouse models with BNIP-H mutations.	6
Figure 1-2 The clinical signs of the <i>dt</i> rat.	7
Figure 1-3 The schematic diagram of homologous BCH domain in BNIP-2 and Cdc42GAP.	8
Figure 1-4 Comparison of predicted three-dimensional structure of BCH domain with other CRAL_TRIO members	9
Figure 1-5 Classifications of BCH domain-containing proteins.	11
Figure 1-6 <i>Atcay</i> /BNIP-H is a neuron-specific gene.	16
Figure 1-7 Functional motifs within BNIP-H.	22
Figure 1-8 Neurite outgrowth proceeds by protrusion, engorgement and consolidation.	23
Figure 1-9 Classification of the regulators for neurite outgrowth.	24
Figure 1-10 Classification of mAChRs.	28
Figure 1-11 The signaling pathways regulated by ACL.	31
Figure 3-1 BNIP-H promotes PC12 cell neurite outgrowth.	50
Figure 3-2 BNIP-H enhances neuronal differentiation of PC12 cell.	51
Figure 3-3 BNIP-H interacts ACL in Neuro2A cells.	52
Figure 3-4 Endogenous BNIP-H interacts with ACL in PC12 cells.	53
Figure 3-5 Overexpression of BNIP-H and ACL enhance PC12 neurite growth.	55

Figure 3-6 Knockdown of BNIP-H inhibits PC12 neurite outgrowth.	56
Figure 3-7 Knockdown of ACL inhibits PC12 neurite outgrowth.....	57
Figure 3-8 ACL fails to restore the neurite outgrowth reduced by BNIP-H knockdown.	59
Figure 3-9 BNIP-H fails to restore the neurite outgrowth reduced by ACL knockdown.	60
Figure 3-10 BNIP-H and ACL co-traffic in the PC12 neurite.	62
Figure 3-11 BNIP-H and ACL co-localize along the microtubule of PC12 neurite.	62
Figure 3-12 "WQ-WED" mutations abolish BNIP-H and KLC1 binding in 293T cells....	64
Figure 3-13 Mobility of BNIP-H 5A is reduced in PC12 neurite.	65
Figure 3-14 BNIP-H promotes KLC1 and ACL association in 293T cells.	66
Figure 3-15 BNIP-H 5A reduces KLC1 and ACL association in 293T cells.	67
Figure 3-16 BNIP-H 5A reduces ACL trafficking in PC12 neurite.....	68
Figure 3-17 BNIP-H accumulates ACL at PC12 neurite terminal.....	70
Figure 3-18 BNIP-H enhances ACL dynamics at PC12 neurite terminal.....	71
Figure 3-19 H760A is an inactive mutant of ACL and BNIP-H has no effect on ACL enzymatic activity.....	73
Figure 3-20 ACL H760A blocks BNIP-H function in PC12 neurite outgrowth.....	74
Figure 3-21 BNIP-H-regulated neurite outgrowth is not affected by cholesterol synthesis inhibitor lovastatin in PC12 cells.	75
Figure 3-22 BNIP-H-regulated neurite outgrowth is not affected by fatty acid	

synthesis inhibitor TOFA in PC12 cells.....	76
Figure 3-23 BNIP-H-regulated neurite outgrowth is blocked by choline transporter inhibitor hemicholinium-3 in PC12 cells.	77
Figure 3-24 Schematic diagram of ACh synthesis and secretion pathway.....	78
Figure 3-25 Synergistic binding of BNIP-H and ACL with ChAT in 293T cells.	79
Figure 3-26 BNIP-H and ACL recruit ChhAT at PC12 neurite terminal.	80
Figure 3-27 BNIP-H localizes at synaptic vesicles of PC12 cells.	81
Figure 3-28 BNIP-H interacts with VAcHT in 293T cells.	81
Figure 3-29 BNIP-H and ACL promote ACh release from PC12 cells.....	82
Figure 3-30 Knockdown of BNIP-H or ACL inhibits ACh release from PC12 cells.....	83
Figure 3-31 BNIP-H-induced neurite outgrowth is blocked by VAcHT inhibitor vesamicol in PC12 cells.	84
Figure 3-32 CCh rescues vesamicol blockage in neurite outgrowth.....	85
Figure 3-33 BNIP-H's function in PC12 neurite outgrowth is blocked by ACh antibody.	86
Figure 3-34 The effect of CCh on neurite outgrowth of PC12 cells.	88
Figure 3-35 BNIP-H-transfected cells promote neurite outgrowth of adjacent wild type cells and this process is blocked by vesamicol.....	89
Figure 3-36 CCh rescues the effect of BNIP-H knockdown on neurite outgrowth.	90
Figure 3-37 BNIP-H-regulated PC12 neurite outgrowth is blocked by muscarinic antagonist atropine, but not by nicotinic antagonist hexamethonium.	92

Figure 3-38 BNIP-H enhances ERK activation through ACh release.....	93
Figure 3-39 BNIP-H-induced PC12 neurite outgrowth is blocked by MEK inhibitor U0126.....	95
Figure 3-40 Constitutive active MEK rescues effect of BNIP-H knockdown on PC12 neurite outgrowth.....	96
Figure 3-41 BNIP-H-regulated PC12 neurite outgrowth is blocked by transcription inhibitor DRB.....	97
Figure 4-1 Mechanism of BNIP-H action in promoting neurite outgrowth.	107
Figure 4-2. Schematic diagram of the future work.....	111

List of tables

Table 1-1 Comparison of BNIP-H mutant models.....	4
Table 2-1 Primers used for mutagenesis.....	39
Table 2-2 RNAi targeting sequences.	39

List of abbreviations

5Gn	Trigeminal ganglion
ACh	Acetylcholine
AChE	Acetylcholinesterase
ACL	ATP citrate lyase
ACS	Acetyl-CoA synthetase
α -TTP	α -Tocopherol transfer protein
BACE	Beta-site APP-cleaving enzyme
BCH	BNIP-2 and Cdc42GAP homology
BMCC1	BCH motif-containing molecule at the carboxyl terminal region 1
BDNF	Brain-derived neurotrophic factor
BNIP-H	BNIP-2 homology
BNIP-S	BNIP-2-similar
BNIP-XL	BNIP-2-extra long
CAM	Cell adhesion molecule
CCh	Carbachol
Cdc42GAP	Cdc42 GTPase activating protein
ChAT	Choline acetyltransferase
CHIP	Hsp70-interacting protein
CNS	Central nervous system
Co-IP	Co-immunoprecipitation
CPT	Camptothecin
CRALBP	Cellular retinaldehyde-binding protein
CREB	cAMP response element binding protein

CSPG	Chondroitin sulfate proteoglycan
DA	Dopamine
DCN	Deep cerebellar nuclei
DMEM	Dulbecco's Modified Eagle's Medium
DMSO	Dimethyl sulfoxide
DRB	5,6-dichloro-1-beta-D-ribofuranosylbenzimidazole
DRG	Dorsal root ganglion cells
dt	Dystonic
ECM	Extracellular matrix
EDTA	Ethylene diamine-tetraacetic acid
FRAP	Fluorescence recovery after photobleaching
GABA	Gamma-aminobutyric acid
GAD	Glutamic acid decarboxylase
GDAP2	Ganglioside-induced differentiation-associated protein 2
HB-GAM	Heparin-binding growth-associated molecule
HRP	Horse radish peroxidase
IAP	Intracisternal A-particle
IRES	Internal ribosome entry site
KGA	Kidney-type glutaminase
KHC	Kinesin heavy chains
KLC1	Kinesin light chain 1
LB	Luria-Bertani

Lbc	Lymphoid blast crisis
mAChR	Muscarinic ACh receptor
MAG	Myelin-associated glycoprotein
MALDI-TOF	Matrix-assisted laser desorption/ionization-time of flight
MAP6	Microtubule-associated protein 6
MAPK	Mitogen-activated protein kinase
MRM	Multiple reaction monitoring
nAChR	Nicotinic ACh receptor
Nasal	Nasal cavity
NE	Norepinephrine
nEnt	Gastrointestinal tract
NGF	Nerve growth factor
NT-3	Neurotrophin-3
NT-4	Neurotrophin-4
PAG	Phosphate-activated glutaminase
PCR	Polymerase Chain Reaction
PI3K	Phosphatidylinositol 3-kinase
Pin1	Protein interacting NIMA
PLC	Phospholipase C
PNS	Peripheral nervous system
PRR	Proline-rich region
RE	Restriction endonuclease
RhoGAP	Rho GTPase activating protein
RhoGEF	RhoA-specific guanine nucleotide exchange factor

Robo	Roundabout
SDS-PAGE	Sodium dodecyl sulfate - Polyacrylamide Gel Electrophoresis
Sec14p	Yeast phosphatidylinositol transfer protein
SEM	Standard errors of the mean
SmgGDS	Small G-protein GDP dissociation stimulator
SPF	Supernatant protein factor
SphPal	Sphenopalatine ganglion
STRP	Short tandem repeat polymorphism
TAE	Tris-acetate EDTA
TOFA	5-tetradecyloxy-2-furoic acid
Trk	Tropomyosin-related kinase
Tuj1	Neuronal class III β -tubulin
VACHT	Vesicular ACh transporter

1. Introduction

Ataxia is a neurological disorder with a lack of muscle coordination. Cayman ataxia is recently identified as one type of such disease. Through genetic screening, defect of brain specific protein BNIP-H is found to be the cause of Cayman ataxia. However, the pathological mechanism of Cayman ataxia and the cellular function of BNIP-H remain unknown, and so far no effective therapeutics to cure this disease has been available. These factors have led to intense investigations on biochemical disturbance which may cause this disease, and on the cellular and molecular functions of BNIP-H in neurons.

1.1 Genetic mental disorder, Cayman ataxia

1.1.1 Ataxia

Ataxia is one of the most common neurological disorders involving involuntary coordination of muscle movements. Based on the dysfunctional parts of the nervous system, which coordinates movement, ataxia can be classified into three types, which are cerebellar ataxia, sensory ataxia and vestibular ataxia.

Cerebellar ataxia is caused by dysfunction of the cerebellum. The cerebellum is important for integrating neuronal signals to coordinate smooth movements and control motor precision and accurate timing. Many diseases affecting the cerebellum can cause ataxia (Schmahmann, 2004). Patients with cerebellar ataxia may have problems in controlling the force, direction, balance, velocity and rhythm of muscle contractions.

Sensory ataxia arises due to loss of sensory input and that of the sensitivity to the positions of body and joints, resulting in poorly judged movements. This is generally caused by dysfunction of the dorsal spinal cord, which sends the information of relative position of body parts up to the brain (Spinazzi et al., 2010). Patients with

sensory ataxia tend to have difficulty in coordinating voluntary movements of their limbs, larynx and eyes. The characteristic symptoms may be absent when the patients can observe their movements, but such symptoms will become worse when they are blindfolded.

Vestibular ataxia occurs due to defects in the vestibular inner ear system. In vestibular ataxia, the information from the inner ear cannot be sent to brainstem and cerebellum. Besides sound detection, the inner ear is important for movement balance. Patients with vestibular ataxia suffer from a loss of balance, but their strength is still preserved. In acute and unilateral cases, the abnormality of such patients is associated with prominent vertigo, such as a feeling that his or her surroundings are spinning.

Although the molecular mechanism underlying ataxia is largely unknown, increasing evidence suggests that neurotransmission plays a crucial role in this disease. The Pogo mouse is an autosomal recessive ataxia mutant (Kim et al., 2003). The cerebellar concentration of glutamate, a most prevalent excitatory neurotransmitter, decreases significantly in the mutant mouse as compared to the control. In Friedreich's ataxia (FA) brains, muscarinic acetylcholine receptors are increased in the inferior olivary nucleus, anterior and posterior cerebellar vermi but is not changed in the cerebellar hemisphere and dentate nucleus (Reisine et al., 1979). In addition, adrenergic receptors are increased in the inferior olivary nucleus but not different from controls in the cerebellar hemisphere, dentate nucleus, and anterior and posterior cerebellar vermi of FA brains. These data suggest that ataxia might be caused by the alteration in neurotransmission.

Among the three types of ataxia, cerebellar ataxia is the most common. The clinical causes of cerebellar ataxia are numerous, including acquired, hereditary and idiopathic ones. Hereditary ataxia can be divided into four categories: autosomal recessive cerebellar ataxia, autosomal dominant cerebellar ataxia, episodic ataxia and X-linked ataxia. Cayman ataxia, the disease we focus on, has been recently

identified as an autosomal recessive cerebellar ataxia.

1.1.2 Cayman ataxia

Cayman ataxia was identified in an isolated island, called Grand Cayman island (Nikali et al., 1995). This isolated region experiences little emigration or immigration. Marriage among individuals with similar genetic background results in a high frequency of consanguinity. Around 8.3% of newborns in the Cayman islands suffer from obvious physical abnormalities (Thurtell and Leigh, 2011). Cayman government reported that Cayman ataxia patients showed cerebellum hypoplasia through imaging studies (Bomar et al., 2003). Cayman cerebellar ataxia is characterized by prominent psychomotor retardation including mental retardation and markedly delayed motor milestones, and non-progressive cerebellar dysfunction, such as truncal ataxia, nystagmus, intention tremor, exo- or esotropia, and a widely based ataxic gait (Nystuen et al., 1996). Symptoms of the disease are often present in early childhood, and patients with such a disease may die as the disease develops.

In Cayman Islands, 26 individuals were diagnosed with Cayman ataxia, and 6 more peoples were accounted for according to the data from personal interviews and public records (Nystuen et al., 1996). Among the 32 patients, 20 of them could be linked to a single person suggesting that this disease might origin from a founder effect (Sheffield et al., 1995). Short tandem repeat polymorphism (STRPs) were used to compare pools of DNA from affected and unaffected individuals. A genetic region on 19p13.3 was identified as homozygous and identical in all affecteds (Nystuen et al., 1996). This region was further narrowed down to 2.0 (Bomar et al., 2003). In parallel, three ataxia mouse mutants, *jittery*, *hesitant* and *sidewinder*, had been identified and two of them had been previously mapped to a region on mouse chromosome 10, which is homologous to human chromosome 19p13.3 (Bomar et al., 2003; Kapfhamer et al., 1996). *Hesitant* mouse suffers from mild ataxia and dystonia, but enjoy normal fertility and life expectancy whereas *jittery* and *sidewinder* mice have severe symptoms and die within 4 weeks of birth (Kapfhamer






et al., 1996). Comparing the affected regions of human and mouse chromosomes identified a region around 150kb covering 7 genes. Sequencing analysis showed that mutations in a single gene named *ATCAY/Atcay* is responsible for this disease (Bomar et al., 2003). In *dystonic (dt)* rats, the *dt* locus was mapped to a region on chromosome 7q11 and the homologous rat gene was mutated (Xiao and Ledoux, 2005). The *ATCAY* gene was first isolated in our laboratory (GenBank accession number AY220297). It encodes a protein called BNIP-H/caytaxin (for BCL2/adenovirus E1B 19kDa interacting protein 2 [BNIP-2] homology), which shares 52% amino acid sequence identity with BNIP-2 (Buschdorf et al., 2006). BNIP-2 was originally identified as one of the partners for the anti-apoptotic proteins Bcl-2 and the adenovirus E1B 19 kDa protein (Boyd et al., 1994).

In different Cayman ataxia models, there are diverse mutations in *ATCAY/Atcay*, which results in different transcripts and expression levels of BNIP-H protein (Table 1-1). Especially in the mouse models, disease severity appears to be correlated with the protein levels of BNIP-H (Bomar et al., 2003; Sikora et al., 2012). The *hesitant* mouse with mild disorder have an intracisternal A-particle (IAP) insertion in the intron 1, which results in a largely reduced expression level of wild type BNIP-H protein (Figure 1-1 A). The *jittery* mouse has a B1 element insertion in the exon 4 and *sidewinder* mice has 2bp shift in the exon 5, which both result in depletion of wild type BNIP-H expression, explaining why these two types of mouse suffer from severe disorder (Figure 1-1 B). The *dt* rat has a similar mutation as *hesitant* mouse (Xiao and Ledoux, 2005) (Figure 1-2). Recent study showed that expression of wild type human BNIP-H could rescue the ataxic phenotype in ataxic mouse, suggesting that the ataxia syndrome is caused by the deficiency of functional BNIP-H expression (Sikora et al., 2012). The current knowledge on the function of BNIP-H and its homologies will be described in the following section.

Table 1-1 Comparison of BNIP-H mutant models.

In human patients with Cayman ataxia, there are two mutations identified: a C->G change in exon 9, which is predicted to cause a serine to arginine substitution at amino acid 301, and a G->T substitution in the intron 9, which is predicted to result in

a shortened protein of 323 amino acids (plus 10 missense) instead of the normal 372 amino acids (Bomar et al., 2003). The *wobbly* mouse has a T->A change in intron 4, which may delete exon 4, resulting in deletion of amino acids 49-119 in BNIP-H protein. The *jittery* mouse has a B1 element insertion, predicting a truncated protein with 62 amino acids (plus 21 missense) (Bomar et al., 2003). In *hesitant* mouse, an insertion of IAP results in the production of larger transcript and reduced amount of normal BNIP-H protein (Bomar et al., 2003; Sikora et al., 2012). The *sidewinder* allele has a 2-bp deletion in exon 5, which is predicted to result in a truncated protein of 181 amino acids (plus 19 missense) (Bomar et al., 2003). The *dt* rat has a similar mutation as *hesitant* mouse, but the mutant rat expresses very low level of BNIP-H protein compared to the *hesitant* mouse (Xiao and Ledoux, 2005). The table is adapted from <http://mutagenetix.utsouthwestern.edu>.

Model	Mutation	Transcripts	Phenotype
		 <p>(wild type)</p>	
Cayman ataxia	C->G in exon9 G->T in intron 9		Gait ataxia, hypotonia, mental retardation, nyctagmus, tremor
<i>wobbly</i> mouse	T->A in intron 4		Ataxia, hind limb dystonia and spasms
<i>jittery</i> mouse	B1 insertion in exon 4		Severe truncal and limb ataxia, dystonic forelimb spasms, die by 3-4 weeks
<i>hesitant</i> mouse	IAP insertion in intron 1	Aberrant larger transcript with small amount normal transcript	Mild ataxia, dystonia
<i>sidewinder</i> mouse	2-bp deletion in exon 5		Severe truncal and limb ataxia, dystonic forelimb spasms, die by 3-4 weeks
<i>dystonic</i> rat	IAP insertion in intron 1	Aberrant larger transcript with small amount normal transcript	Severe generalized dystonia, die by 4-5 weeks

A



B



Figure 1-1 The clinical signs of the mouse models with BNIP-H mutations.

A. Adult *hesitant* mouse suffers frozen on tiptoes (indicated by arrow). B. 3 week old *jittery* mouse cannot walk (indicated by arrow). The picture is adapted from Bomar et al., 2003.

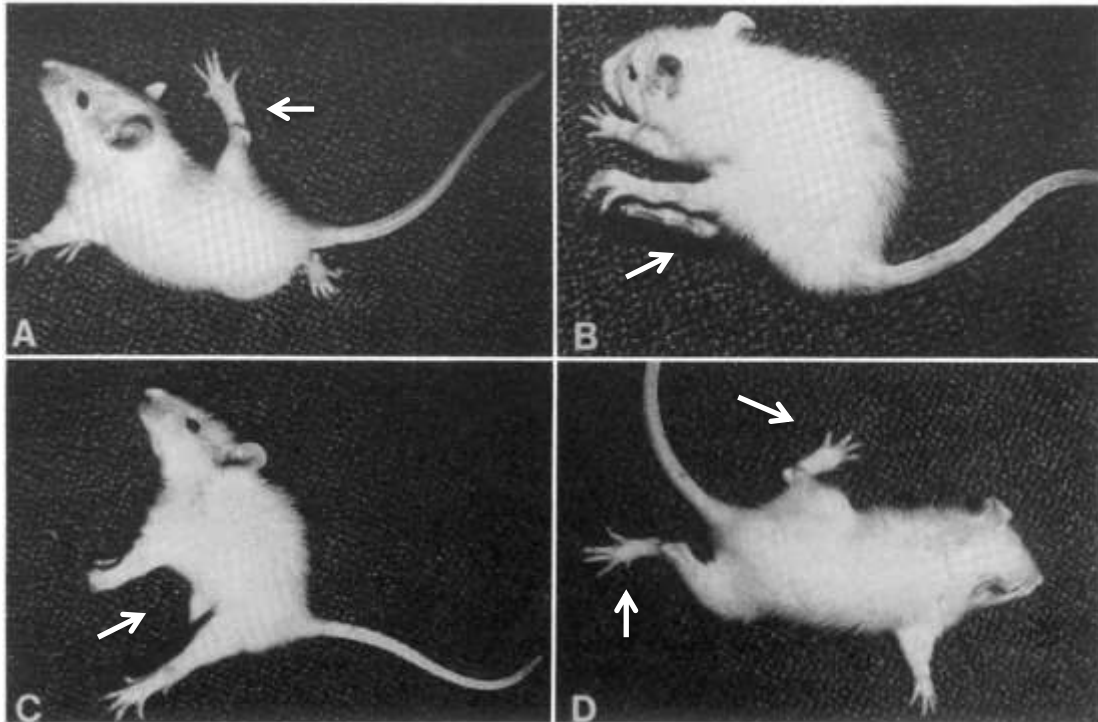


Figure 1-2 The clinical signs of the *dt* rat.

A. Torticollis (indicated by arrow). B. Falling to one side and hyperflexion of the trunk (indicated by arrow). C. Self-clasping of the limbs (indicated by arrow). D. Abnormal limb placement during locomotion (indicated by arrow). The picture is adapted from Lorden et al., 1984.

1.2 BNIP-H protein

1.2.1 BCH domain

As described previously, BNIP-H protein is similar to BNIP-2, especially at the C-terminal region (Pan and Low, 2012). This conserved region was first identified at the C-terminal of BNIP-2 protein, named the BNIP-2 and Cdc42 GTPase activating protein (Cdc42GAP) homology (BCH) domain, because it is similar to the N-terminal non-catalytic domain of Cdc42GAP (Low et al., 1999; Low et al., 2000b; Pan and Low, 2012) (Figure 1-3). BCH domain also shares 14% amino acids sequence identity with the CRAL_TRIO domain (Pan and Low, 2012). CRAL_TRIO domain is a structural scaffold based on the sequences of cellular retinaldehyde-binding protein (CRALBP) and the triple functional domain of the Trio protein (Crabb et al., 1991; Debant et al.,

1996), functioning in binding small lipophilic molecules (Panagabko et al., 2003). BCH domain shares a low sequence similarity with other CRAL_TRIO domain containing proteins, such as α -Tocopherol transfer protein (α -TTP), yeast phosphatidylinositol transfer protein (Sec14p) and supernatant protein factor (SPF), but they exhibit similar three-dimensional structures, suggesting that BCH domain is a novel member of CRAL_TRIO superfamily (Gupta et al., 2012; Panagabko et al., 2003) (Figure 1-4).

BNIP-2 and Cdc42GAP Homology (BCH) domain

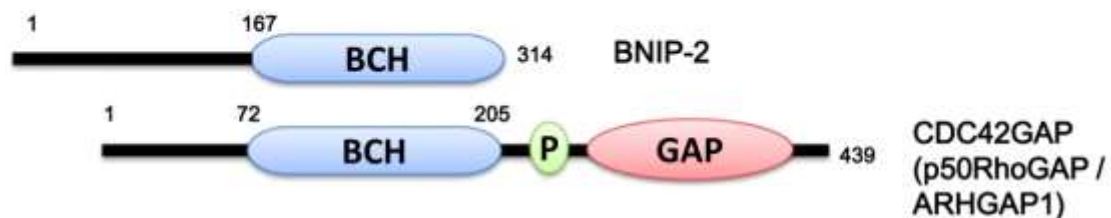


Figure 1-3 The schematic diagram of homologous BCH domain in BNIP-2 and Cdc42GAP.

The C-terminal region of BNIP-2 and N-terminal region of Cdc2GAP (also known as p50RhoGAP and ARHGAP1) is homologous (labeled by blue color), thus named BNIP-2 and Cdc42GAP homology (BCH) domain. This figure is adapted from Pan and Low, 2012.

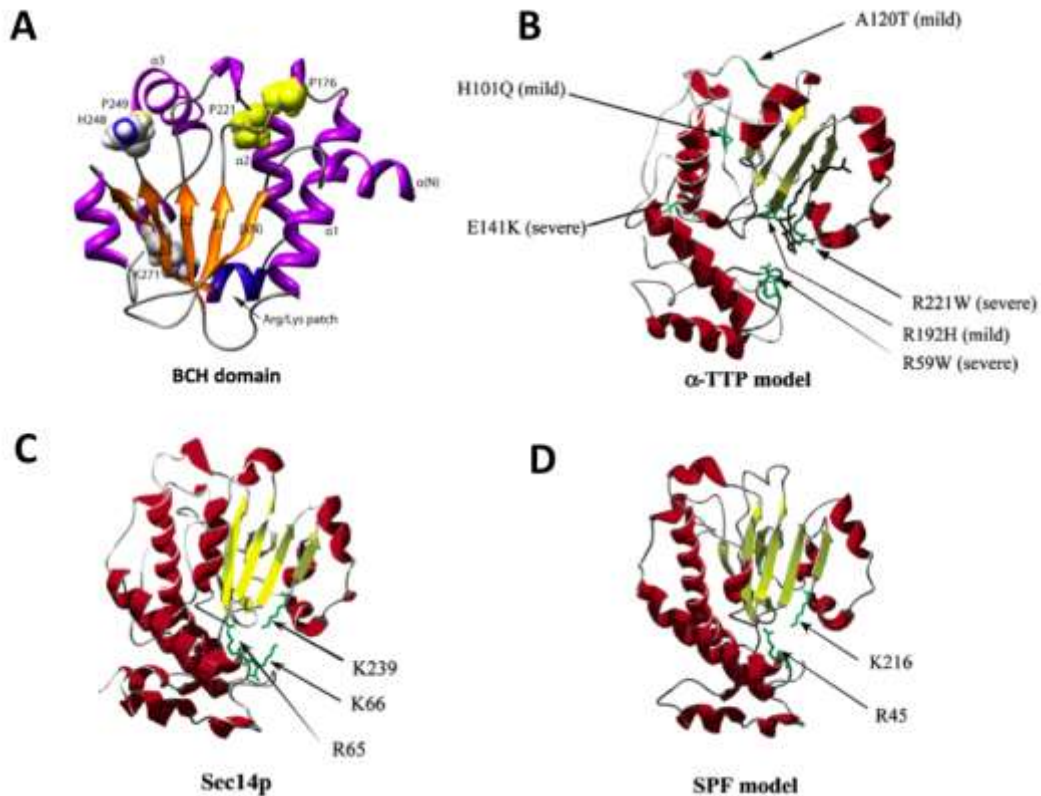


Figure 1-4 Comparison of predicted three-dimensional structure of BCH domain with other CRAL_TRIO members

A. A predicted 3D structure of BCH domain of BNIP-2 protein. The patch of positively charged residues (Arg/Lys patch) is highlighted in blue, and the conserved residue K271 is marked. The picture is adapted from Gupta et al. 2012.

B. A predicted 3D structure of α -TTP. The highlighted residues indicate the mutations in patients with α -TTP related disease ataxia with Vitamin E deficiency. Inspection of the structure model shows that R221 is homologous to K271 in BCH domain. The picture is taken from Panagabko et al. 2003.

C. A 3D structure of Sec14p obtained by X-ray diffraction. The mutations of the highlighted residues have been shown to affect the transfer of phosphoinositides (Phillips et al., 1999) and K239 in Sec14p is homologous to R221 in α -TTP. The picture is taken from Panagabko et al. 2003.

D. A predicted 3D structure of SPF. K216 highlighted is homologous to R221 in α -TTP. R45 is homologous to R65 of Sec14p, as well as to R59 in α -TTP, but this site is missing in BCH domain. The picture is taken from Panagobko et al. 2003.

1.2.2 Members of BCH family

Through bioinformatics analysis, at least 175 proteins with a putative BCH domain were identified in a wide range of eukaryotic species, including slime molds, plants,

yeasts and animals, suggesting that it is important during the evolution (Gupta et al., 2012). Based on the phylogenetic clustering and associated protein domains, these BCH domain-containing proteins could be divided into three subgroups as group-1, group-2 and group-3 (Figure 1-5) (Gupta et al., 2012; Pan and Low, 2012). The group-1 proteins only contain BCH domain at the C-terminal, including BNIP-2, BNIP-S (BNIP-2-Similar), BNIP-XL (BNIP-2-Extra Long), BMCC1 (BCH motif-containing molecule at the carboxyl terminal region 1) and BNIP-H (BNIP-2 homology). BMCC1-isoforms are the extended isoforms of BNIP-XL, from different transcriptional starting sites of the locus *BMCC1/PRUNE2*. Ganglioside-induced differentiation-associated protein 2 (GDAP2) is classified into group-2, as the BCH domain is associated with macro domain. The group-3 proteins contain BCH domains at the N-terminal, while Rho GTPase activating protein (RhoGAP) domains at the C-terminal. The highly conserved BCH domains in different members, function as the scaffold protein domains that regulate cell growth, apoptosis, migration, morphogenesis and differentiation via Rho, Ras and mitogen-activated protein kinase (MAPK) pathways. The cellular functions of these BCH-containing proteins will be described in the following sections.

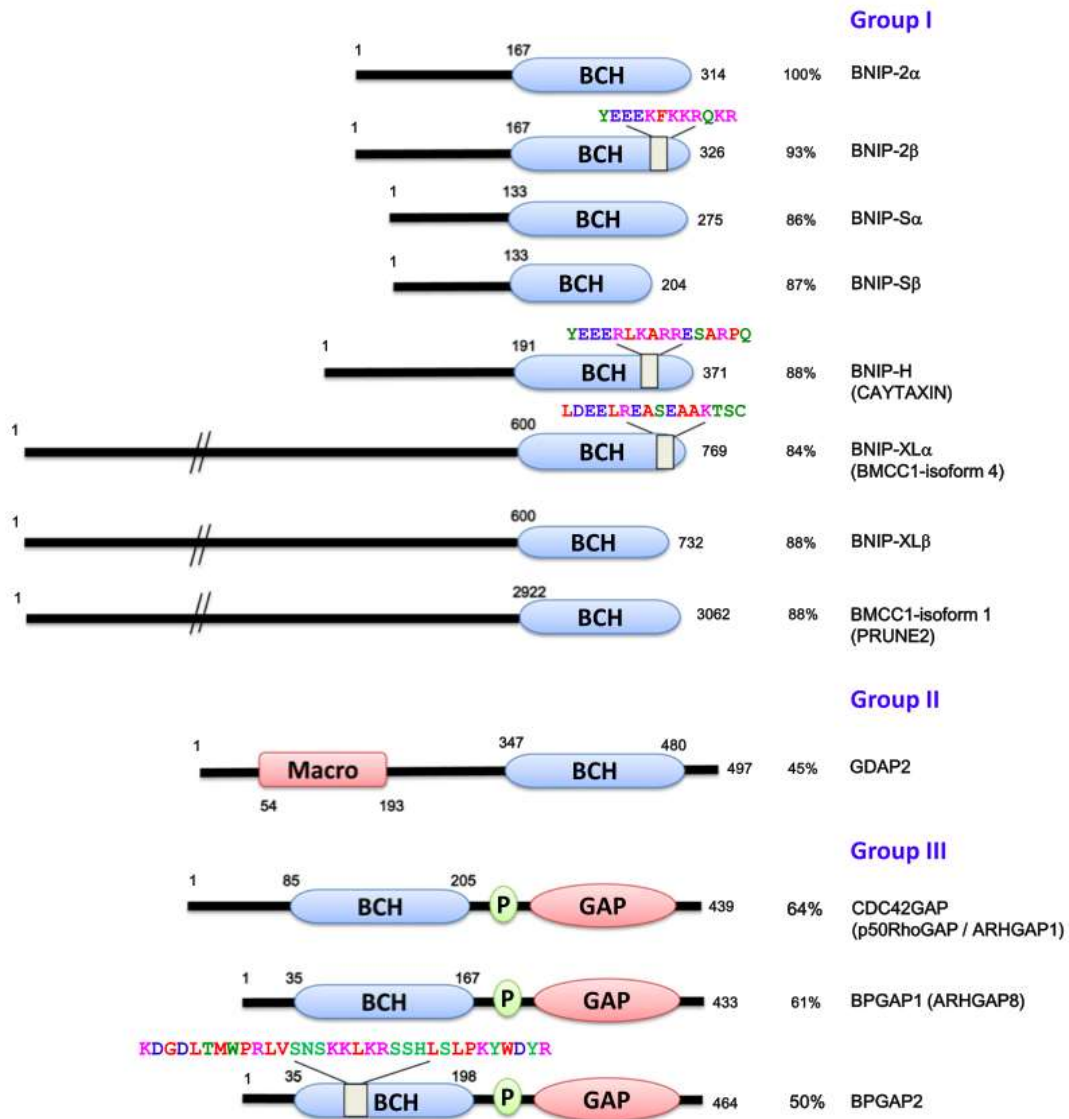


Figure 1-5 Classifications of BCH domain-containing proteins.

Group-1 type proteins contain single BCH domain at C-terminal. Group-2 type protein GDAP2 contains a macro domain at N-terminal. Group-3 type proteins locate the BCH domain at N-terminal and RhoGAP domain at C-terminal. The percentages indicate the similarity of BCH domain (amino acid sequence) compared to the one of BNIP-2. The highlighted amino acid sequences within the BCH domains indicate the different the alternative RNA splicing. The picture is adapted from Pan and Low, 2012.

1.2.2.1 BNIP-2

BNIP-2 is the earliest identified BCH domain-containing protein and mostly well

studied molecule in BCH family. It has been reported that BNIP-2 could form a homophilic dimer with itself, or form a heterophilic dimer with Cdc42GAP through the “RRKMP” patch within the BCH domain (Low et al., 2000a). BNIP-2 also interacts with Cdc42 through “EYV” motif in BCH domain (Low et al., 2000b). BNIP-2 itself has the Cdc42 GAP activity and homophilic or heterophilic interactions via BCH domains affect its GAP activity (Low et al., 2000a). BNIP-2 induces membrane protrusion and cell elongation via Cdc42, as deletion the binding between BNIP-2 and Cdc42, or introducing dominant negative form of Cdc42 inhibits this effect (Yi et al., 2005). In muscle cells, BNIP-2 interacts with cell surface Cdo receptor and induces myogenic differentiation (Kang et al., 2008). In particular, BNIP-2 and Cdo receptor both negatively regulate Cdc42 activity. Through Cdo receptor, BNIP-2 and p38 MAPK pathway scaffold protein JLP form a complex. Overexpression of BNIP-2 or downregulation of Cdc42 activity could inhibit p38 activation, suggesting that BNIP-2 might regulate muscle cells differentiation via Cdc42-p38 MAPK pathway. Similarly, BNIP-2 also takes part in the regulation of Cdc42 and p38 MAPK pathway by Cdo receptor, leading to neuronal differentiation (Oh et al., 2009). Besides, BNIP-2 contains a RhoA binding domain like motif (aa 183-211) within the BCH domain, and could enhance RhoA activity, which inhibits cell spreading and collective cell migration of MDCK epithelia cells (Kenny Lim, unpublished data). At the N-terminus of BNIP-2, EF-hand motif (DGLD) is recognized and cleaved by caspase proteins or under camptothecin (CPT) induced apoptosis condition (Valencia et al., 2007). And the “IEAD” motif at the N-terminus of BNIP-2 could be cleaved by granzyme B *in vitro* during the natural killer cell-induced killing (Scott et al., 2010). Although the function of BNIP-2 cleavage by these enzymes is unknown, these results suggest that BNIP-2 might be regulated under apoptotic condition.

1.2.2.2 BNIP-S

BNIP-S has two isoforms namely BNIP-S α and BNIP-S β (Zhou et al., 2002). BNIP-S α locates at the cytoplasm and induces cell round and apoptosis, while BNIP-S β

concentrates at the nuclei and has no this pro-apoptosis effect. This rounding effect is independent of the caspase apoptotic pathway. Unlike BNIP-2, BNIP-S α only targets to RhoA, but not Cdc42 and Rac (Zhou et al., 2006). Cdc42GAP induces membrane protrusion when it is overexpressed in cells, while this effect is inhibited when BNIP-S α is co-transfected. Immunoprecipitation study showed that introduction of BNIP-S α reduces the binding between Cdc42GAP and RhoA and restores the activation of RhoA. Dominant negative mutant of RhoA or BNIP-S α mutant which could not bind with RhoA, completely inhibits cell rounding and apoptosis, suggesting that BNIP-S α functions through RhoA pathway for cell apoptosis.

1.2.2.3 BNIP-XL and BMCC1

BNIP-XL was firstly isolated by our laboratory and has been found to specifically target RhoA through its BCH domain (Soh and Low, 2008). Mutagenesis study demonstrated that, unlike the RhoA-binding domain of BNIP-S α , BNIP-XL requires the whole BCH domain to bind with RhoA. BNIP-XL negatively regulates RhoA activity and affects stress fiber formation. Immunoprecipitation study showed that the BCH domain of BNIP-XL associates with the catalytic domain of the lymphoid blast crisis (Lbc), a RhoA-specific guanine nucleotide exchange factor (RhoGEF). Lbc induces cell transformation through regulation of RhoA activity. Introduction of full-length BNIP-XL or BCH domain alone partially inhibited this effect, suggesting that the BCH domain of BNIP-XL may regulate RhoA through its regulator RhoGEF.

BMCC1 is upregulated in the favorable subset of primary neuroblastomas (Machida et al., 2006). Further studies show that the expression of BMCC1 is regulated during differentiation and apoptosis. In newborn mice superior cervical ganglion neurons, BMCC1 expression is downregulated after nerve growth factor (NGF) induced-neuronal differentiation, and upregulated after NGF-deletion-induced apoptosis. Consistently, in CHP134 neuroblastomas, BMCC1 expression is increased during retinoic acid-induced apoptosis. This study suggested that BMCC1, as a prognostic

factor, might regulate neuronal differentiation, survival and tumor aggressiveness. In addition, a shorter isoform of BMCC1, BMCC1s, was found to regulate microtubule dynamics through interaction with microtubule-associated protein 6 (MAP6) (Arama et al., 2012). MAPs is a class of proteins that can bind with, stabilize and enhance the assembly of microtubules (Mandelkow and Mandelkow, 1995). Overexpression of BMCC1s displaces MAP6 from microtubules and blocks MAP6-induced microtubule stability. BMCC1s also promotes membrane protrusion in a MAP6-dependent manner. This study provides a novel molecular mechanism on how BMCC1s regulate cytoskeleton dynamics and morphology change in neurons.

1.2.2.4 Cdc42GAP

Cdc42GAP is also known as p50RhoGAP and ARHGAP1. Cdc42GAP belongs to the type 3 of BCH protein with a BCH domain at N-terminal and a GAP domain at C-terminal. It acts as a negative regulator of Cdc42 and Rho, through catalyzing the hydrolysis of GTP to GDP by small GTPase (Lancaster et al., 1994). It regulates multiple cellular processes by regulating the activation of Cdc42. In liver, Cdc42 is specifically upregulated by knockout of Cdc42GAP (Wang et al., 2006). The Cdc42GAP $-/-$ liver shows increased apoptosis through the activation of JNK pathway. In hematopoietic stem/progenitor cells with Cdc42GAP $-/-$, the cortical actin assembly is impaired, leading to the defective cell adhesion and migration. In contrast, the Cdc42GAP $-/-$ neutrophils show enhanced cell mobility and deficiency in directed migration (Szczur et al., 2006). Cdc42GAP regulates cell mobility through ERK/MAPK pathway, and regulates migration direction through p38/MAPK pathway. In addition, Cdc42GAP knockdown also enhances myogenic differentiation through p38/MAPK pathway (Kang et al., 2008). Although the properties of the GAP domain are well studied, little is known on the function of BCH domain located at the N-terminal.

Recently, it was found that the BCH domain within Cdc42GAP only targets RhoA, but not Cdc42 or Rac, suggesting that Cdc42GAP may regulate its RhoA GAP activity through the BCH domain (Zhou et al., 2010). Functional studies reveal that the BCH

domain prevents RhoA inactivation by sequestering RhoA from the adjacent GAP domain. Deletion of the RhoA binding motif (aa 85-120) within the BCH domain reduced BCH inhibition on GAP activity and GAP-mediated cell rounding. This is the first evidence to show that how Cdc42GAP regulates small GTPase activity by its intramolecular BCH domain.

1.2.2.5 BPGAP1

BPGAP1 is a homolog of Cdc42GAP (Shang et al., 2003). It contains a BCH domain at the N-terminal, a proline-rich region (PRR) in the middle, and a GAP domain at the C-terminal. BPGAP1 specifically enhances RhoA GTPase activity although it interacts with Cdc42 and Rac. BPGAP1 induced pseudopodia formation and increased migration of MCF7 cells. Mutagenesis studies showed that the pseudopodia induction requires BCH the GAP domains, while the cell migration enhancement requires all the three regions. Specifically, the PRR interacts with cortactin (Lua and Low, 2004). BPGAP1 facilitates translocation of cortactin to the periphery. There, cortactin induces the formation of branching actin network, leading to enhanced cell migration.

In addition, BPGAP1 interacts with endophilin 2 through its PRR to enhance EGF-induced receptor endocytosis to promote ERK signaling (Lua and Low, 2005). Furthermore, the active Mek2 would release an auto inhibition on the PRR and promote the interaction between peptidyl-prolyl isomerase 1 (Pin1) and BPGAP1, leading to suppress BPGAP1-enhanced ERK signaling and cell mobility (Pan et al., 2010). The BCH domain of BPGAP1 also binds with K-Ras and its regulator, the small G-protein GDP dissociation stimulator (SmgGDS) (Ravichandran and Low, 2013). Through binding to K-Ras, the BCH domain enhances ERK activation and neuronal differentiation, revealing a novel function of BCH on Ras/ERK signaling.

The functions of different BCH domain-containing proteins are diverse *in vivo*. BNIP-H, as a brain specific member of BCH family, has drawn more and more attention

since it has been shown to be responsible for the human disease Cayman ataxia.

1.2.3 Physiological studies on BNIP-H

BNIP-H is specifically expressed in the nervous system, such as cerebrum, cerebellum, brain stem, spinal cord and dorsal root ganglion (Bomar et al., 2003; Buschdorf et al., 2006) (Figure 1-6). Subcellular localization study indicated that BNIP-H is concentrated at presynaptic sites of neurons (Hayakawa et al., 2007), implying that BNIP-H may function at synapse. The expression of BNIP-H is upregulated during development in cerebellum and hippocampus of mouse (Hayakawa et al., 2007). BNIP-H expression variation during development coincides with the synaptic and neuronal maturation, suggesting that BNIP-H may play an important role in brain development.

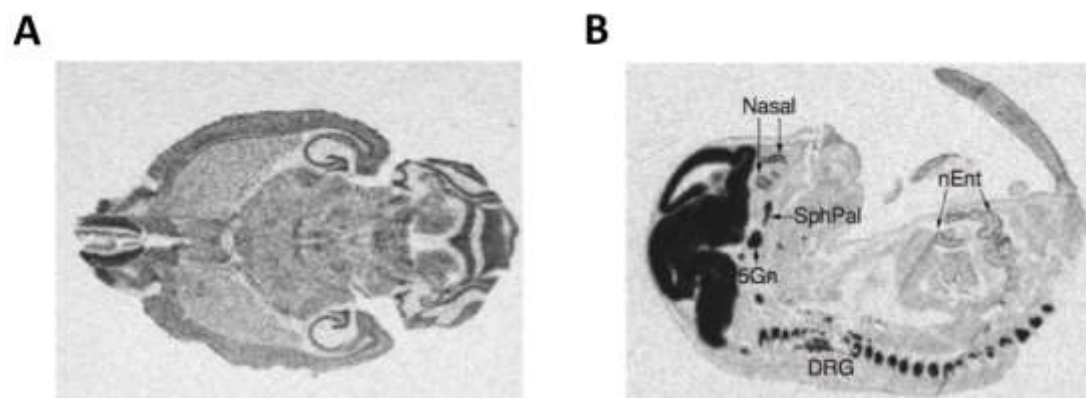


Figure 1-6 Atcay/BNIP-H is a neuron-specific gene.

A. In situ hybridization of a normal mouse brain. BNIP-H is expressed in all parts of the brain. B. In situ hybridization of an embryo at embryonic day 16. BNIP-H is expressed in some regions below the brain, including the sphenopalatine ganglion (SphPal), the trigeminal ganglion (5Gn), the nasal cavity (Nasal), the gastrointestinal tract (nEnt) and the dorsal root ganglion cells (DRG). The picture is adapted from Bomar et al., 2003.

Many neuronal physiological studies have been done in *dt* rat before BNIP-H mutation was identified in this model. The *dt* rat displays clinical signs on day 10 and

the signs include twisting trunk musculature, poor balance during locomotion and self-clasping of forelimbs and hindlimbs (Lorden et al., 1984), so that this rat was identified as a model for Huntington's and Parkinson's disease, and other dystonia diseases. No anatomical differences of neural or non-neural tissues are observed with routine light microscopes (Lorden et al., 1984). However neurochemical analysis shows a significant elevation of norepinephrine (NE) in the cerebellum of the mutant rats compared to normal littermates. And in the *dt* rat, glutamic acid decarboxylase (GAD) activity is significantly higher only in the deep cerebellar nuclei (DCN) than that in the control (Oltmans et al., 1984). GAD activity is known to indicate the neuronal activity in gamma-aminobutyric acid (GABA) system (Collins, 1972). Purkinje cells release GABA as the inhibitory neurotransmitter to DCN. GABA receptors in the DCN are reduced (Beales et al., 1990), reflecting that GABA release from Purkinje cells may be enhanced by the up-regulated GAD activity. To assess whether the difference in DCN neuronal activity is caused by the neurotransmission from the afferent information, the response of DCN cells to harmaline treatment was observed in *dt* rat (Lorden et al., 1992; Lorden et al., 1985). Harmaline induce tremors by activating the inferior olive cells in cerebellum (de Montigny and Lamarre, 1973; Lamarre et al., 1971). The inferior olive neurons activate the climbing fiber pathway to change Purkinje cell complex spikes (Davie et al., 2008). However, harmaline fails to induce tremor and any reliable change in the average firing rate or rhythmicity of the medial nucleus neurons in the *dt* rat (Lorden et al., 1992; Lorden et al., 1985). These data indicate the abnormalities in the cerebellum of *dt* rat, especially olivo-cerebellum pathway. Purkinje cells in the cerebellum adopt a unique anatomical and functional position for processing neuronal information (Apps and Garwicz, 2005) and these cells are the only output signal required for motor coordination (Strick, 1985). Although the biochemical and metabolic studies show that cerebellum is affected in the mutant rat, all the observation and measurements were made after the dystonic syndrome had been developed. Therefore, the animals may develop these abnormalities to compensate and attenuate the dystonia, but not the causes of the disease. To rule out this possibility, a total cerebellectomy was

performed, and found to greatly improve the motor function and prevent the early death of *dt* rats, suggesting that abnormal cerebellar output is the cause of dystonic syndrome (LeDoux et al., 1995). Study from oligonucleotide microarrays identified a huge number signaling pathways affected in the cerebellum of *dt* rats, especially the extracellular matrix interactions, phosphatidylinositol signaling pathways and calcium homeostasis (Xiao et al., 2007).

Besides, regional cerebral glucose utilization is reduced in widespread motor system of the *dt* rat, such as cerebellum, substantia nigra, basal ganglia and so on, suggesting there are widespread abnormalities in *dt* rats (Brown and Lorden, 1989). In particular, these rats display a reduced behavioral response to the dopaminergic blocker, haloperidol, indicating there may be a defect in striatum pathway (McKeon et al., 1984). As dopamine (DA) is one of the major neurotransmitters in striatum system, McKeon et al. measured the striatal DA levels, turnover rates and receptor density (McKeon et al., 1984). No change was observed in the mutant rat compared to the control, suggesting that there might be a defect in the efferent pathway to the striatum system (McKeon et al., 1984).

The above studies indicated the affected regions of the brain by BNIP-H mutation in *dt* rat. However, the cellular and molecular aspects of BNIP-H have not been well characterized. That drives others and us to study the functions of BNIP-H protein in cell by identifying its cellular binding partners.

1.2.4 Cellular binding partners of BNIP-H

Recently, five binding partners of BNIP-H have been identified, namely carboxyl terminus of Hsp70-interacting protein (CHIP) (Grelle et al., 2006), kidney-type glutaminase (KGA) (Buschdorf et al., 2006), Pin1 (Buschdorf et al., 2008), caspase-3 (Itoh et al., 2011) and kinesin light chain 1 (KLC1) (Aoyama et al., 2009) (Figure 1-7). Besides, the BCH domain of BNIP-H contains a RBD-like motif and a CRIB-like motif, suggesting that BNIP-H might interact with RhoA and Cdc42 (Figure 1-7).

1.2.4.1 Hsp70-interacting protein (CHIP)

CHIP is known as a co-chaperone, which interacts with Hsp70, Hsc70, and Hsp90 (Wanker et al., 1997). Recent studies have shown that it acts as an E3 ubiquitin ligase and regulates the polyubiquitination and degradation of chaperone substrates (Clapp et al., 2012; Kravtsova-Ivantsiv and Ciechanover, 2012; Yang et al., 2011). Grelle et al. showed that GST-tagged CHIP interacts with His-tagged BNIP-H on overlay experiments using protein arrays (Grelle et al., 2006). Their functional analysis showed that CHIP, which has E3 ubiquitin ligase activity, stimulates the ubiquitination of BNIP-H *in vitro*. This evidence suggests that degradation of BNIP-H could be regulated by CHIP in cell.

1.2.4.2 Kidney-type glutaminase (KGA)

BNIP-H is strictly expressed in neuronal tissues (Bomar et al., 2003), and its expression increases during development of the cerebellum (Hayakawa et al., 2007; Xiao and Ledoux, 2005), suggesting that BNIP-H is likely to play important roles in neuronal function and/or development of the brain. The first identified BNIP-H binding partner is CHIP, which may regulate BNIP-H turnover, but does not elucidate the neuronal function of BNIP-H (Grelle et al., 2006). Subsequently, another BNIP-H binding partner KGA was found (Buschdorf et al., 2006). KGA is one isoform of phosphate-activated glutaminase (PAG). PAG localizes to mitochondrial to convert glutamine to glutamate, which is the most abundant neurotransmitter in neuronal tissues (Kvamme et al., 2000). In Buschdorf et al. (2006), bacterial GST-tagged BNIP-H pulled down KGA in rat brain whole-cell lysate, mouse neuroblastoma Neuro2A cells and rat pheochromocytoma PC12 cells. Their immunoblotting study showed that endogenous BNIP-H and KGA interact *in vivo*. Two regions (amino acid residues 191-235 and 288-331) within BNIP-H were identified to bind KGA (Figure 1-17). It was also found that BNIP-H is upregulated during neuron differentiation and could re-localize KGA from mitochondria to neurite terminals in differentiated PC12 cells. The glutamate assay results showed that BNIP-H inhibits KGA enzyme activity and

thereby reduces steady-state levels of glutamate. On top of that, this study suggested that BNIP-H might regulate glutamate neurotransmission in brain.

1.2.4.3 Protein interacting NIMA (Pin1)

The certain region (aa 190-287) of the BNIP-H BCH domain could form an intramolecular interaction, suggesting that BNIP-H might undergo protein folding or conformational control (Buschdorf et al., 2008). Though the “candidate” approach screening, Buschdorf et al. identified Pin1, a peptidyl-prolyl cis/trans-isomerase that also interacts with BPGAP1, as a binding partner of BNIP-H. Through progressive mutagenesis, it was identified that two regions (amino acid residues 191-206 and 288-331) within BCH domain are crucial for their interaction and the WW domain of Pin1 is important for the interaction with BNIP-H (Figure 1-17). The immunoprecipitation study showed that the interaction between these two molecules is upregulated during NGF-induced neuron differentiation, and Pin1 displaces KGA binding with BNIP-H during this differentiation process. These results suggested that Pin1 might regulate the conformational change of BNIP-H during neuronal differentiation, which could be important for the cellular activity of BNIP-H. However, it is still not yet known how exactly Pin1 functions on BNIP-H.

1.2.4.4 Caspase-3

Caspase is an important protease in apoptosis, necrosis and inflammation that regulates its substrates by cleavage. Interestingly, it has become evident that caspase may regulate signaling cascades, such as neurogenesis, synaptic plasticity, cell migration and so on (Bravarenko et al., 2006; Fernando et al., 2005; Geisbrecht and Montell, 2004). *In vitro* cleavage assay identified BNIP-H as a substrate of caspase-3 and caspase-7 (Itoh et al., 2011). BNIP-H could be cleaved by caspase-3 in cerebellar granule neurons, further confirming that BNIP-H is a substrate of caspase-3. Caspase-3 preferentially cleaves BNIP-H at the N-terminal (aa 102-105), which results in a C-terminal fragment of 366 amino acids (Figure 1-17). Overexpression of full-length

BNIP-H slightly inhibits constitutively active MEK2-induced ERK activation, and the C-terminal fragment of BNIP-H further enhances this inhibition effect. This study suggested that BNIP-H might regulate MAPK signaling pathway through caspase-3 mediated cleavage. However, the ERK activation experiments were done in HEK293T cells. The ERK stimulator might be different in neurons from HEK293T cells. The function of BNIP-H on MAPK pathway remains to be investigated in neuronal cells.

1.2.4.5 Kinesin light chain 1 (KLC1)

Re-localization of KGA by BNIP-H raises a possibility that BNIP-H might interact with motor protein to regulate this dynamic process. In 2009, Aoyama et al. identified KLC1 as a binding partner of BNIP-H through yeast two-hybrid assay (Aoyama et al., 2009). Kinesin proteins belong to a class of motor proteins. A kinesin is activated by hydrolysis of ATP to move along the microtubule filaments. The active movement of kinesins supports axonal transport of cellular cargos (Hirokawa and Takemura, 2005; Salinas et al., 2008). KLC is a component of kinesin-1, which is a heterotetrameric complex consisting of 2 kinesin heavy chains (KHCs) and 2 KLCs. KLC of kinesin 1 contains four members: KLC1, KLC2, KLC3 and KLC4. Aoyama et al. found BNIP-H binds with KLC1 and is transported by kinesin in neurites (Aoyama et al., 2009). Three amino acid residues (aa 118-120) of BNIP-H at the N-terminal domain have been identified as the binding site to KLC1 (Figure 1-17). Their electron microscopy data indicated that BNIP-H resides at the out membrane of mitochondria. Deletion of BNIP-H from neurons diminished the number of mitochondria at neurite terminals. These results suggested that BNIP-H acts as an adaptor to link mitochondria and kinesin 1 and facilitates the transport of mitochondria from cell body to neurite terminals. However, the accumulation of mitochondria at neurite terminals was not observed by Buschdorf et al. (Buschdorf et al., 2006), which might be caused by the different types of cells used. In addition, it was found that BNIP-H enhances neurite outgrowth in hippocampus neuron, while knockdown of BNIP-H inhibited this effect. However, the molecular mechanism underlying the pro-neurite growth effect of

BNIP-H is still largely unknown.

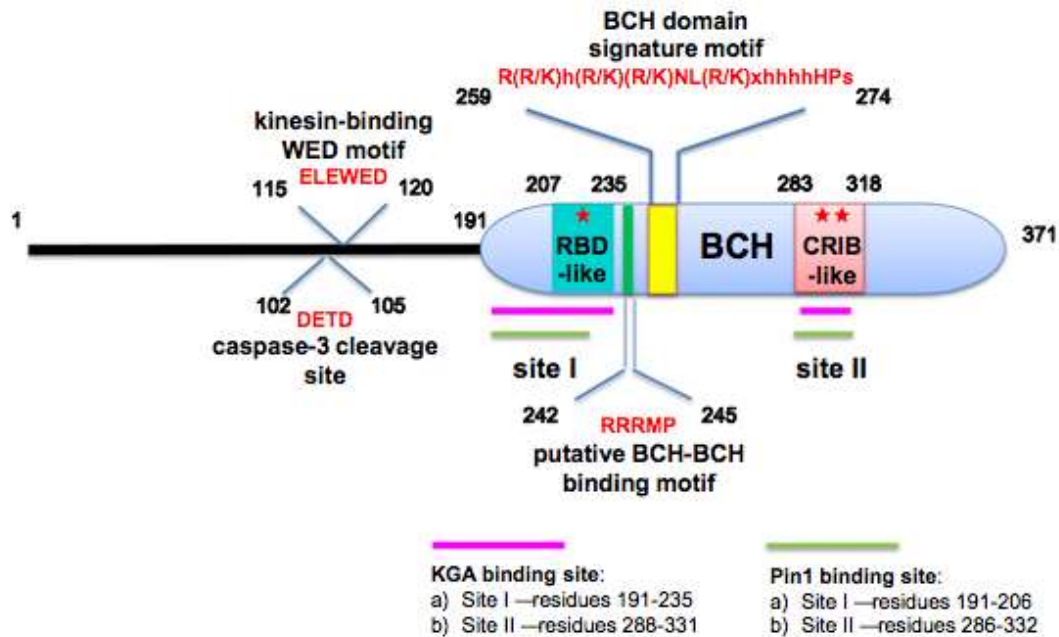


Figure 1-7 Functional motifs within BNIP-H.

In this schematic diagrams of BNIP-H, the known or putative functional motifs are highlighted, including the Rho-binding domain (RBD), CRIB-like motif, BCH signature motif, BCH/BCH interaction motif, caspase-3 cleavage site and kinesin-binding motif. The picture is adapted from Pan and Low, 2012.

1.3 Neurite outgrowth

Aoyama's study suggested that BNIP-H might function in regulating neurite outgrowth (Aoyama et al., 2009). The neurite initiation followed by elongation is the major morphological characteristic of neuronal differentiation, which is the fundamental event in the development of the nervous system. Defective neurite outgrowth induced by disrupting axon guidance, affects the development of cerebellar neurons, leading to severe ataxic phenotype (Berglund et al., 1999). Neurite outgrowth is known to involve three stages, including (1) membrane protrusion of the growth cone, (2) engorgement of organelles and vesicles and microtubules invasion to the growth cone, and (3) consolidation of the newly formed

central of the growth cone into the leading edge of the neurite shaft (Goldberg and Burmeister, 1986; Mortimer et al., 2008) (Figure 1-8).

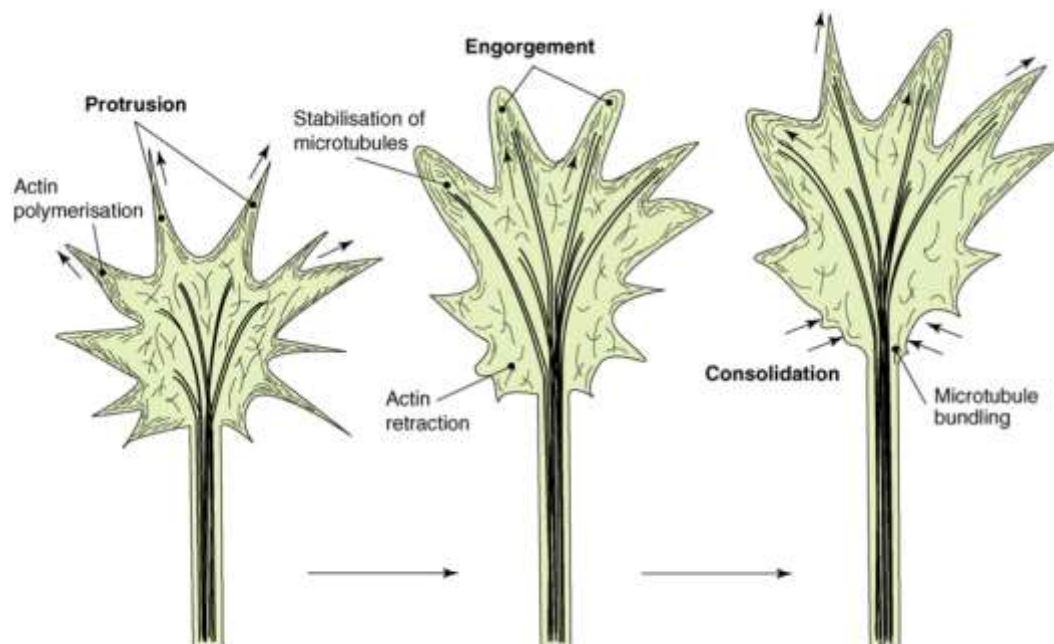


Figure 1-8 Neurite outgrowth proceeds by protrusion, engorgement and consolidation.

Actin polymerization generates forces on the membrane, leading to membrane protrusion. And then the stabilization of microtubules facilitates the vesicles and organelles transportation from the central zone of the growth cone into the periphery, leading to engorgement. Finally, a nascent axon segment becomes consolidated through the crosslinking of microtubules into a stable bundle. The picture is taken from Mortimer et al., 2008.

1.3.1 Signals regulating neurite outgrowth

The initiation of a neurite is guided by positive, negative or guiding signals from the extracellular space (Kiryushko et al., 2004) (Figure 1-9). These signals could arise from the extracellular matrix (ECM), the surface of other cells and autocrine/paracrine factors.

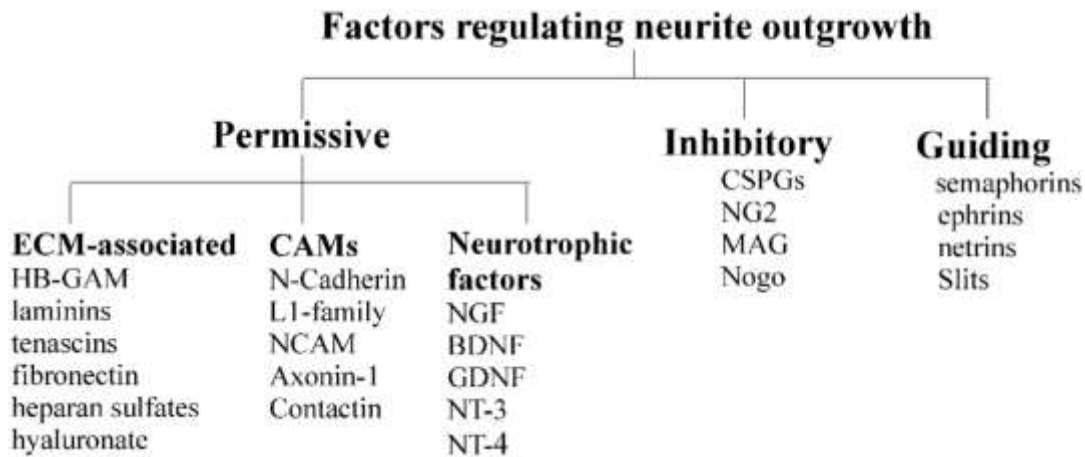


Figure 1-9 Classification of the regulators for neurite outgrowth.
The picture is taken from Kiryushiko et al., 2004.

1.3.1.1 Permissive signals

The ECM not only provides the extracellular structural support for cell adhesion and migration, but also sequesters growth factors and concentrates them for the cellular receptors (Zagris, 2001). Heparin-binding growth-associated molecule (HB-GAM) is a secretory protein that was isolated by screening for factors that enhance neurite outgrowth in rat brain neurons (Rauvala, 1989). It has been reported that HB-GAM has neurite-promoting activity in central nervous system (Li et al., 1990). In addition to central neurons, the peripheral neurons chicken dorsal root ganglia neurons also protrude longer neurite after treatment with HB-GAM (Nolo et al., 1996).

The precise axonal targeting and synapse formation could be driven by cell-cell contact as well (Sperry, 1963). Cell adhesion molecule (CAM) is able to regulate cell adhesion and triggering intracellular signaling, resulting in neurite outgrowth. It has been demonstrated that dominant negative cadherin blocks neurite outgrowth of retinal neurons *in vivo* (Riehl et al., 1996). The CAMs could activate the cAMP response element binding protein (CREB) and the downstream transcription factor c-Fos which is crucial for pro-neurite growth effect (Kiryushko et al., 2004).

Neurotrophic factors are another type of cue, positively regulating neurite extension. This family contains several highly related polypeptides, including NGF, neurotrophin-3 (NT-3), neurotrophin-4 (NT-4) and brain-derived neurotrophic factor (BDNF). They could interact with two classes of receptors, the high affinity tropomyosin-related kinase (Trk) receptors and the low affinity p75 neurotrophin receptors (Huang and Reichardt, 2001). Activation of these receptors by neurotrophic factors could trigger neurite outgrowth through several intracellular signaling cascades, such as Ras, MAPK, phospholipase C (PLC), phosphatidylinositol 3-kinase (PI3K) and so on (Lentz et al., 1999; Sofroniew et al., 2001).

1.3.1.2 Inhibitory signals

To establish a correct neuronal architecture, the inhibitory signals are necessary to control the neurite extension. In addition, these inhibitory factors supply a nonpermissive environment for the mature central nervous system to block neurite regeneration after neural injury (Richardson et al., 1980). The well-studied inhibitory factors include chondroitin sulfate proteoglycans (CSPGs), Nogo-A and myelin-associated glycoprotein (MAG). CSPGs are produced by glial cells during central nervous system (CNS) maturation and after CNS injury (Bovolenta and Feraud-Espinosa, 2000). It has been reported that CSPGs interfere with ECM or CAM to block neurite outgrowth (Dou and Levine, 1994; Friedlander et al., 1994). MAG induces intracellular inhibitory signals through the neurophin receptor p75 (Yamashita et al., 2002), while it is capable of promoting neurite outgrowth in young neurons (Tang, 2003). Nogo-A activates its cell surface receptor, and recruits Rho GTPase to modify the growth cone cytoskeleton and alter the expression of growth cone-associated proteins (Ng and Tang, 2002).

1.3.1.3 Neuronal guiding signals

Neurite can grow in a highly directed manner *in vivo*, which is accomplished by the combination of attractive and repulsive signals during development and regeneration

(Kiryushko et al., 2004). The axons and dendrites are navigated by the guiding cues through the growth cone, a highly sensitive and motile structure. The mobility of growth cone is mediated by F-actin bundles called filopodia, which is a long thin protrusion at the periphery of the growth cone. The interplay of actin polymerization and retrograde flow of these filaments determines whether the filopodia extends or retract (Mallavarapu and Mitchison, 1999). Evidence has suggested that assembly of these actin filaments in growth cone is crucial for axon guidance (Challacombe et al., 1996), but is not required for axon growth (Marsh and Letourneau, 1984), indicating that neurite elongation and direction are two independent but highly co-operated processes for neural development. Several neuronal guidance cues exhibit bifunctionality, which is either attractive or repulsive depending on the physiological condition and cell type. The most well-understood guidance molecules are semaphorins, ephrins, netrins, and slits.

Semaphorins are secreted proteins, functioning through multimeric receptor complexes (Song and Poo, 2001). Semaphorins primarily function as short range inhibitory cues, resulting in growth cone collapse and preventing neurite growth from inappropriate brain regions, But they can also act as attractive signals for some axons (Song and Poo, 2001). Ephrins are membrane-bound ligands, acting through the Eph family of receptor protein-tyrosin kinases (Himanen and Nikolov, 2003). Ephrins function as both attractive and inhibitory guiding cues and control axonal pathfinding in many regions (Brown et al., 2000). Netrins are secreted proteins and act as both attractive and repulsive signals to guide growth cone at short (cell surface) and long (a few millimeters) range distances (Manitt and Kennedy, 2002). Netrins function through the “deleted in colorectal cancer” family (UNC-40) receptor for the growth cone attraction and repulsion, and function through the unc-5 homolog family (UNC-5) receptor for the repulsive effect (Keleman and Dickson, 2001). Slits are secreted proteins functioning through the Roundabout (Robo) receptors, and they have been identified as the major repulsive cues preventing inappropriate axons crossing the midline (Brose et al., 1999; Tang, 2003).

1.3.2 Acetylcholine and neurite outgrowth

1.3.2.1 Acetylcholine signaling pathway

Acetylcholine (ACh) is the first identified neurotransmitter in both peripheral nervous system (PNS) and CNS. Its abnormal blockade would result in many brain motor related diseases, such as Alzheimer's disease, Parkinson's disease, schizophrenia, multiple system atrophy, ataxia and so on (Eglen et al., 2001; Felder et al., 2000; Livingstone et al., 1981; Polinsky et al., 1989). ACh is synthesized by the enzyme choline acetyltransferase (ChAT) (Nachmansohn and Machado, 1943), and the produced ACh would be loaded into synaptic vesicles by vesicular ACh transporter (VAChT) (Song et al., 1997). Synaptic vesicles filled with ACh, would dock at presynaptic plasma membrane and are triggered to exocytose ACh by a transient increase of Ca^{2+} , which is the conserved mechanism of neurotransmitter release (Jackson and Chapman, 2006). Acetylcholinesterase (AChE) hydrolyses and inactivates ACh, to regulate the concentration of ACh at the synapse (Silver, 1963). The ACh-induced actions are mediated by two types of ACh receptors, the nicotinic ACh receptors (nAChRs) and the muscarinic ACh receptors (mAChRs).

The mAChRs are members of the G protein-coupled receptors family (Caulfield and Birdsall, 1998; Wess, 1996). This type of receptors is metabotropic, and would affect targeting cells over a long time frame. They are stimulated by endogenous ACh and selectively stimulated by muscarine. Atropine is one of the effective antagonists of mAChRs. Molecular studies have identified five mammalian mAChR subtypes, M1-M5 (Caulfield and Birdsall, 1998; Wess, 1996). These five members can be further divided into two functional classes according to their coupling preference of G-protein. The M₁, M₃ and M₅ receptors specifically couple to the G_q/G₁₁-type G-proteins, while the M₂ and M₄ receptors selectively activate G-proteins of G_i/G₀ family (Caulfield and Birdsall, 1998; Wess, 1996) (Figure 1-10). A wide range of biochemical responses like activation of MAPK pathway is induced by mAChRs (Wess et al., 2007) (Figure 1-10). The nAChRs are ligand-gated ion channels involved in the

rapid effects of ACh. They are activated by ACh and nicotine, and blocked by hexamethonium. nAChRs comprise five identical or homologous subunits symmetrically arranged to form a central ionic channel (Taly et al., 2009). The active nAChRs are permeable to sodium, potassium and calcium, causing a depolarization of the plasma membrane and intracellular cascades (Albuquerque et al., 2009).

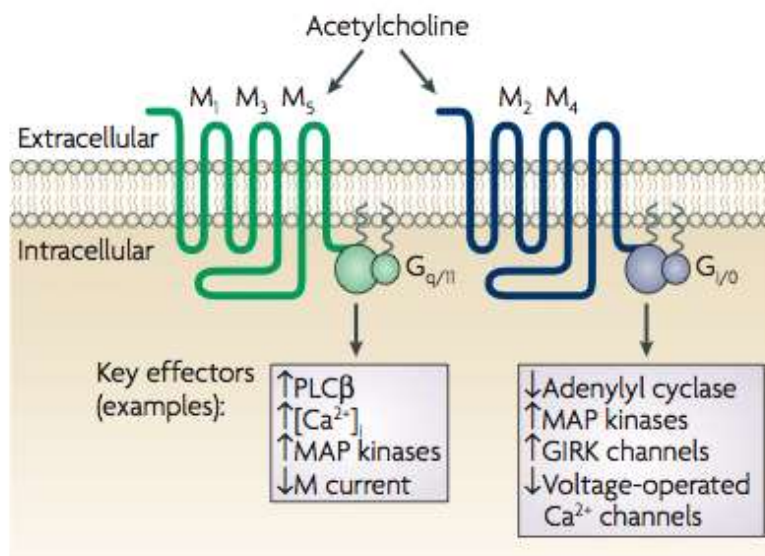


Figure 1-10 Classification of mAChRs.

The M₁, M₃ and M₅ receptors preferentially couple to the G_q/G₁₁-type G-proteins, while the M₂ and M₄ receptors specially activate G-proteins of G_i/G_o family. Distinct mAChRs can modulate phospholipases, protein kinases, ion channels and other signaling cascades. GIRK, G protein-activated inwardly rectifying potassium channel; PLCβ, phospholipase Cβ. The picture is taken from Wess et al., 2007.

1.3.2.2 Effect of ACh on neurite outgrowth

Neurotransmitter system used for communication in mature nervous system is expressed during the brain development, suggesting that these molecules might also play important roles in neuron differentiation (Lipton and Kater, 1989). Neurotransmitters induce caution movement, which would modulate cytoskeleton remodeling at the growth cone. In addition, neurotransmitters also activate various signal transduction pathways to elicit their cellular effects, which is similar to the NTs. Utilizing the common signaling components provides a mechanism for functional

crosstalk between neurotransmitters and neurite modulators (Weiss et al., 1998). A series of investigations has indicated that neurotransmitters contribute to neurite outgrowth and affect neuronal architecture. It has been reported that glutamate promotes neurite sprouting in rat hippocampus and *Helisoma* neurons (Patterson, 1988). Dopamine has been shown to inhibit neurite outgrowth in chick retina and *Helisoma* (Lankford et al., 1988), and serotonin also inhibits neurite outgrowth in *Helisoma* (Haydon et al., 1987).

Interestingly, ACh displays multiple functions in regulating neurite growth in different cell lines and physiological conditions. It has been shown that applying ACh or its agonist carbachol (CCh) blocks neurite outgrowth in rat retinal ganglion and chick retina neurons, suggesting that it acts as an inhibitory cue in these cells (Lankford et al., 1988; Lipton et al., 1988). In particular, nAChRs are crucial for this inhibitory effect as treating rat retinal neurons with nAChR antagonist promotes neurite growth (Lipton et al., 1988). Recently, it was indicated that ACh might function through nAChR α_7 subtype to inhibit G protein pathway complex comprising $G\alpha_{i/o}$, GAP43 and the G protein regulated inducer of neurite outgrowth 1, leading to neurite reduction (Nordman and Kabbani, 2012). Subsequently, it was reported that ACh could act as an attractive cue to turn the direction of nerve growth cone (Zheng et al., 1994). Applying embryonic spinal neurons from *Xenopus* with extracellular ACh turns the growing neurite to the direction of ACh source and this process is mediated by Ca^{2+} calmodulin dependent protein kinase 2 (Zheng et al., 1994). In neuroblastoma, overexpression of ChAT induces the synthesis and secretion of ACh, and promotes fiber outgrowth through mAChRs (Bignami et al., 1997; De Jaco et al., 2002). Similarly, ACh also functions through mAChRs to promote neurite outgrowth in rat Pyramidal hippocampal neurons (De Jaco et al., 2002; VanDeMark et al., 2009) and in PC12 cells expressing M_1 receptor (Pinkas-Kramarski et al., 1992). Further studies suggested that activating mAChRs induces MAPK activation and early response genes for neurite growth (Altin et al., 1991; Berkeley and Levey, 2000; Salani et al., 2009). The above evidences suggested that ACh might regulate neurite outgrowth through

distinct signaling pathways.

1.4 A novel BNIP-H binding partner of BNIP-H, ATP citrate lyase

BNIP-H could regulate neurite outgrowth while the mechanism is elusive (Aoyama et al., 2009). Different mutations of BNIP-H in several models result in diverse phenotypes (Table 1-1), suggesting that BNIP-H may take part in multiple signaling pathways in nervous system. That drove us to identify the novel BNIP-H binding partner and signaling pathway involved to better understand the role of BNIP-H in regulating neurite growth. Through proteomics pull down, ATP citrate lyase (ACL) was identified as a novel BNIP-H associated protein, which will be elaborated in chapter 3.

ACL is formed by four identical subunits each approximately 120 kDa (Singh et al., 1976). It is a key metabolic enzyme that catalyzes cytoplasmic citrate and Coenzyme A to produce acetyl-CoA and oxaloacetate (Srere, 1961). Histidine 760 is the active site of ACL and mutation of ACL His760 (ACL H760A) eliminates its enzymatic activity in producing acetyl-CoA (Fan et al., 2012). ACL is widely distributed in mammalian tissues, especially in liver, adipose tissue and brain (Elshourbagy et al., 1990; Szutowicz and Srere, 1983). There are five enzymes to produce acetyl-CoA in cell, including pyruvate dehydrogenase, carnitine acetyl-transferase, citrate synthase, acetyl-CoA synthetase (ACS) and ACL (Sterri and Fonnum, 1980). In these five enzymes, only ACL and a small portion of ACS (ACS2) locate at cytoplasm, while others locate at mitochondria (Beigneux et al., 2004a; Hatzivassiliou et al., 2005; Hayashi and Kato, 1978; Szutowicz and Lysiak, 1980b). Acetyl-CoA is mainly produced in mitochondria and used in citric acid cycle (Krebs cycle) for energy production. At the meantime, acetyl-CoA supplies the acetyl group in many reactions in cytoplasm. However, the acetyl-CoA produced in the mitochondria is not permeable to the mitochondrial membrane. Therefore it is converted to citrate, which is then transported to cytoplasm to be catalyzed to acetyl-CoA again by ACL.

ACL has been shown to regulate lipogenesis and cholesterol genesis in cytoplasm, and histone acetylation in nuclei (Elshourbagy et al., 1990; Hatzivassiliou et al., 2005; Wellen et al., 2009) (Figure 1-11). Interestingly, several studies suggested that ACL might cooperate with ChAT, and participate in ACh synthesis pathway (Figure 1-11). In rat brain, ChAT and ACL activities are mostly found in synaptosome where ACh is synthesized, and are significantly correlated in cholinergic regions of the brain, whereas ACS activity is relatively low in these regions (Szutowicz et al., 1983; Szutowicz and Lysiak, 1980a; Szutowicz et al., 1982). ACL was also shown to co-localize with ChAT and VAcHT in cholinergic neurons of the mouse hippocampus (Beigneux et al., 2004b). In vitro study also showed the importance of ACL in ACh synthesis whereby inactivation of ACL by histidine phosphatase (dephosphorylating His760) reduces ACh content in SN56 cholinergic neuroblastoma cells (Eissing et al., 2012). These results suggested ACL might supply acetyl group for ACh synthesis. However, it remains elusive that how functions of ACL and ChAT are coordinated.

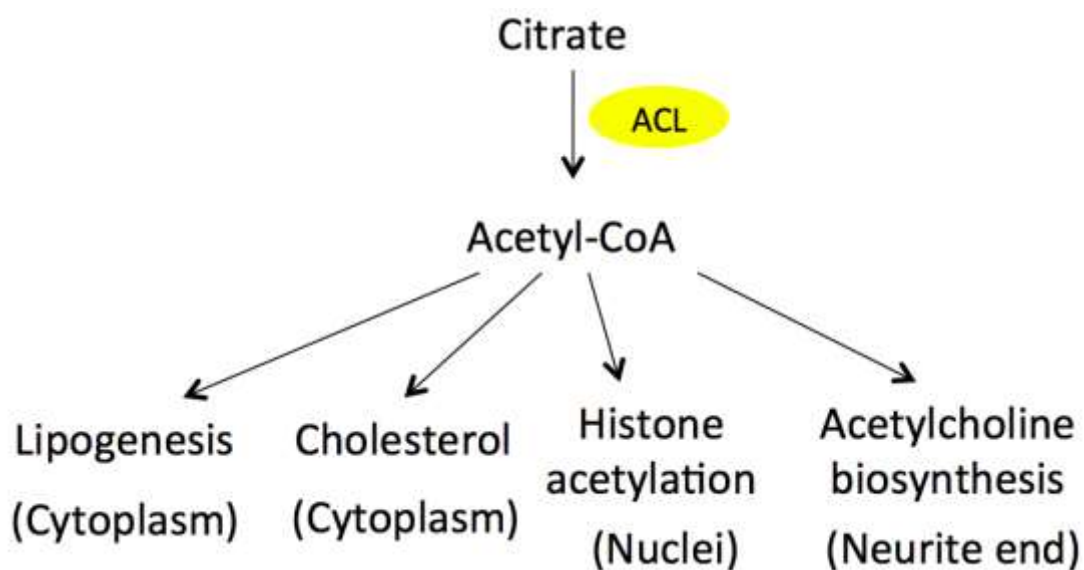


Figure 1-11 The signaling pathways regulated by ACL.

ACL is an enzyme that represents important functions in fatty acid biosynthesis and cholesterologenesis in cytoplasm, and histone acetylation in nuclei (Elshourbagy et al., 1990; Hatzivassiliou et al., 2005; Wellen et al., 2009). At neurite terminals of neurons, ACL takes part in ACh synthesis regions (Szutowicz et al., 1983; Szutowicz and Lysiak, 1980a; Szutowicz et al., 1982).

1.5 Gaps in understanding the functional mechanism of BNIP-H

BNIP-H deficiency is linked with ataxic phenotype and mental retardation in patients with Cayman ataxia, *jittery* mice and *dt* rats (Bomar et al., 2003; Xiao and Ledoux, 2005). However, the pathophysiologic mechanism through which it acts is still largely unknown. Cellular studies indicated that overexpression of BNIP-H enhances neurite outgrowth in hippocampal neurons (Aoyama et al., 2009; Buschdorf et al., 2006). While this finding suggested that BNIP-H affects neurite outgrowth and neuronal differentiation, it remains unclear what role BNIP-H plays in neuronal differentiation and what molecular signaling pathway is involved in this process.

1.6 Objectives of this study

The investigation on the cellular and molecular mechanism of BNIP-H functions will provide us important knowledge of ataxia disease and neuritogenesis. This study focused on the functional investigations of BNIP-H at the molecular level. The overall aim of this study was to investigate how BNIP-H regulates neurite outgrowth. More specifically, the aims of this study were:

1. To identify BNIP-H binding partner in neuronal cells.
2. To determine the effect of BNIP-H and its binding partner ACL on neurite outgrowth.
3. To explore the mechanism by which BNIP-H regulates neurite outgrowth through its interaction with ACL.

This thesis demonstrates that BNIP-H regulates the dynamics trafficking of ACL on kinesin motor to neurite terminals and accumulates ACh biosynthesis enzymes ACL and ChAT there to enhance the local production and release of ACh. The released ACh exerts an autocrine/paracrine feedback loop to activate MEK/ERK pathway and potentiate neurite outgrowth through mAChRs. The investigation of the regulatory

effects of BNIP-H in ACh release in this study may extend our understanding on how motor proteins actively transport the metabolic enzymes in neurons and how scaffold proteins regulate this process. This finding could also provide novel therapeutic strategies for Cayman ataxia and related diseases.

In order to achieve the aims mentioned above, proteomics pull down assay was employed to identify its putative binding partner to analyze the mechanism in regulating neurite outgrowth. Besides, co-immunoprecipitation was applied to study protein-protein interaction, and confocal microscopes were used to study the localization and dynamics of interested proteins inside the cells. The signaling pathway BNIP-H takes part in to regulate neurite growth was identified through pharmacological treatments. Mass spectrometry was employed to study the ACh content secreted by PC12 cells upon NGF stimulated differentiation. The detailed methods have been described in the following chapter.

2. Materials and methods

2.1 DNA cloning techniques

2.1.1 Polymerase Chain Reaction (PCR)

To obtain the desired DNA sequence (sub-cloning and site-directed mutagenesis), PCR was conducted by using high fidelity DNA polymerase PfuUltra™ (Stratagene) with specific primer pairs in DNA thermal cycler model iCycler (BIO-RAD). The components of a 50 µl reaction are as follows: 5 µl of 10× reaction buffer, 0.2 mM dNTPs, 5 ng DNA template, 1 µl of 10 µM sense primer, 1 µl of 10 µM anti-sense primer, 1 µl of polymerase and top up to 50 µl with distilled water (dH₂O). The PCR reaction mix was subjected to the following typical PCR condition: initial denaturation at 94°C for 5 min, followed by 35 cycles of denaturation at 94°C for 30 sec, annealing at 56°C for 30 sec and extension at 72°C for 1-4 min (1 min per kb) and final extension at 72°C for 10 min.

2.1.2 Agarose gel electrophoresis

The DNA electrophoresis was performed in 1% (w/v) agarose gel. The agarose powder (Bio-Rad) was dissolved in Tris-acetate Ethylene diamine-tetraacetic acid (EDTA) (TAE) buffer. SYBR® safe DNA gel stain (Life technologies) was added into the agarose solution at the ratio of 1:100,000. PCR product was mixed with 10× DNA loading dye (3.9 ml glycerol, 500 µl 10% (w/v) SDS, 200 µl 0.5 M EDTA, 0.025 g bromophenol blue, 0.025 g xylene cyanol ff in 10 ml dH₂O) and ran with a voltage of 5 V/cm for 20-30 min. The gel was visualized using Gel Doc UV-transilluminator (Bio-Rad).

2.1.3 Gel extraction

A gel extraction kit (Qiagen) was used to isolate the DNA sample. The desired DNA band was excised using a clean sharp scalpel. After that, a typical gel extraction was

conducted following the manufacturer's protocol. Briefly, 1 volume of the gel was mixed with 3 volumes of buffer QG and incubated at 50°C for 10 min with occasional mixation to dissolve the agarose gel. If the desired DNA sample was greater than 4 kb or smaller than 500 bp, additional 1 volume of isopropanol was added into the mixture. Then the mixture was transferred into a QIAquick column and spun at 13,000 rpm in a centrifuge (Eppendorf) for 1 min. The column was washed with 0.5 ml of buffer QG and spun at 13,000 rpm for 1 min, and washed again with 0.75 ml of buffer PE. The empty column was centrifuged for an additional 2 min to remove any residual ethanol. The DNA sample was eluted with 30-50 µl of dH₂O.

2.1.4 Restriction endonuclease (RE) digestion

All the REs used for this study were from New England Biolabs. The plasmid used as the backbone, plasmid containing the insert of interest or PCR product was restriction digested in a 50 µl reaction containing 5 µl of 10× specific buffer, 1 µl of enzyme (20 Units), 0.5 µl of 100× BSA and made up to 50 µl with dH₂O. The mixture was incubated at 37°C for 3 h. The digested product was then separated by agarose gel electrophoresis and gel extracted as explained above.

2.1.5 Ligation

The ligation reaction was set up following the manufacturer's instruction (Promega). In a 10 µl reaction, 1 µl of 10× DNA ligase buffer (300 mM Tris-HCl at pH 7.8, 100 mM MgCl₂, 100 mM DTT and 10 mM ATP), 1 unit of T4 DNA ligase, 50 ng vector and corresponding amount of DNA insert, was mixed and incubated 4°C overnight. The molar ratio between vector and DNA insert was 1:3 to 1:5.

2.1.6 Transformation

The standard transformation was performed using calcium chloride based chemically competent *E.coli* DH5α cells (Seidman et al., 2001). The desired plasmid or ligation product was added into the competent cells and mixed by tapping. The mixture was

incubated on ice for 30 min. Heat shock was conducted by incubation at 42°C water bath for 90 s. The tube was cooled on ice for 2 min. Then 1 ml of Luria-Bertani (LB) media (5 g yeast extract, 10 g tryptone and 10 g of NaCl in 1 l of H₂O) was added into the mixture of bacteria and plasmid and incubated for 1 h at 37°C in a bacterial shaker swaying at 250 rpm. The cells were spun down, spread on a LB plate with 50 µg/ml ampicillin or other appropriate antibiotics and incubated at 37°C overnight

2.1.7 Colony PCR screening

Colony PCR is used to screen the presence of the desired DNA insert. The colonies on the LB plate is picked by a 10 µl pipette tip and resuspended in 5 µl of dH₂O as the DNA template source. The primer pair consists of one primer from the sequence of the vector and another primer from the sequence of the DNA insert. The 10 µl PCR reaction (DyNAzyme 2, Thermo) contains 1 µl of DNA template, 1 µl of 10× Buffer, 0.2 mM dNTPs, 0.4 µl of 10 µM forward primer, 0.4 µl of 10 µM reverse primer and 0.2 µl of DNA polymerase. The PCR parameters were: initial denaturation at 94°C for 3 min, followed by 25 cycles of denaturation at 94°C for 30 s, annealing at 56°C for 30 s, extension at 72°C for 1-3 min (40 sec per kb) and final extension of 72°C for 5 min. The positive colonies were picked and expanded for plasmid isolation.

2.1.8 Plasmid isolation

The bacterial was culture in 3 ml of LB medium with 50 µg/ml ampicillin or appropriate antibiotics at 37°C overnight with vigorous shaking at 250 rpm in a bacterial shaker. The plasmid mini prep was conducted based on manufacturer's instructions (Axygen). Briefly, the bacterial culture was spun down at 13,000 rpm for 1 min and resuspended in 250 µl of buffer S1. Another 250 µl of buffer S2 was added into the bacterial solution and mixed gently by inverting 10 times. Then 350 µl of buffer S3 was added and mixed by inverting 10 times. The solution was spun down at 13,000 rpm for 10 min. The supernatant was transferred into the column and bond to its membrane by centrifugation. The column membrane was washed by 500 µl of

buffer W1 and 700 μ l of buffer W2. Empty column was centrifuged to remove residual ethanol. Elution was done by addition of 30-50 μ l of dH₂O.

2.1.9 DNA sequencing

DNA sequencing was performed by BigDye[®] terminator (Applied Biosystems Inc.). The components for a 10 μ l sequencing PCR are as follows: around 300 ng DNA template, 0.4 μ l of 10 μ M forward primer, 4 μ l of the BigDye premix and dH₂O. The PCR condition is 25 cycles of 96°C for 30 s, 50°C for 15 s and 60°C for 1 min. The PCR product was purified by ethanol precipitation. The 10 μ l PCR product was mixed with 62.5 μ l of ethanol, 3 μ l of 3 M sodium acetate and 24.5 μ l dH₂O. After 10 min, the mixture was spun down at 13,000 rpm for 15 min. The pellet was washed twice with 1 ml 70% ethanol and centrifuged at 13,000 rpm for 10 min. The pellet was air-dried and resuspended in 13 μ l of ABI HiDi formamide buffer. The solution was loaded into a 96 well reaction plate and sequencing was performed using the 377 ABI PRISM automated DNA sequencer (Applied Biosystems Inc.).

2.1.10 Plasmids

The ACL cDNA (NCBI: J05210.1) and BNIP-H cDNA (NCBI: NM_001040190.1) were created previously in the lab by amplifying the CDS from rat PC12 cells cDNA, and were cloned in pXJ40 vectors between BamH1 and Not1. They were used as the templates to generate all the mutation constructs. The primer pairs used in mutagenesis are shown in Table 2-1. The KLC1 cDNA (NCBI: NM_008450.2) was created previously in the lab by amplifying the CDS from mouse Neuro2A cells cDNA, and were cloned in pXJ40 vectors between BamH1 and Kpn1. The mouse ChAT cDNA (NCBI: NM_009891.2) was purchased from Origene and sub-cloned in pXJ40 vectors between BamH1 and Not1. The rat VACHT cDNA (NCBI: U09838.1) was a generous gift from Zu-Hang Sheng (National Institute of Neurological Disorders and Stroke, National Institutes of Health, Maryland), and sub-cloned in pXJ40 vectors between BamH1 and Not1. Knockdown by plasmid-based RNAi was carried out with the pGFP-

V-RS and pRFP-C-RS vectors (Origene) that expressed BNIP-H and ACL targeting sequences (designed with Ambion siRNA Designer). Two independent targeting sequences for BNIP-H and ACL are shown in table 2-2. A nontargeting RNAi (scramble) was used as control.

Table 2-1 Primers used for mutagenesis.

Name	Sequence	Description
BNIP-H 3A F	ggcaatgaacttgaggcggcagctgacacccca	Primers used for BNIP-H WED (aa 118-120) mutant.
BNIP-H 3A R	tggggtgtcagctgccgctcaagttcattgcc	
BNIP-H 2A F	cgtgagggatgaagcggcggatgaagatctgc	Primers used for BNIP-H WQ (aa 19-20) mutant.
BNIP-H 2A R	gcagatcttcatccgcttcatccctcacg	
ACL H760A F	gaggtccagttggcgccgctggggcttgtgcc	Primers used for ACL Histiding 760 mutant.
ACL H760A R	ggcacaagccccagcggcgccaaactggacctc	
GFP-BNIP-H ^{re} F	ctggctgaagaaatgctatcatatgattgacag	Primers used for the synonymous mutant of BNIP-H.
GFP-BNIP-H ^{re} R	ctgtcaatcatatgatagcatttcttcagccag	
mCherry-ACL ^{re} F	gctgtgcaaggtatgctagatttcgactacgtg	Primers used for the synonymous mutant of ACL.
mCherry-ACL ^{re} R	cacgtagtcgaaatctagcatcaccttgacacgc	

Table 2-2 RNAi targeting sequences.

Targeting gene	Number	Targeting sequence
BNIP-H	1	CTACATTACGAATGGAAA
	2	AAGTGTTACCACATGATT
ACL	1	ATCTTTACTTCACCTACC
	2	GCATGCTGGACTTTGACT

2.2 Cell culture

2.2.1 PC12 cell culture

PC12 cells were cultured in Dulbecco's Modified Eagle's Medium (DMEM) supplied with 4500mg glucose, 10mM HEPES, 5% fetal bovine serum (all from Hyclone) and 10% horse serum (Gibco) in a 10 cm tissue culture dish (NUNC) at 37°C in a humidified incubator (Thermo) with 5% CO₂. Cell culture medium was changed once every other day. When they reach around 80-90% confluence, PC12 cells were washed once with DMEM supplied with 0.25% fetal bovine serum and 0.5% horse serum. And then the cell culture medium was used to wash the cells off the plate. The cells were split into new dishes at the passage ratio of 1:3. Cells within passage 3 to passage 15 were used for all the experiments.

2.2.2 PC12 cells transfection

For PC12 cells transfection, cells were firstly seeded in a 10 cm dish or a 6-well plate coated with poly-D-lysine (Sigma) and culture for 24 h. For imaging studies, 2×10^4 cells were seeded in a 35 mm tissue culture dish, and for biochemical studies, 2×10^5 cells were seeded in a 35 mm tissue culture dish. And then cells were changed into the medium containing 0.25% fetal bovine serum and 0.5% horse serum, and transfected with Lipofectamine 2000 reagent (Invitrogen) according to the manufacturer's instructions. It was comprised of DNA: Lipofectamine 2000 in a ratio of 1:2.5 in Opti-MEM® (Gibco). Plasmid DNA of 0.1-0.5 µg and 2 µg was used for transfection for imaging studies and biochemical studies respectively. Briefly, plasmid DNA and Lipofectamine 2000 reagent were resuspended in 150 µl Opti-MEM respectively and mixed by gently tapping. The two solutions were mixed by gently tapping after 5 min incubation at room temperature. This transfection mix was incubated for another 20 min at room temperature before adding onto the cells dropwisely.

2.2.3 Chemical treatment on PC12 cells

2.2.3.1 Reagents used for cell treatment

NGF, lovastatin, 5-tetradecyloxy-2-furoic acid (TOFA), hemicholinium-3, (±)-vesamicol hydrochloride, carbachol (CCh), atropine, hexamethonium bromide, eserine, 1,4-diamino-2,3-dicyano-1,4-bis [2-aminophenylthio] butadiene (U0126) and 5,6-dichloro-1-beta-D-ribofuranosylbenzimidazole (DRB) were all from Sigma. Polyclonal antibody against ACh was from Millipore.

2.2.3.2 Procedure

For neuronal differentiation, PC12 cells were incubated for 24 h after transfection, and then were induced to differentiate with 20 ng/ml NGF (for overexpression experiments) or 100 ng/ml NGF (for knockdown experiments) in the absence of

serum for another 24 h. To study the effect of different drugs or ACh antibody on PC12 differentiation, specific drug or antibody was added together with NGF for 24 h.

For ERK activation, PC12 cells were incubated for 24 h, after transfection or in the medium containing 0.25% fetal bovine serum and 0.5% horse serum without transfection. The inhibitors used in this study were added into the medium 30 min before NGF stimulation. And then the cells were treated with 20 ng/ml NGF in the absence of serum for the indicated time.

2.2.4 Neuro2A cell culture and transfection

Mouse Neuro2A cells were grown in DMEM supplemented with 4.5 g glucose, 10 mM HEPES, 10% (v/v) fetal bovine serum in a 10 cm tissue culture dish in the same condition as PC12 cells. Cell culture medium was changed once every other day. When they reach around 80-90% confluence, Neuro2A cells were washed once with PBS and rinsed by Trypsin-EDTA solution (Gibco). The dish was incubated at 37°C incubator for 2-3 min till the cells have detached from the plate. The trypsin-EDTA was neutralized using complete media. The cells were split at the passage ratio of 1:5.

Neuro2A cells at 60-80% confluence in 10 cm plates were changed into complete media without antibiotics, and transfected with 10 µg plasmid using Lipofectamine 2000 reagent. The procedure is similar to the one of PC12 cells.

2.2.5 HEK293T cell culture and transfection

HEK293T cells were grown in RPMI 1640 medium (Hyclone) supplied with 10% fetal bovine serum, 10mM HEPES. Cell culture medium was changed once every other day. When they reach around 80-90% confluence, HEK293T cells were washed once with PBS and rinsed by Trypsin-EDTA solution (Gibco). The dish was incubated at 37°C incubator for 1 min till the cells have detached from the plate. The trypsin-EDTA was neutralized using complete media. The cells were split at the passage ratio of 1:10.

The cells at 60-80% confluence in 35 mm plates were transfected with TransIT-LT1 (Mirus Bio LLC), according to the manufacturer's instructions. It was comprised of DNA: TransIT-LT1 in a ratio of 1:3 in Opti-MEM and 1 µg of each plasmid was used for transfection. Briefly, plasmid DNA and transfection reagent were mixed in 300 µl Opti-MEM by gently pipetting. This transfection mix was incubated for 30 min at room temperature before adding onto the cells dropwisely.

2.2.6 Cell number quantification

The quantification of cell number was done by using Luna™ Automated Cell Counter. The cell suspension was mixed with an equal volume of Trypan Blue Stain (Invitrogen) and loaded into a cell counting slide. The slide was later inserted into the instrument slot. Then the program was run to calculate the cell number.

2.2.7 Cryopreservation and recovery of cell lines

The cell lines at 80-90% confluence were resuspended and spun down at 800 g for 3 min. The cell pellets were resuspended in their culture medium containing 5% Dimethyl sulfoxide (DMSO). Around 2×10^6 cells were transferred into a 1 ml cryovial. Cryovials were sealed tightly and placed in Mr. Frosty (Thermo) before transferring in -80°C freezer. After 24 h, the cryovials were transferred into liquid nitrogen tank. Cell recovery was performed by rapid thawing the cryovials in a 37°C water bath. The cells were centrifuged at 800 g for 3 min to remove DMSO and resuspended in fresh culture medium. After that, the cells were seeded onto a 10 cm dish for further incubation.

2.3 Immunoassays

2.3.1 Antibodies

Goat polyclonal anti-BNIP-H antibody was purchased from Santa Cruz Biotechnology. Polyclonal antibody against FLAG, monoclonal antibody against activated ERK1/2, IgG from goat serum and horse radish peroxidase (HRP)-conjugated antibodies were all

from Sigma. Polyclonal antibodies against ACL and total ERK1/2 were from Cell Signaling Technology. Monoclonal antibodies against β -tubulin, GAPDH and polyclonal antibody against HA were from Invitrogen. Polyclonal antibody against ACh was from Millipore and monoclonal antibody against neuronal class III β -tubulin (Tuj1) was from Covance. All secondary antibodies conjugated with Alexa Fluor dyes (405, 488 and 568) were from Invitrogen.

2.3.2 Cell lysis

Briefly, cells were rinsed twice with PBS. Then HEPES lysis buffer containing 25 mM PIPES, 115 mM potassium acetate, 5 mM sodium acetate, 5 mM MgCl₂, 0.5 mM EGTA, 1% Triton-X-100, 5 mM sodium orthovanadate, 25 mM glycerol 2-phosphate, 2 mM sodium fluoride and 1 \times protease inhibitor cocktail solution (Roche) was added dropwisely on the cells. The cells were immediately harvested by cell scraper and incubated on a nutator at 4°C for 15 min. The undissolving cell debris was removed by centrifugation at 13,000 rpm at 4°C for 15 min. For western blotting analysis (described in 2.3.4), the supernatant was mixed with SDS loading dye and boiled at 85°C for 5 min.

2.3.3 Identify the binding partner of BNIP-H

One 10 cm dish of Neuro2A cells were transfected with FLAG-BNIP-H for 24 h. The sample transfected with FLAG empty vector was used as the control. The cells were lysed in 1 ml lysis buffer per well. The lysates were incubated with 20 μ l of anti-FLAG antibody conjugated to agarose beads (Sigma) at 4°C overnight. The beads were extensively washed with lysis buffer for three times and boiled with 2 \times SDS loading buffer. After that, the protein samples were applied for SDS-PAGE and silver staining that will be described 2.3.4.1. The specific band showed in FLAG-BNIP-H pull down was identified by matrix-assisted laser desorption/ionization-time of flight (MALDI-TOF) mass spectrometer (AB SCIEX).

2.3.3 Co-immunoprecipitation (Co-IP)

Transfected cells were lysed in 250 μ l lysis buffer per well. The lysates were either directly analysed by Western blotting or used for binding studies. For use in binding study, lysates were incubated with 8 μ l of anti-FLAG antibody conjugated to agarose beads at 4°C for 2 h. The beads were extensively washed with lysis buffer and analysed by western blotting. For Co-IP of endogenous proteins, 2 μ g of anti-BNIP-H antibody was conjugated to 20 μ l of protein A/G sepharose (GE healthcare) for 2 h at 4°C. PC12 cells were lysed in lysis buffer. After centrifugation, the lysate were incubated with anti-BNIP-H antibody conjugated to sepharose beads at 4°C overnight. After washing with lysis buffer, samples were analysed by western blotting.

2.3.4 Western blotting

2.3.4.1 Sodium dodecyl sulfate - Polyacrylamide Gel Electrophoresis (SDS-PAGE)

8-15% polyacrylamide gel was used according to the molecular weight of the protein band and was manually casted in Mini-PROTEAN® 3 Cell (Bio-Rad) SDS-PAGE apparatus following the manufacturer's instruction. The gel was placed into the Mini-PROTEAN® 3 electrophoresis module assembly filled with the SDS-running buffer (15 g/L Tris base, 72 g/L Glycine, pH 8.3, SDS 5g). The comb in the gel was gently removed. The protein marker (Bio-Rad) and samples were loaded into the wells. The electrical leads were connected to a power pack and run at 150 V for 1.5 h.

To visualize protein bands, the resolving gel was carefully transferred into a 20 cm culture dish and applied for silver staining (Bio-Rad). Briefly, the gel was fixed with fixative reagent (40% methanol/10% acetic acid (v/v)) at room temperature for 30 min. And then the gel was incubated with Oxidizer for 5 min and washed with dH₂O for 15 min. After that, the gel was incubated with silver reagent for 20 min and developed with developer till the protein bands were clear. The development was stopped by 5% acetic acid (v/v) for 15 min.

2.3.4.2 Gel transfer

Proteins separated by SDS-PAGE were transferred into the PVDF membrane (Millipore) by wet electroblotting transfer system (Bio-Rad). Briefly, the PVDF membrane was firstly activated by methanol for 2 min. And then the PVDF membrane, chromatography papers (Whatman) and foam pads were pre-soaked in transfer buffer (25mM Tris, 195mM glycine, 0.1% (w/v) SDS, 20% (v/v) methanol). Gel covered by the membrane was sandwiched between chromatography papers on each side followed by a foam pad in the plastic holder. Care was taken to avoid any bubble in this step. Then the holder was inserted into the cassette placed inside the electrophoresis system. A bio-ice cooling unit was placed into the tank. After that, the transfer buffer was poured into the tank. The protein transfer was performed at 100V at 4°C for 1.5 h.

2.3.4.3 Immunoblotting

The PVDF membrane with transferred protein was placed in a plastic box and blocked by 10 ml of 1% BSA in 1× PBS with 0.1% tween-20 (PBST) at room temperature with gentle shaking for 1 h. The blocking solution was replaced by the primary antibody with appropriate dilution prepared in 1% BSA in 1× PBST with 0.2% sodium azide and shaken overnight at 4°C. After incubation, the membrane was washed for five times with PBST for 5 min each on a shaker. The matching secondary antibody conjugated with HRP with 1:2500 dilution in 1% BSA in PBST was added to the membrane and shaken at room temperature for 1 h. This was followed by five times washes with PBST for 5 min each.

2.3.4.4 Chemiluminescent detection

After immunoblotting, the HRP activity was detected by enhanced chemiluminescent substrate (Pierce Biotechnology, Inc.). Equal volumes of the luminol/enhancer and the peroxide buffer were mixed and added dropwisely on the membrane. After 5 min incubation, the membrane was transferred into the developing cassette and placed

between transparency sheets. Signal detection was performed by exposure to X-ray film (Fuji Photo Film) for appropriate time and developed in a RP X-OMAT Processor (Kodak).

2.3.5 Immunostaining

PC12 cells were cultured on poly-D-lysine-coated glass coverslips. Cells were washed three times with PBS and fixed with 4% formaldehyde for 15 min at room temperature. To deplete the cytosolic pool of ACL protein, cells were permeabilized before fixation with 0.01% saponin for 2 min. After fixation, cells were washed three times with PBS and permeabilised with 0.1% Triton X-100 in PBS for 10 min at room temperature. Permeabilised cells were blocked with 2% bovine serum albumin and 7% fetal bovine serum in PBS for 60 min at room temperature. Cells were incubated with primary antibodies appropriately diluted in blocking buffer for 60 min at room temperature. Samples were washed five times with 0.1% Triton X-100 containing PBS, and then incubated with Alexa Fluor conjugated antibodies in blocking buffer (1:500 dilution) for 60 min at room temperature. To mount the stained cells to a glass slide, a drop of FluorSave™ (Millipore) was applied on the slide and the coverslip with cells facing the slide was placed onto the slide. To image PC12 cells transfected with fluorescence tagged protein, the coverslip with cells was fixed and mounted to a glass slide without staining.

2.4 Imaging and image processing

2.4.1 Fixed sample imaging and image processing

To image the protein localization of the fixed sample, pictures were taken with a Nikon A1R confocal microscope equipped with 60 × and 100 × oil immersion lenses. To image cells differentiation, cells were imaged with an EVOS FL Cell imaging system (Invitrogen). The fluorescence intensity and neurite length were analyzed with NIH ImageJ software.

2.4.2 Live cell imaging and image processing

To image protein trafficking along the neurite, PC12 cells were cultured on poly-D-lysine-coated glass bottom dish (ibidi). Live imaging was captured with PerkinElmer UltraVIEW VoX confocal microscope equipped with a 100 × oil immersion lens, at maximum speed (2-7 frames per second) for 1 min. In transfection-positive PC12 cells in culture, 20 μm length of neurite was selected and kymography was processed with ImageJ software. To image PC12 cells differentiation, a wide field Olympus IX81 inverted microscope was used and images were analyzed with ImageJ software.

2.4.3 Fluorescence recovery after photobleaching (FRAP) assay

For the FRAP assay at neurite terminals, samples were observed using PerkinElmer UltraVIEW VoX confocal microscope equipped with a 100 × oil immersion lens. A rectangular ROI (3 μm × 11 μm) was defined and photobleached using 488 nm laser line. Subsequent recovery was monitored at the rate of 1 frame every 5 seconds. A ROI was selected from cell body for acquisition bleaching corrections. Images were analyzed with Volocity software.

2.5 ACL enzyme assay

The enzymatic activity of ACL in the cell lysate was determined by the malate dehydrogenase-coupled procedure as described (Srere, 1959). After 24 h of transfection, the cells were lysed and an aliquot of the lysate was analysed by western blotting for protein expression. 50 μL of the rest lysate in a final volume of 100 μL was incubated with 100 mM Tris/HCl pH 8.7, 20 mM of potassium citrate, 10 mM dithiothreitol, 10 mM MgCl₂, 0.5 unit/ml malate dehydrogenase, 0.33 mM CoA, 0.14 mM NADH and 5 mM ATP for 10 min at room temperature. The absorbance at 340 nm was measured with TECAN Infinite spectrophotometer.

2.6 Quantification of ACh by mass spectrometry

ACh content was measured and analysed following the method as described (Fu et al., 2008). PC12 cells were transfected and stimulated in the medium containing NGF and 40 μ M AChE inhibitor eserine for 24 h. The stimulation medium was collected and centrifuged at 1200 rpm for 10 min. The supernatant was transferred into a 1.5 ml amber autosampler vial (Alpha Analytical, Singapore) and placed into Agilent 6490 UHPLC-QqQ mass spectrometry. A ZORBAX HILIC column (2.1 \times 100 mm, 3.5 μ m, Agilent) was used for the separation. The mobile phase was a mixture of 10 mM ammonium formate aqueous solution and acetonitrile (all from Sigma). The column was eluted isocratically at a flow rate of 0.2 ml/min. The injection volume was 1 μ L. Analyses were carried out in the positive ion mode using multiple reaction monitoring (MRM) with the mass transition (m/z) 146->87. All data were collected and processed with the Agilent MassHunter Workstation Data Acquisition software and QUANTITATIVE Analysis software.

2.7 Statistical analysis

Data were expressed as standard errors of the mean (\pm SEM). Statistical significance was determined using Student's t-test. N. S., not significant; *p < 0.05; **p < 0.01; ***p < 0.001.

3. RESULTS

3.1 BNIP-H binds ACL to promote neurite outgrowth

3.1.1 BNIP-H promotes neurite outgrowth

As BNIP-H could enhance neurite extension of hippocampal neurons (Aoyama et al., 2009), my study mainly focused on how BNIP-H regulated this process. To better understand that, I employed rat adrenal pheochromocytoma PC12 cells that have been widely used for studying neuronal differentiation (Greene, 1978), and in which properties of BNIP-H have previously been characterized (Buschdorf et al., 2008; Buschdorf et al., 2006). PC12 cells would protrude neurites and express neuro-specific markers upon NGF stimulation (Damon et al., 1990; Das et al., 2004; Perrone-Bizzozero et al., 1993). Normally, the stimulation of PC12 cell neurite outgrowth was dependent on the concentration of NGF. For example, 100 ng/ml of NGF was sufficient to induce neural outgrowth while 20 ng/ml was not as potent as 100 ng/ml in neurite induction (Mark et al., 1995).

I chose the overexpression system to study the role of BNIP-H in neurite outgrowth. As BNIP-H has the ability to enhance neurite outgrowth, gain of function may potentiate this process compared to the control. Treating PC12 cells with sub-optimal concentration (20 ng/ml) of NGF barely induced neurite outgrowth over the 6-24 h period (Figure 3-1 A, indicated by red arrow). However, this deficiency was rescued by BNIP-H overexpression (Figure 3-1 B, indicated by red arrow). This proneurite growth effect of BNIP-H in PC12 cells is similar to primary hippocampal neuron (Aoyama et al., 2009). Figure 3-2 shows the immunostaining for specific neuro-marker Tuj1 (Lee et al., 1990). The cell overexpressing BNIP-H induced longer neurite growth and more Tuj1 expression, especially along the neurite, confirming that this morphogenetic change was associated with neuronal differentiation (Figure 3-2).

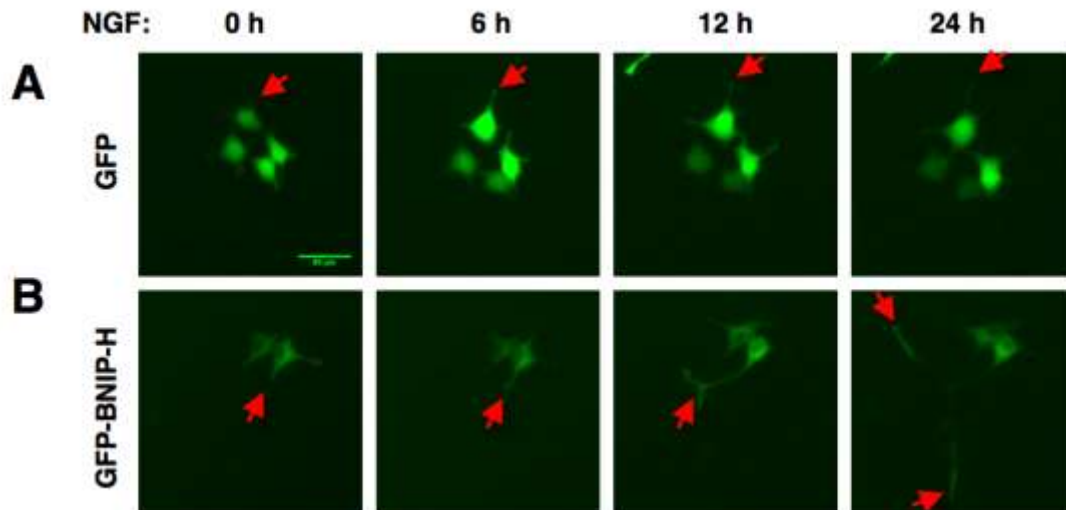


Figure 3-1 BNIP-H promotes PC12 cell neurite outgrowth.

A. Neurite outgrowth of wild type cell. PC12 cells were transfected with GFP empty vector. The neurite outgrowth process was imaged immediately after 20 ng/ml NGF stimulation. The red arrows indicate the localization of neurite tips within 24 h period. B. Neurite outgrowth of BNIP-H overexpressing cell. PC12 cells were transfected with GFP-BNIP-H. The red arrows indicate the neurite outgrowth upon 20 ng/ml NGF stimulation. Scale bar, 50 μ m.

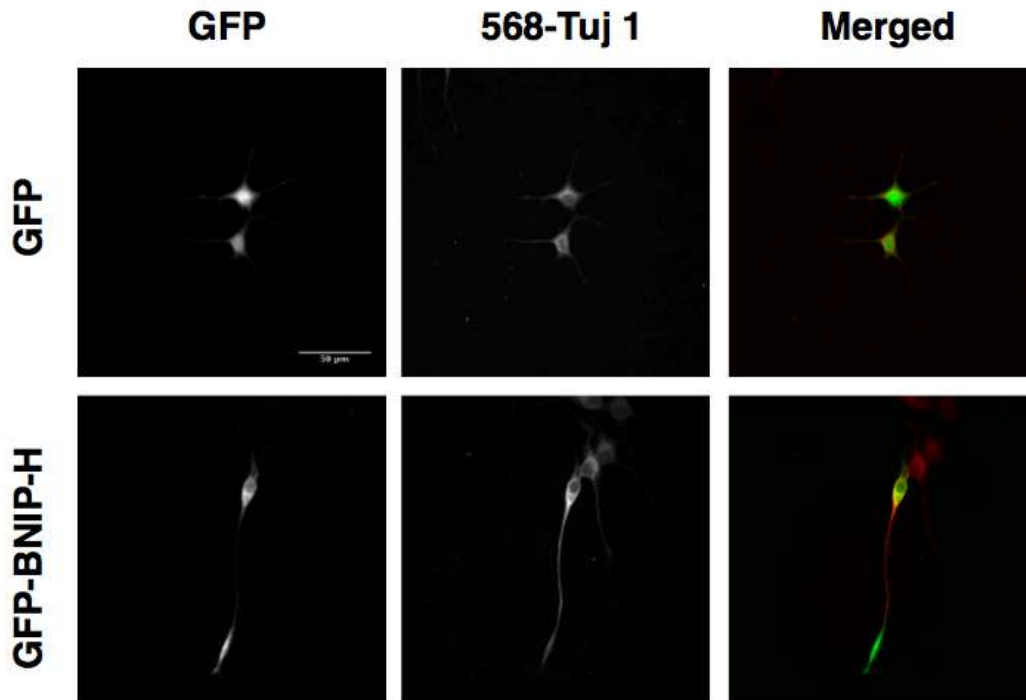


Figure 3-2 BNIP-H enhances neuronal differentiation of PC12 cell.

Transfected cells were immunostained with an antibody against Tuj 1. Images are maximum intensity projections of z stacks. Scale bar, 50 μ m.

3.1.2 ACL is identified as a novel BNIP-H binding partner

The above data suggested that BNIP-H might have pro-neurite outgrowth function in PC12 cells. However, the molecular mechanism underlying is largely unknown. Besides, mutations of BNIP-H result in diverse phenotypes (Table 1-1), suggesting that BNIP-H may take part in multiple signaling pathways in nervous system. I hypothesized that BNIP-H might regulate neurite growth through a novel signaling pathway. To identify the potential signaling pathway related to BNIP-H, I employed proteomics pulldown assay to identify its putative cellular binding partners. As Neuro2A cells are much more easier to be transfected than PC12 cells, Neuro2A cell was used for sufficient BNIP-H transfection. Co-IP of FLAG-tagged BNIP-H from Neuro2A cells revealed a 120 kDa protein (Figure 3-3 A, indicated by arrow), identified as ACL by mass spectrometry analyses. To confirm this, the pull down assay

was analyzed by Western blotting with an ACL specific antibody where ACL was detected in BNIP-H pull down complex (Figure 3-3 B). Co-IP using an antibody specific to BNIP-H also pulled down endogenous ACL from PC12 cells (Figure 3-4), validating their physiological interaction in vivo.

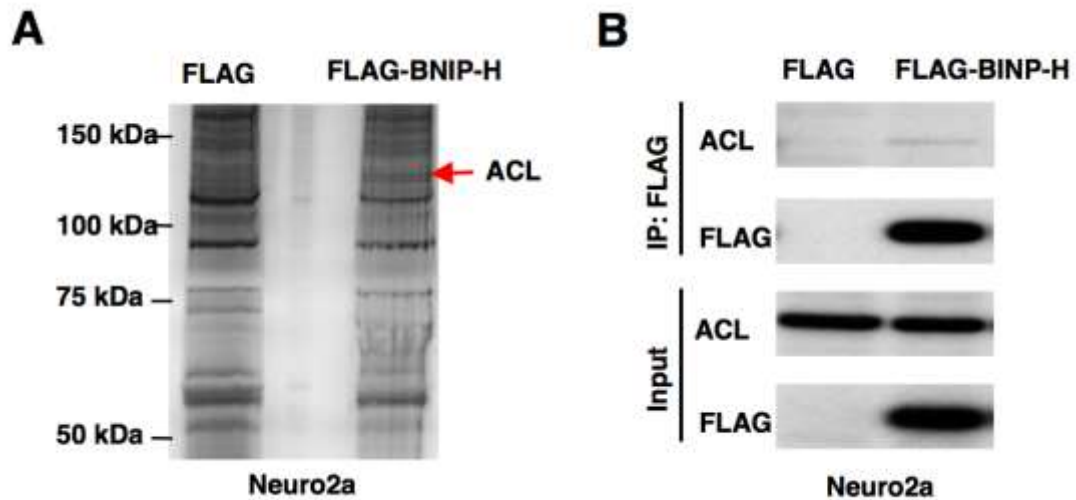


Figure 3-3 BNIP-H interacts ACL in Neuro2A cells.

A. Overexpressed BNIP-H pulled down ACL. FLAG-BNIP-H protein was pulled down by M2 beads, and the protein band indicated by arrow was identified by mass spectrometry analyses. B. The identification was confirmed by western blotting with antibody against ACL.

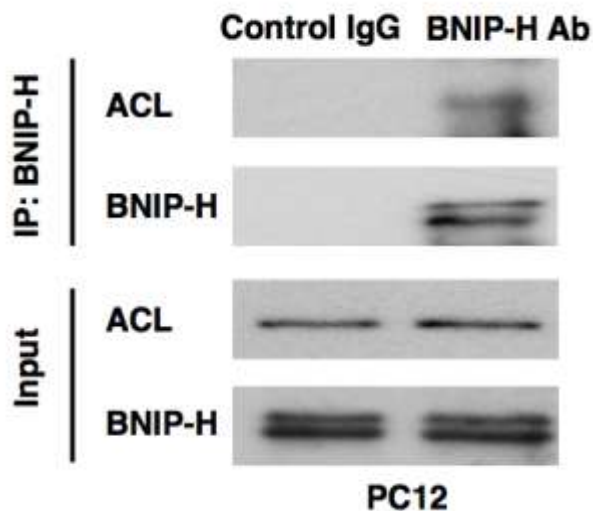
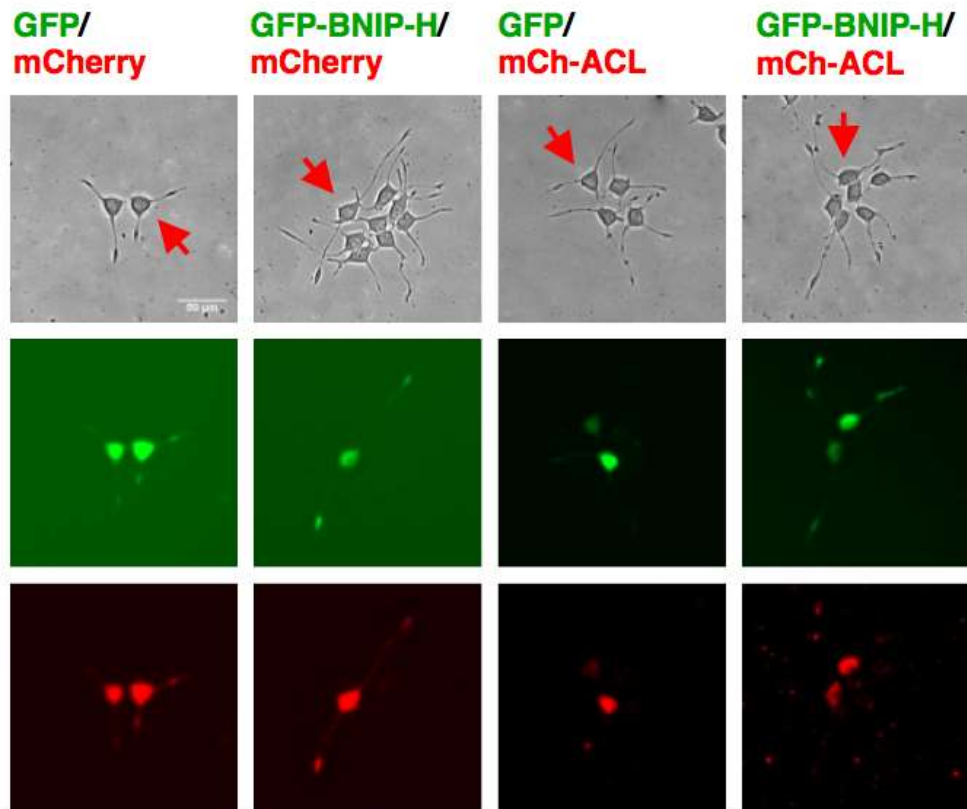
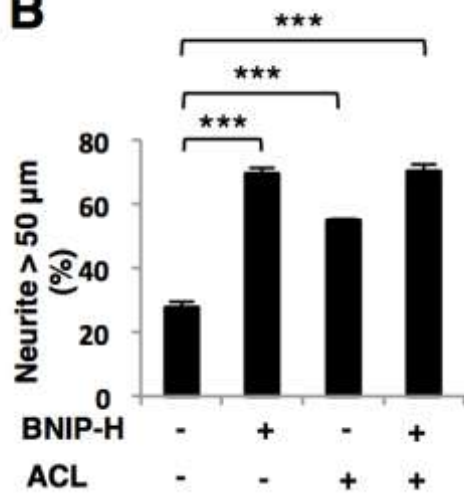


Figure 3-4 Endogenous BNIP-H interacts with ACL in PC12 cells.

Endogenous BNIP-H protein was pulled down by polyclonal BNIP-H antibody. The ACL was detected in BNIP-H pull down complex. Goat IgG protein was used as the control.

3.1.3 BNIP-H and ACL both promote neurite outgrowth

Next, I studied whether BNIP-H and ACL had similar effect on regulating neurite outgrowth. At first, the effect of ACL on neurite outgrowth was investigated by gain of function study (Figure 3-5 A). Under 20 ng/ml of NGF stimulation for 24 h, ACL exerted the similar effect of pro-neurite growth as BNIP-H. BNIP-H and ACL both increased the population of cells with neurite longer than 50 μm , from 27.7% (control) to 69.5% and 55% respectively (Figure 3-5 B). However, the whole profile of neurite length showed that, BNIP-H overexpression induced 32.5% cells to protrude neurite longer than 100 μm , while ACL only induced 15.2%, indicating that ACL is less potent than BNIP-H on promoting neurite growth (Figure 3-5 C). Interestingly, overexpression of BNIP-H and ACL together did not augment the effect by BNIP-H, suggesting that these two proteins could have converged to a saturating step and might function in the same signaling pathway to regulate neurite outgrowth.

A**B**

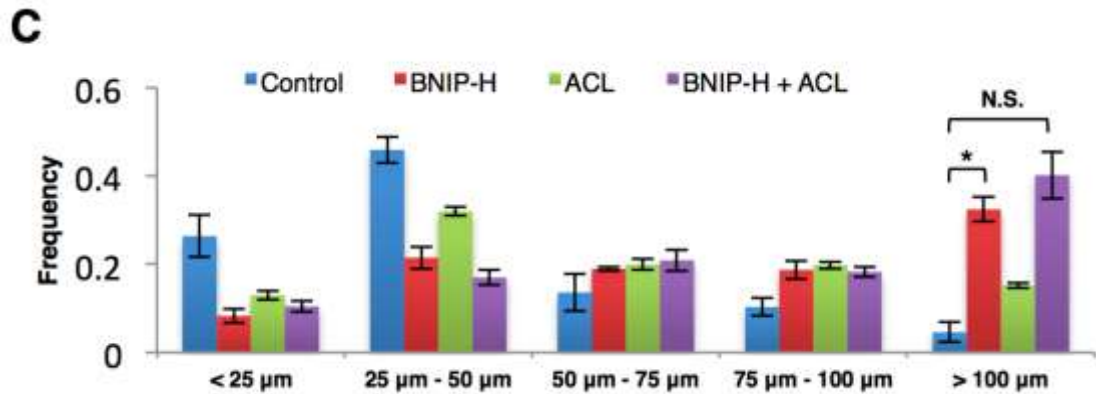


Figure 3-5 Overexpression of BNIP-H and ACL enhance PC12 neurite growth.

A. Neurite outgrowth of BNIP-H and ACL overexpressing cell. The red arrows indicate the transfected cells. B. Quantification of neurite outgrowth. Percentage (%) of cells with neurites longer than 50 μm is presented. C. Quantification of neurite outgrowth. Percentage (%) of cells with different neurite lengths is presented. For all quantification in this figure, n = 50-100 cells/category from three experiments (*p < 0.05; **p < 0.01; ***p < 0.001; N. S., not significant). mCh = mCherry. Scale bar, 50 μm.

As 20 ng/ml NGF itself was not sufficient to induce neurite outgrowth in PC12 cells, this treatment regime was used in subsequent overexpression experiments to determine the potentiation effects. When the wild type cells were treated with 100 ng/ml NGF, the cells would protrude normal neurite. This optimal NGF dose was used in BNIP-H and ACL knockdown experiments to show the neurite deficiency caused by defect of BNIP-H and ACL. Consistent with the overexpression results, knockdown of BNIP-H or ACL alone using two independent shRNA constructs (RFP-shRNA BNIP-H 1 and 2; GFP-shRNA ACL 1 and 2) inhibited neurite outgrowth despite being under the optimal dose of NGF stimulation (Figure 3-6 and 3-7), suggesting that BNIP-H and ACL both are crucial for neurite growth. Here, the BNIP-H shRNAs are co-transcribed with internal ribosome entry site (IRES)-RFP, so the expression of RFP indicates the transfection of shRNA construct. Similarly, the ACL shRNA transfection is indicated by GFP protein expression.

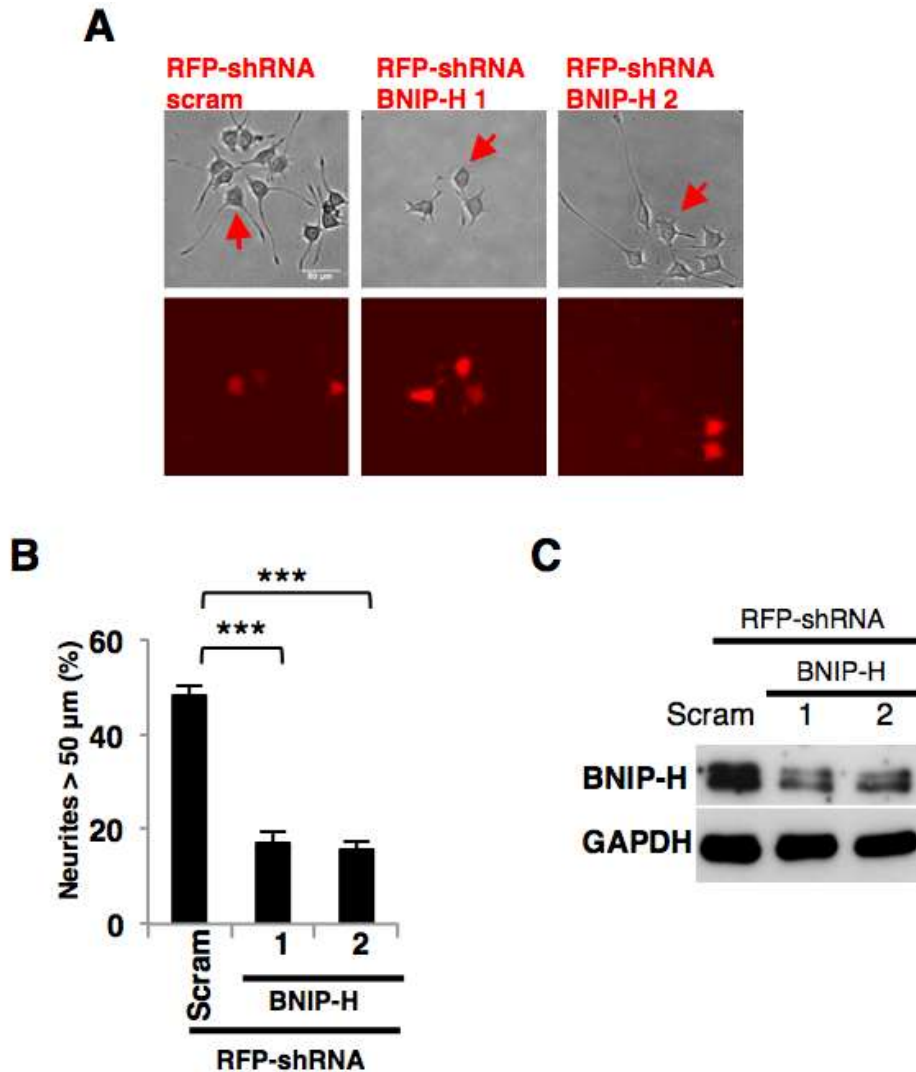


Figure 3-6 Knockdown of BNIP-H inhibits PC12 neurite outgrowth.

A. Neurite outgrowth of BNIP-H knockdown cells. The red arrows indicate the shRNA-transfected cells. B. Quantification of neurite outgrowth. Percentage (%) of cells with neurites longer than 50 μm is presented. n = 50-100 cells/category from three experiments (**p < 0.01). C. Detection of knockdown efficiency by western blotting. The blots show the protein levels of endogenous BNIP-H and GAPDH. Scale bar, 50 μm.

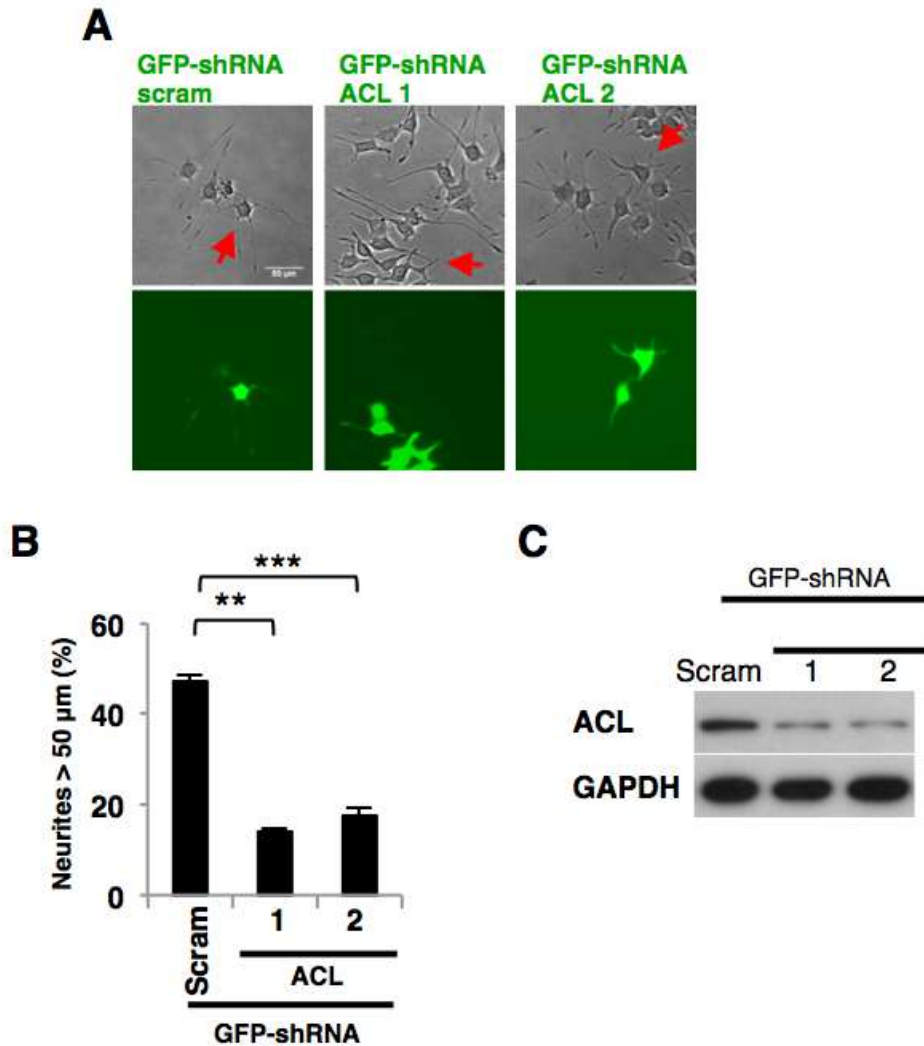


Figure 3-7 Knockdown of ACL inhibits PC12 neurite outgrowth.

A. Neurite outgrowth of ACL knockdown cells. The red arrows indicate the shRNA-transfected cells. B. Quantification of neurite outgrowth. Percentage (%) of cells with neurites longer than 50 μm is presented. $n = 50\text{-}100$ cells/category from three experiments (** $p < 0.01$; *** $p < 0.001$). C. Detection of knockdown efficiency by Western blotting. The blots show the protein levels of endogenous ACL and GAPDH. Scale bar, 50 μm .

3.1.4 BNIP-H and ACL require each other for neurite outgrowth

The above data demonstrated that BNIP-H and ACL are both important for neurite outgrowth. In addition, BNIP-H interacted with ACL and double overexpression of both molecules did not show synergic effect on neurite growth, suggesting that these

two molecules might act in the same signaling pathway to regulate neural outgrowth. To further confirm that BNIP-H and ACL cooperate to regulate neurite growth and determine the hierarchical relationship of BNIP-H/ACL, BNIP-H and ACL effects on neurite growth were examined by overexpressing one but knockdown of the other (Figure 3-8 and 3-9). In BNIP-H knockdown cells, the deficiency in neurite outgrowth was completely rescued by the re-introduction of a synonymous mutant of BNIP-H (GFP-BNIP-H^{re}), which could not be recognized by shRNA of BNIP-H (RFP-shRNA BNIP-H 2) (Figure 3-8). However, overexpressing ACL could not restore the ability of neurite growth reduced by the loss of BNIP-H, implying that ACL requires BNIP-H to elicit its pro-neurite outgrowth effect. In comparison, under ACL knockdown, re-introduction of an un-suppressible ACL (mCherry-ACL^{re}) fully rescued the neurite outgrowth (Figure 3-9). However, overexpression of BNIP-H also failed to enhance neurite growth in these ACL knockdown cells. These data strongly indicated that both BNIP-H and its binding partner ACL act together to enhance neurite outgrowth. As the result suggested that ACL requires BNIP-H to enhance neuronal outgrowth, intracellular disposition of these two molecules would be investigated in the following section.

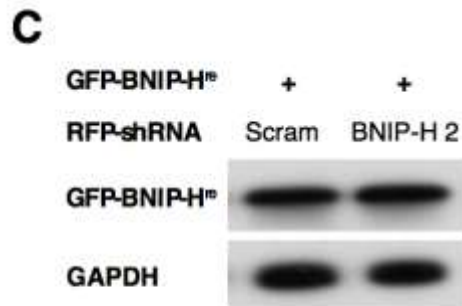
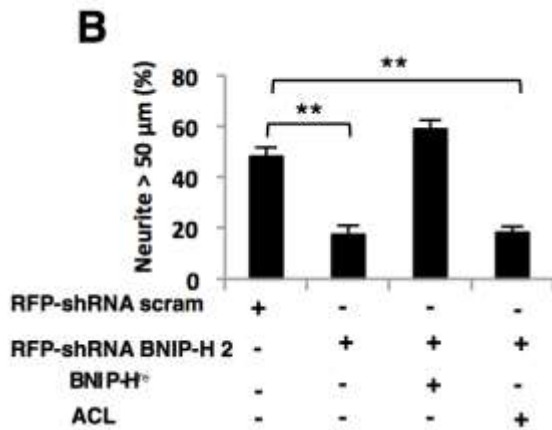
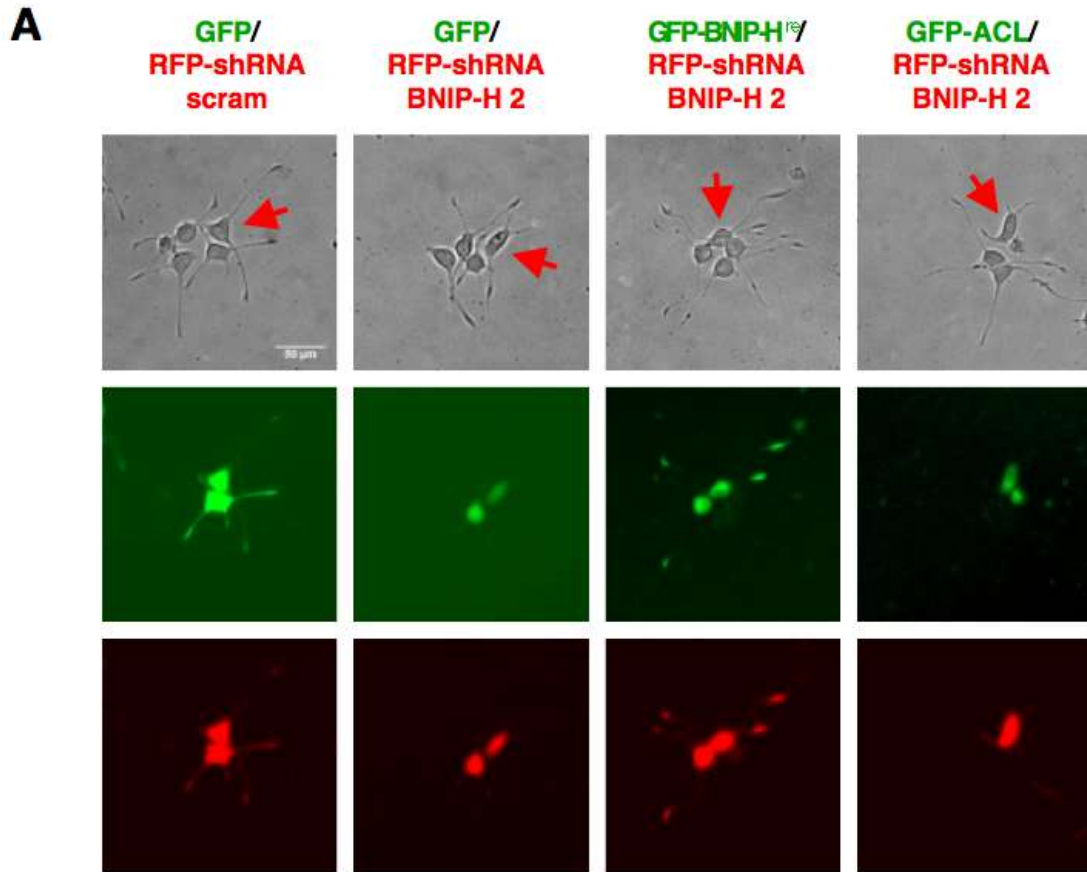


Figure 3-8 ACL fails to restore the neurite outgrowth reduced by BNIP-H knockdown.

A. PC12 neurite outgrowth with BNIP-H knockdown and rescue. The red arrows indicate the transfected cells. B. Quantification of neurite outgrowth. Percentage (%) of cells with neurites longer than 50 μm is presented. n = 50-100 cells/category from three experiments (**p < 0.01). C. Detection of the synonymous mutant of BNIP-H by western blotting. The blots show the protein levels of GFP-BNIP-H^{re} and GAPDH. Scale bar, 50 μm.

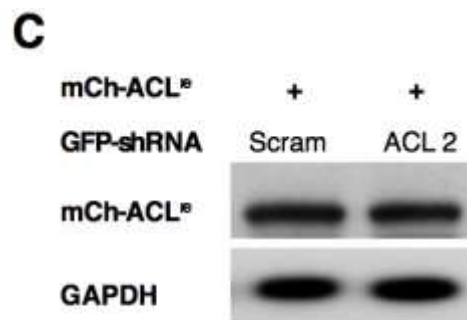
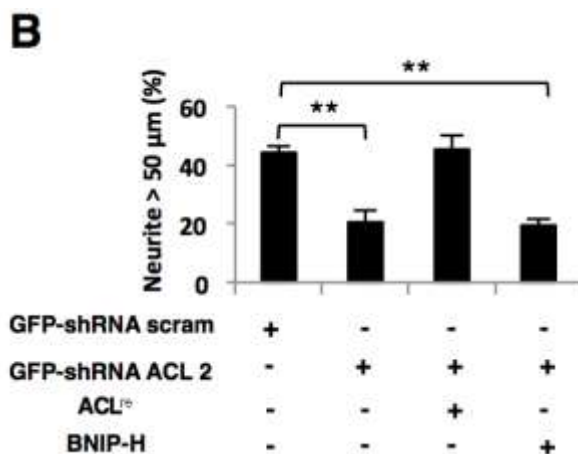
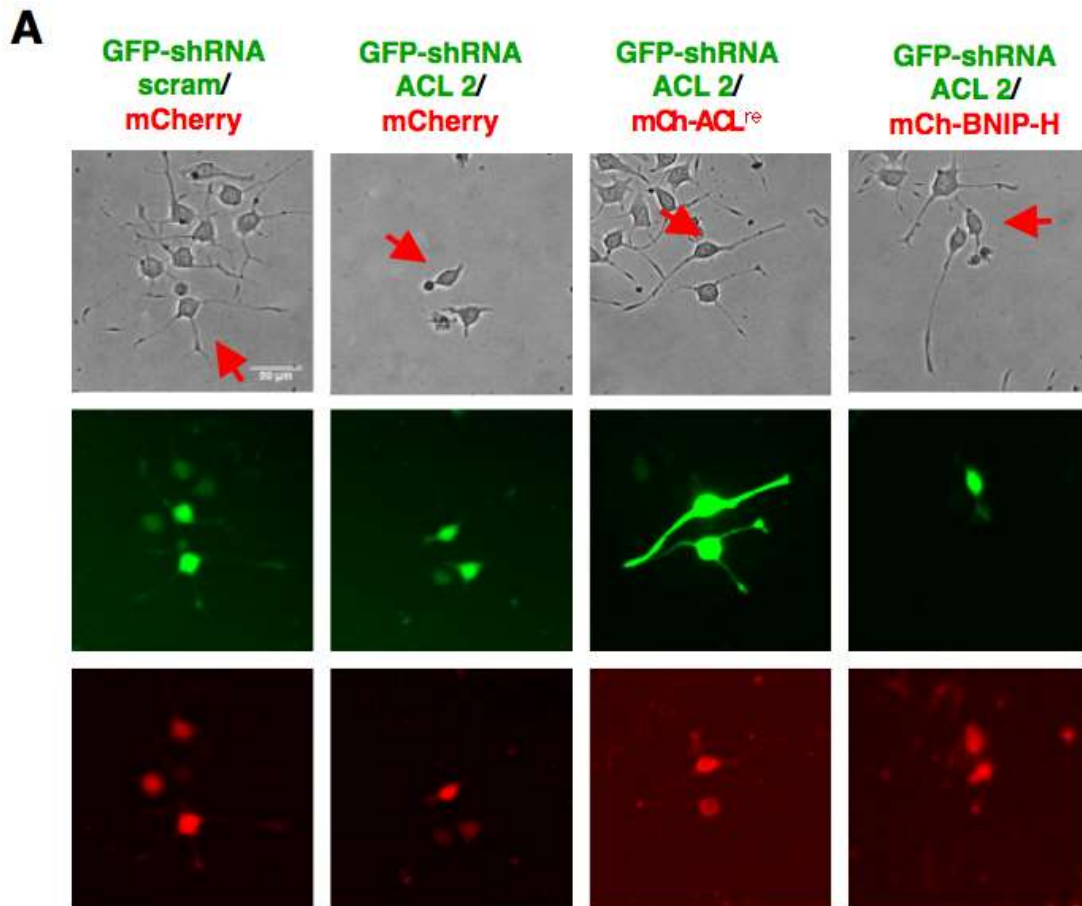


Figure 3-9 BNIP-H fails to restore the neurite outgrowth reduced by ACL knockdown.

A. PC12 neurite outgrowth with ACL knockdown and rescue. The red arrows indicate the transfected cells. B. Quantification of neurite outgrowth. Percentage (%) of cells with neurites longer than 50 μm is presented. n = 50-100 cells/category from three experiments (**p < 0.01). C. Detection of the synonymous mutant of ACL by western blotting. The blots show the protein levels of mCherry-ACL^{re} and GAPDH. mCh = mCherry. Scale bar, 50 μm.

3.2 BNIP-H transports ACL via kinesin-1

3.2.1 BNIP-H and ACL co-traffic along the neurite

BNIP-H has previously been shown to interact with KLC1 and traffic along the neurite (Aoyama et al., 2009), but the physiological function of the BNIP-H trafficking remains unknown. It was hypothesized that BNIP-H might transport ACL along the neurite by KLC1. To test this hypothesis, I studied the cellular localization and dynamics of BNIP-H and ACL in differentiating PC12 cells. By time-lapse confocal microscopy, BNIP-H and ACL were found to co-localize at granular structures (indicated by arrowheads) and most profoundly co-traffic in an anterograde manner along the neurites (Figure 3-10) at approximately 1 $\mu\text{m/s}$, consistent with a kinesin-based microtubule event, and also with the previous report for the trafficking speed of BNIP-H (Aoyama et al., 2009). Furthermore, immunostaining was employed to study the intracellular localization of BNIP-H and ACL. GFP-ACL showed diffused distribution in the cytoplasm while mCherry-BNIP-H displayed as puncta, which might be caused by the reason that the cytosolic pool of overexpressed GFP-ACL protein obscured the signal of granule bound pool. Therefore, saponin permeabilization before fixation was used to deplete the cytosolic pool of ACL. By using this method, it was shown that that GFP-ACL and mCherry-BNIP-H co-localized in the same granules and were located on the microtubule track (Figure 3-11), implying that BNIP-H and ACL undergo microtubule-based transport along the neurites.



Figure 3-10 BNIP-H and ACL co-traffic in the PC12 neurite.

Representative confocal images of neurite at 100 × magnification are shown juxtaposed with nucleus at left and neurite terminal at right (time lapse as indicated). Arrowheads indicate the co-trafficking granules. mCh = mCherry. Scale bar, 10 μm.

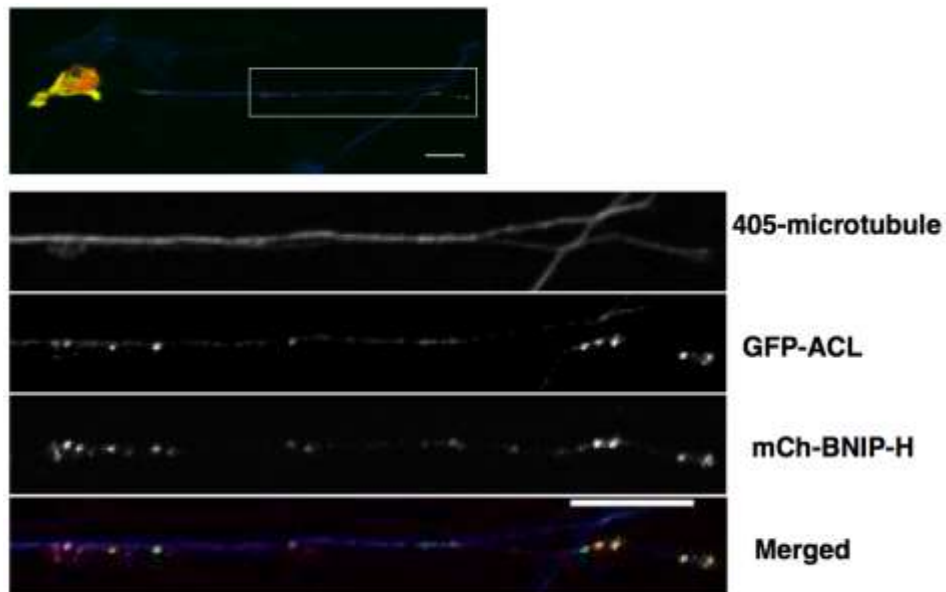


Figure 3-11 BNIP-H and ACL co-localize along the microtubule of PC12 neurite.

The cells were permeabilized with saponin before fixation to deplete the cytosolic pool of ACL. And then the cells were immunostained with an antibody against β -tubulin. Insets show the magnified view of the boxed area. Scale bar, 10 μm.

3.2.2 BNIP-H binds with KLC1 through “WQ-WED” motif

As BNIP-H is known to interact with kinesin motor, BNIP-H was hypothesized to act as a scaffold to mediate trafficking of ACL on kinesin. To test this, I examined the binding of BNIP-H to KLC1. Three amino acids WED (aa 118-120, as indicated in Figure 3-12 A) have been shown to be important for BNIP-H and KLC1 binding (Aoyama et al., 2009). However, Aoyama et al. used bacterial expressed BNIP-H and mutants to pull down mammalian cell expressed KLC1 (Aoyama et al., 2009). The posttranslational modification of BNIP-H expressed in prokaryotic cells might be different from the one expressed in eukaryotic cells, so the binding between BNIP-H and KLC1 was examined again by using HEK293T as surrogate cells, conveniently used for verification of protein-protein interactions. As shown in Figure 3-12 B, BNIP-H 3A (replacing of WED motif with alanines) caused only partial inhibition of its binding with KLC1. Based on recent prediction (Dodding et al., 2011), two other amino acids WQ (aa 19-20, as indicated in Figure 3-12 A) might also be involved in the interaction between BNIP-H and KLC1. Indeed, BNIP-H 2A (replacing of WQ with alanines) also led to partial loss in binding to KLC1 while the interaction was completely blocked when both WQ and WED motifs were mutated (BNIP-H 5A) (Figure 3-12 B). Consistently, live imaging analysis revealed that mutation of WQ-WED reduced the anterograde transport of BNIP-H along the neurites (Figure 3-13). This lesser granular movement of BNIP-H reflected the impaired ability of BNIP-H 5A to associate with and co-transport on kinesin-1.

A BNIP-H amino acids sequence
 --RDE**WQ**DED----ELE**WED**DTP--
 19-20 118-120

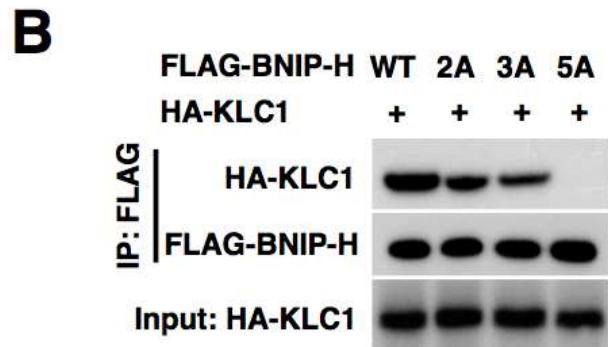
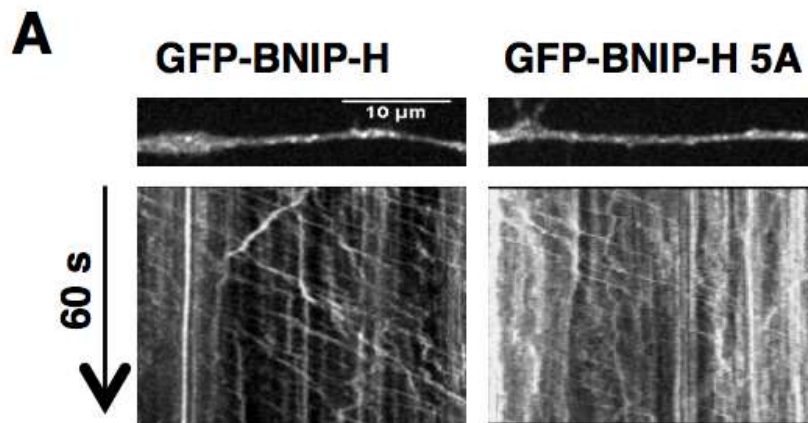


Figure 3-12 "WQ-WED" mutations abolish BNIP-H and KLC1 binding in 293T cells.
 A. BNIP-H amino acids sequence shows the localization of "WQ-WED" sites. B. The interaction between BNIP-H and KLC1. FLAG-BNIP-H mutants: 2A, WQ to AA; 3A, WED to AAA; 5A, WQ-WED to AA-AAA.



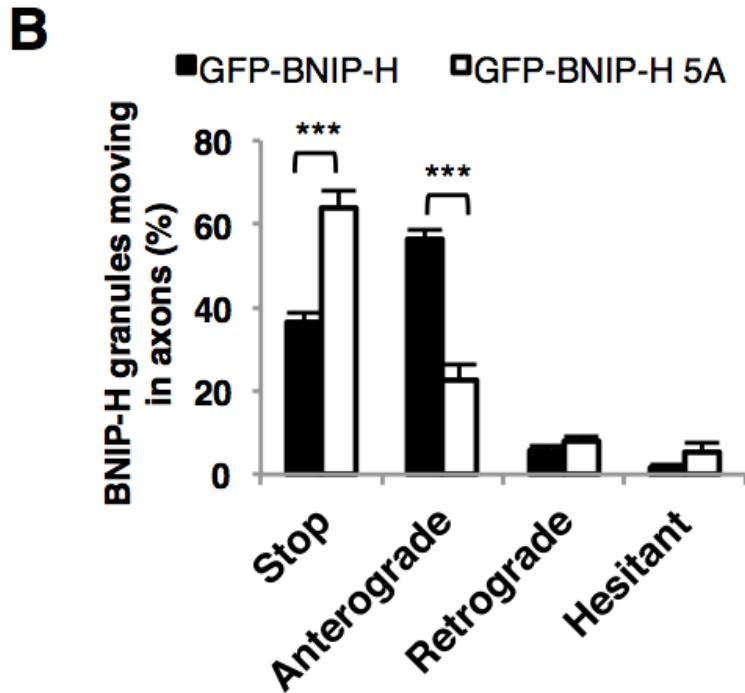


Figure 3-13 Mobility of BNIP-H 5A is reduced in PC12 neurite.

A. The mobility of BNIP-H and BNIP-H 5A along the neurites. The upper images are pictures of GFP-BNIP-H from movies recorded with confocal microscope with nucleus at left and neurite terminal at right. The lower images show the kymographs of the movies (time as indicated). B. The graph indicates percentages (%) of BNIP-H granules moving in anterograde, retrograde, hesitant, or stationary manners. Cells expressing GFP-BNIP-H (n = 12) and GFP-BNIP-H 5A (n = 11) were quantified (***) p < 0.001). Scale bar, 10 μ m.

3.2.3 BNIP-H functions as a scaffold to traffic ACL

The above section has indicated that BNIP-H interacts with KLC1 through the “WQ-WED” motif. Next, I examined whether BNIP-H indeed bridges ACL to kinesin-1 to form a functional complex. To prove this, the effect of increasing amounts of BNIP-H on the binding of ACL to KLC1 was investigated in 293T cells. The result showed that while the control cells exhibited detectable level of interaction between ACL and KLC1, increasing amount of BNIP-H enhanced their binding to a maximum, before it declined to the control level (Figure 3-14). This observation revealed that an optimal level of BNIP-H is required to bridge their interaction. With excessive amount of

BNIP-H, binary BNIP-H/ACL and BNIP-H/KLC1 complexes would be formed, instead of the ternary complex ACL/BNIP-H/KLC1. Therefore, BNIP-H functions as a scaffold to facilitate ACL interaction with KLC1 in this ternary complex. And then, the BNIP-H 5A mutant that lost the binding with KLC1 was used to study its effect on this ternary complex formation. The results showed that BNIP-H 5A mutant failed to augment the interaction between ACL and KLC1 (Figure 3-15 A), despite the fact that the binding between BNIP-H 5A and ACL remained intact (Figure 3-15 B), further confirming that ACL requires BNIP-H to enhance its binding with KLC1. In addition, the presence of ACL also enhanced the interaction between BNIP-H and KLC1 (Figure 3-15 A), indicating that BNIP-H and ACL function synergistically to promote their assembly with kinesin motor protein.

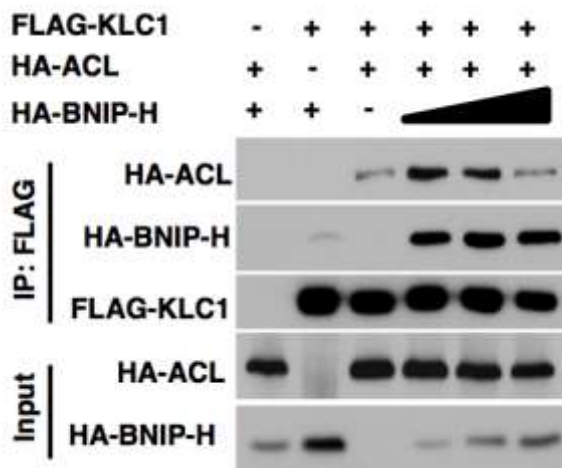


Figure 3-14 BNIP-H promotes KLC1 and ACL association in 293T cells.

The interaction between ACL and KLC1 regulated by the expression level of BNIP-H. The following amounts of each construct were used, as indicated, per well of 6-well plate: 2 μ g of FLAG-KLC1; 2 μ g of HA-ACL; and 0.5, 2, 4 μ g of HA-BNIP-H.

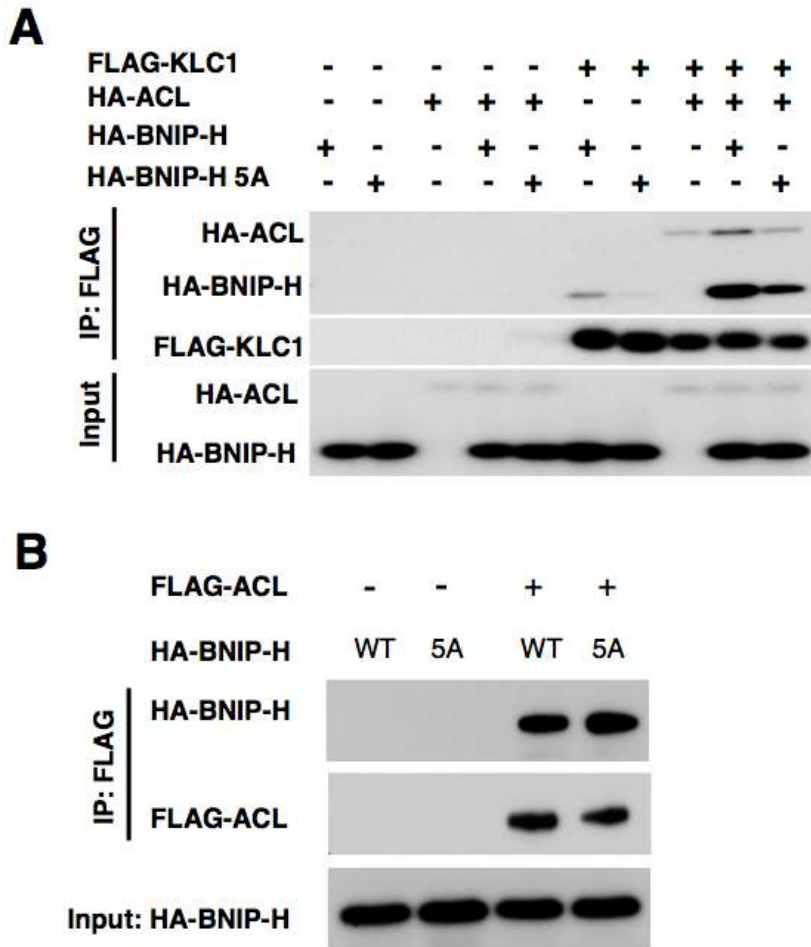


Figure 3-15 BNIP-H 5A reduces KLC1 and ACL association in 293T cells.

A. The interaction between ACL and KLC1 regulated by BNIP-H 5A mutant. B. The interaction between ACL and BNIP-H 5A mutant.

To recapitulate the significance of this functional ACL/BNIP-H/kinesin complex in PC12 cells, live imaging analyses of ACL movements were performed. The result showed that co-expression of BNIP-H and ACL facilitated ACL movement along the neurites of differentiating PC12 cells (Figure 3-16). Under this condition, 45% of mCherry-ACL containing granules exhibited anterograde movement in the neurites while 27% of them did not move. The disposition of ACL granules is similar to BNIP-H as shown in Figure 3-13. In contrast, in the absence of BNIP-H or in the presence of BNIP-H 5A, only 10% of mCherry-ACL containing granules moved from cell bodies to neurite terminals, while over 50% of them were stalled.

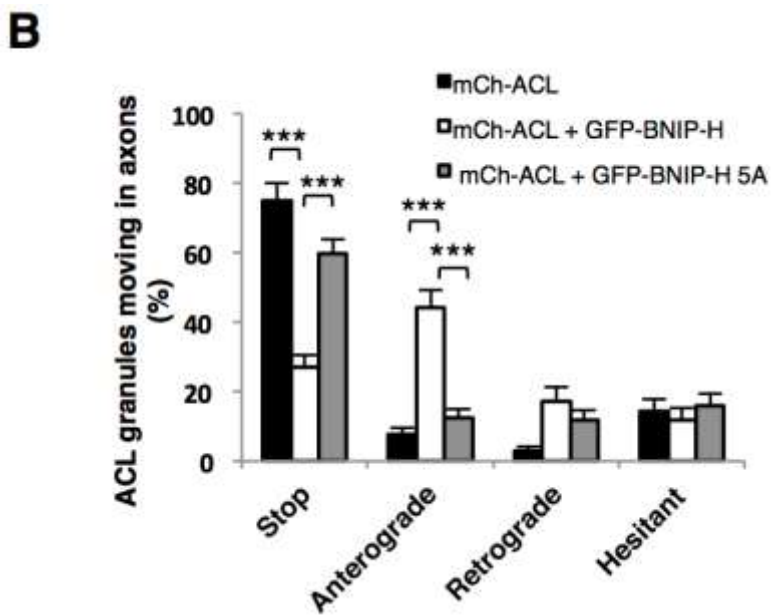
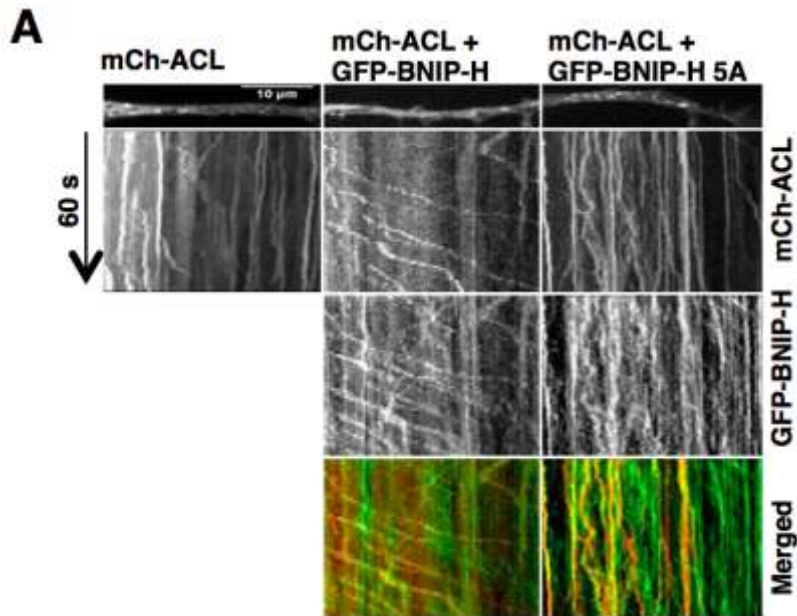


Figure 3-16 BNIP-H 5A reduces ACL trafficking in PC12 neurite.

A. The mobility of ACL along the neurites. The upper images are pictures of mCherry-ACL granules from movies recorded with confocal microscope, with nucleus at left and neurite terminal at right. The lower images show the kymographs of the movies (time as indicated). B. The graph indicates percentages (%) of ACL granules moving in anterograde, retrograde, hesitant, or stationary manners. Cells without BNIP-H overexpression ($n = 15$), with GFP-BNIP-H ($n = 15$) and GFP-BNIP-H 5A ($n = 13$) were quantified ($***p < 0.001$). mCh = mCherry. Scale bar, 10 μ m.

3.2.4 BNIP-H regulates ACL accumulation and dynamics at neurite terminal

Previous studies showed that BNIP-H is concentrated at presynaptic site of neurons (Buschdorf et al., 2006; Hayakawa et al., 2007). My data suggested that BNIP-H facilitates the anterograde trafficking of ACL. To determine whether BNIP-H would progressively accumulate ACL at neurite terminals, I examined the effect of BNIP-H on the distribution of ACL. More ACL molecules were shown concentrated at neurite terminals of BNIP-H overexpressing cells compared to the control (Figure 3-17). Most importantly, overexpression of BNIP-H 5A reduced the accumulation of ACL molecules at these terminals. These results suggested that ACL is transported and accumulated at neurite terminals by BNIP-H. To confirm the dynamics of such process, the FRAP of ACL molecules at neurite terminals was investigated (Figure 3-18). ACL recovered at a significantly higher rate in the presence of wild type BNIP-H ($\tau_{1/2} = 12$ s) compared to the control ($\tau_{1/2} = 37$ s). These results indicated that trafficking of ACL along the neurite and its dynamic disposition at neurite terminals are regulated by BNIP-H.

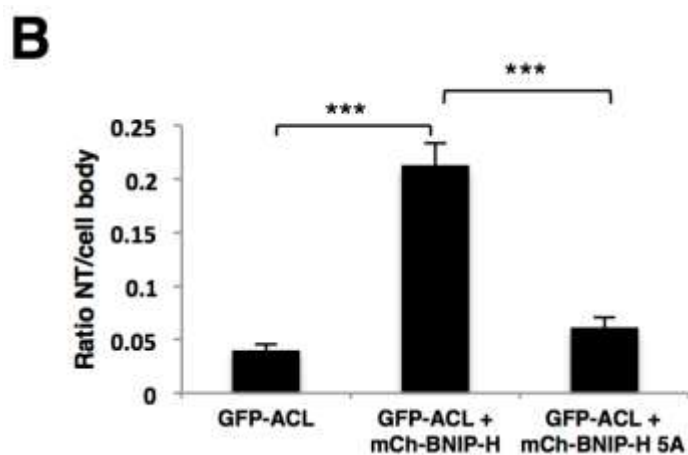
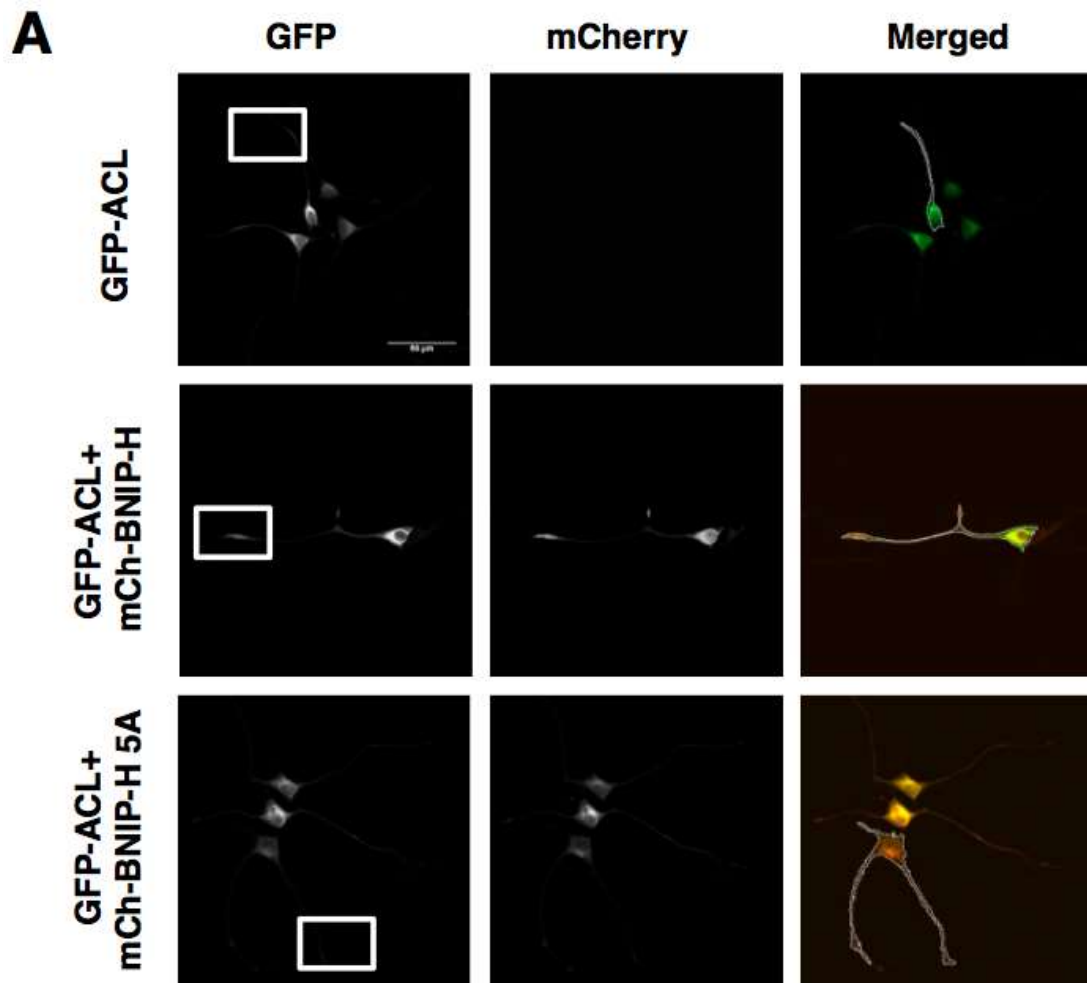


Figure 3-17 BNIP-H accumulates ACL at PC12 neurite terminal.

A. Localization of ACL in PC12 cells. Cells were fixed and imaged with confocal microscope. Images are maximum intensity projections of z stacks. B. Quantification of the ratio of GFP-ACL fluorescent density between the neurite terminal (white boxes) and cell body. Cells without GFP-BNIP-H (n = 10), with GFP-BNIP-H (n = 13) and with GFP-BNIP-H 5A (n = 10) were quantified (***p < 0.001). mCh = mCherry.

Scale bar, 50 μm .

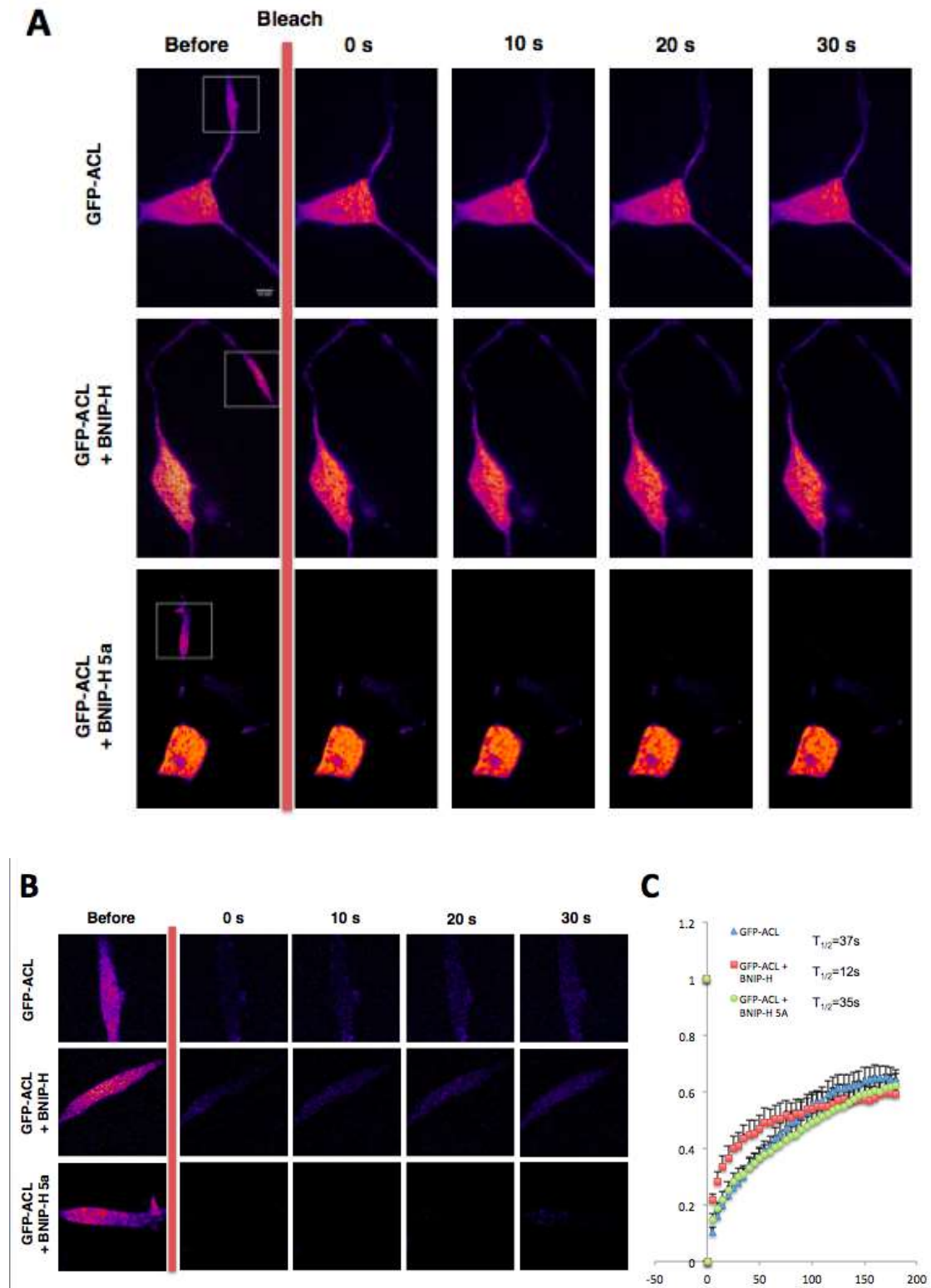


Figure 3-18 BNIP-H enhances ACL dynamics at PC12 neurite terminal.

A. FRAP of GFP-ACL at PC12 neurite terminals. The intensity changes are depicted in

pseudo color. The first row indicates the pre-bleaching images. The recovery images are shown in the subsequent panels. The photobleached ROI is shown as a white box (20 μm \times 20 μm) in the first row. B. Magnified images of neurite terminals inside the white squares in A. C. Quantification of FRAP data.

3.3 BNIP-H requires ACL enzymatic activity for neurite outgrowth

3.3.1 ACL enzyme dead mutant blocks BNIP-H function in neurite outgrowth

In section 3.1, it has been demonstrated that BNIP-H and ACL require each other to regulate neurite growth. In section 3.2, the results suggested that BNIP-H function as a scaffold protein to transport and accumulate ACL at neurite terminals. The next question need to be answered would be how ACL regulates BNIP-H function on neural outgrowth.

ACL is an important cytoplasm enzyme to supply acetyl-CoA (Singh et al., 1976), thus I asked whether the enzymatic activity of ACL was essential for BNIP-H in promoting neurite outgrowth. To test this, I set out to nullify the activity of ACL while retaining its ability to bind BNIP-H. Histidine 760 is the active site of ACL and mutation of ACL His760 (ACL H760A) eliminates its enzyme activity in producing acetyl-CoA (Fan et al., 2012). 293T cells were transfected with BNIP-H, ACL and ACL H760A, and used for ACL enzyme activity assay (Figure 3-19). The results showed that H760A mutation eliminates ACL enzymatic activity, and overexpression of BNIP-H had no effect on ACL activity, either on the endogenous or overexpressed ACL proteins. Co-transfection with ACL H760A blocked the effect of BNIP-H on neurite outgrowth compared to the cells without ACL co-transfection or with wild type ACL (Figure 3-20). Co-IP study showed that ACL H760A has similar binding affinity with BNIP-H as compared to wild type ACL (Figure 3-20 C), suggesting that ACL H760A could function as a dominant negative mutant to block neurite outgrowth through competing with the endogenous ACL for BNIP-H. These results also implied that BNIP-H requires ACL enzymatic activity to promote neurite growth.

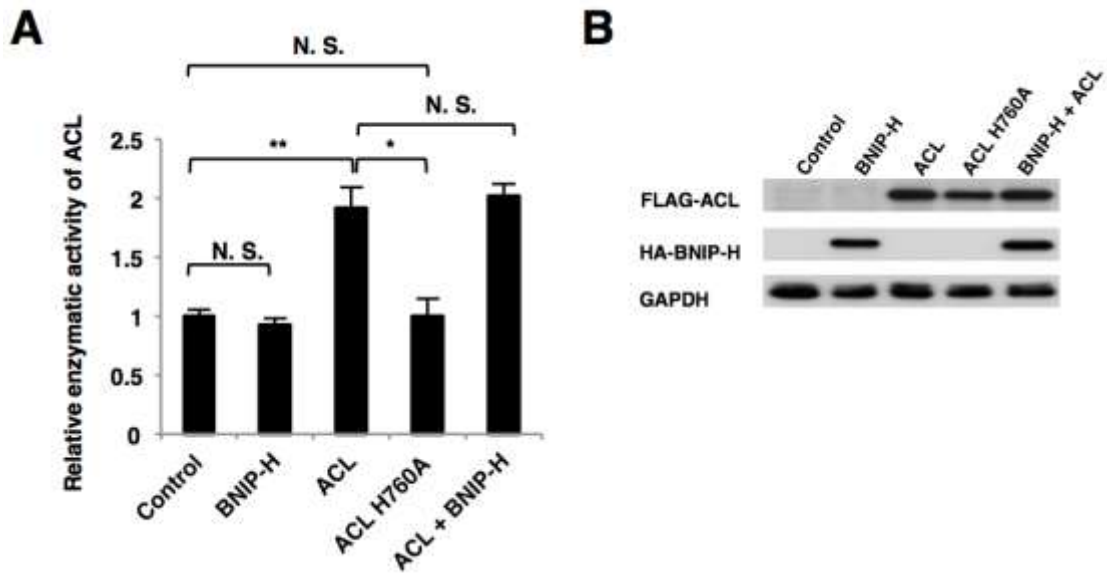


Figure 3-19 H760A is an inactive mutant of ACL and BNIP-H has no effect on ACL enzymatic activity.

A. Quantification of ACL enzymatic activity. 293T cells were transfected with indicated constructs and harvested for analysis after 24 h. Relative enzymatic activity is presented from three experiments. (* $p < 0.05$; ** $p < 0.01$; N. S., not significant). B. Detection of proteins expression levels in A.

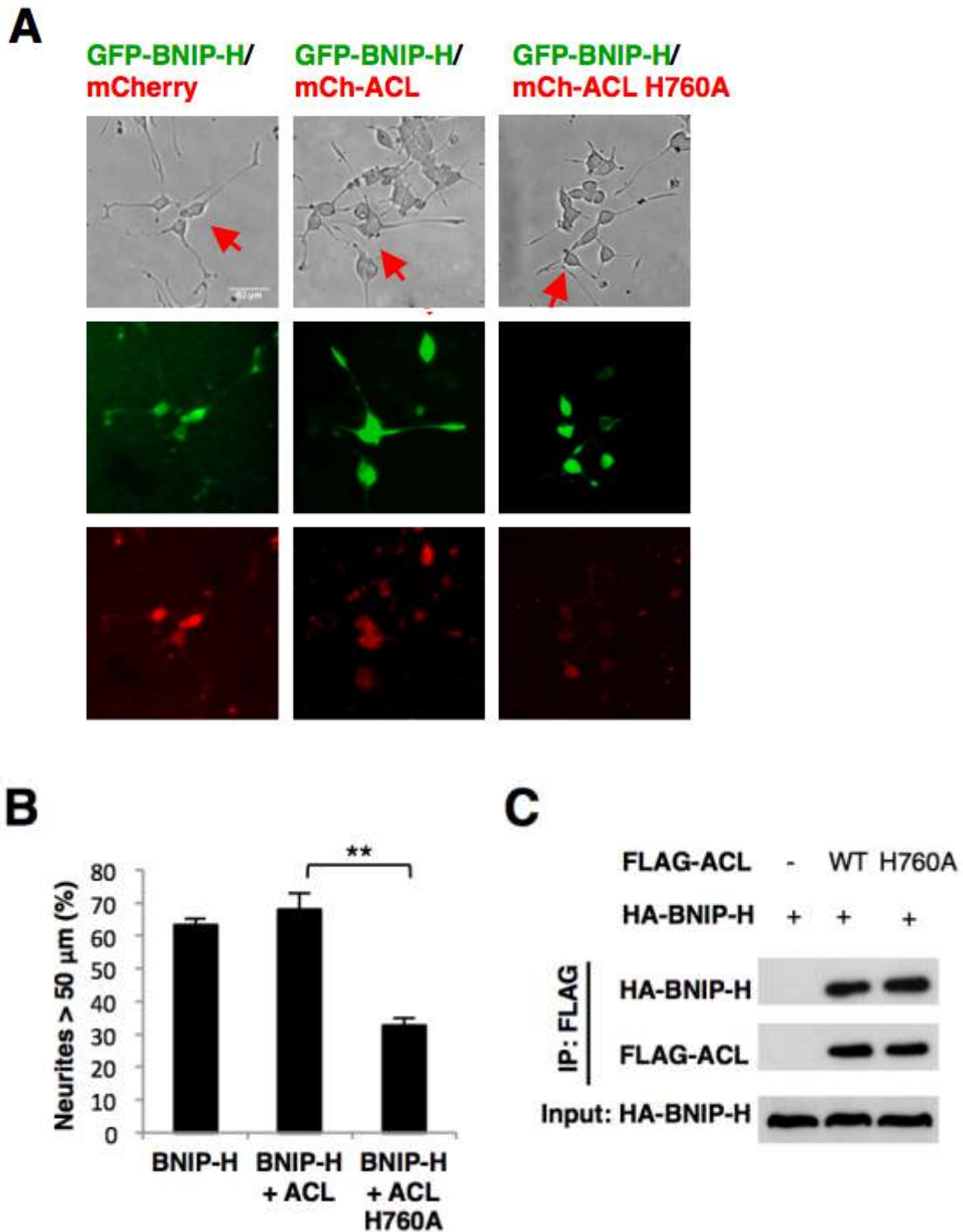


Figure 3-20 ACL H760A blocks BNIP-H function in PC12 neurite outgrowth.

A. Neurite outgrowth of BNIP-H and ACL overexpressing cell. The red arrows indicate the transfected cells. B. Quantification of neurite outgrowth. Percentage (%) of cells with neurites longer than 50 μm is presented. n = 50-100 cells/category from three experiments (**p < 0.01). C. The interaction between ACL H760A and BNIP-H. mCh = mCherry. Scale bar, 50 μm.

3.3.2 BNIP-H requires ACh synthesis for neurite outgrowth

As ACL has been known to regulate lipogenesis, cholesterol and ACh synthesis in cytoplasm (Elshourbagy et al., 1990; Hatzivassiliou et al., 2005; Szutowicz et al., 1982), the next question was that which of these pathway(s) was essential for this process. Treatments with cholesterol synthesis inhibitor lovastatin and fatty acid synthesis inhibitor TOFA did not block neurite outgrowth promoted by BNIP-H (Figures 3-21 and 3-22). However, choline transporter inhibitor hemicholinium-3, which blocked ACh synthesis, significantly inhibited this effect (Figure 3-23). These data suggested that ACh biosynthesis pathway regulated by ACL is required for BNIP-H to promote neurite outgrowth.

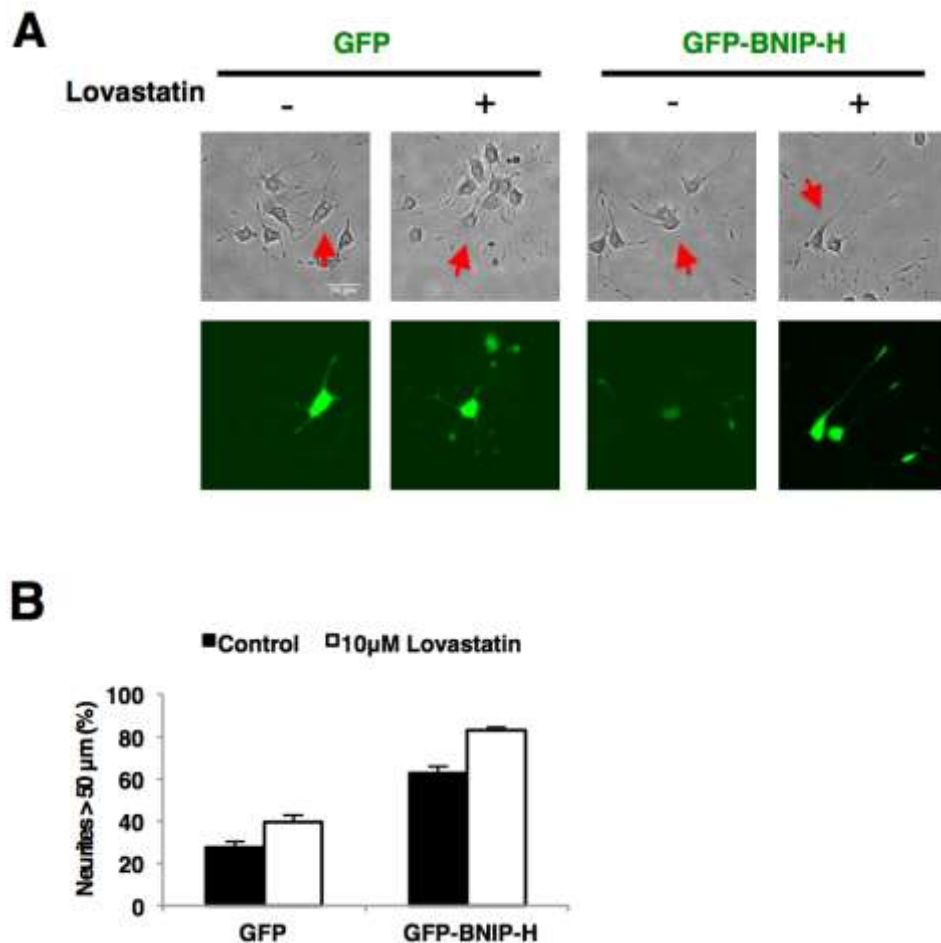


Figure 3-21 BNIP-H-regulated neurite outgrowth is not affected by cholesterol synthesis inhibitor lovastatin in PC12 cells.

A. Neurite outgrowth with lovastatin treatment. The red arrows indicate the

transfected cells. B. Quantification of neurite outgrowth. Percentage (%) of cells with neurites longer than 50 μm is presented. $n = 50-100$ cells/category from three experiments. Scale bar, 50 μm .

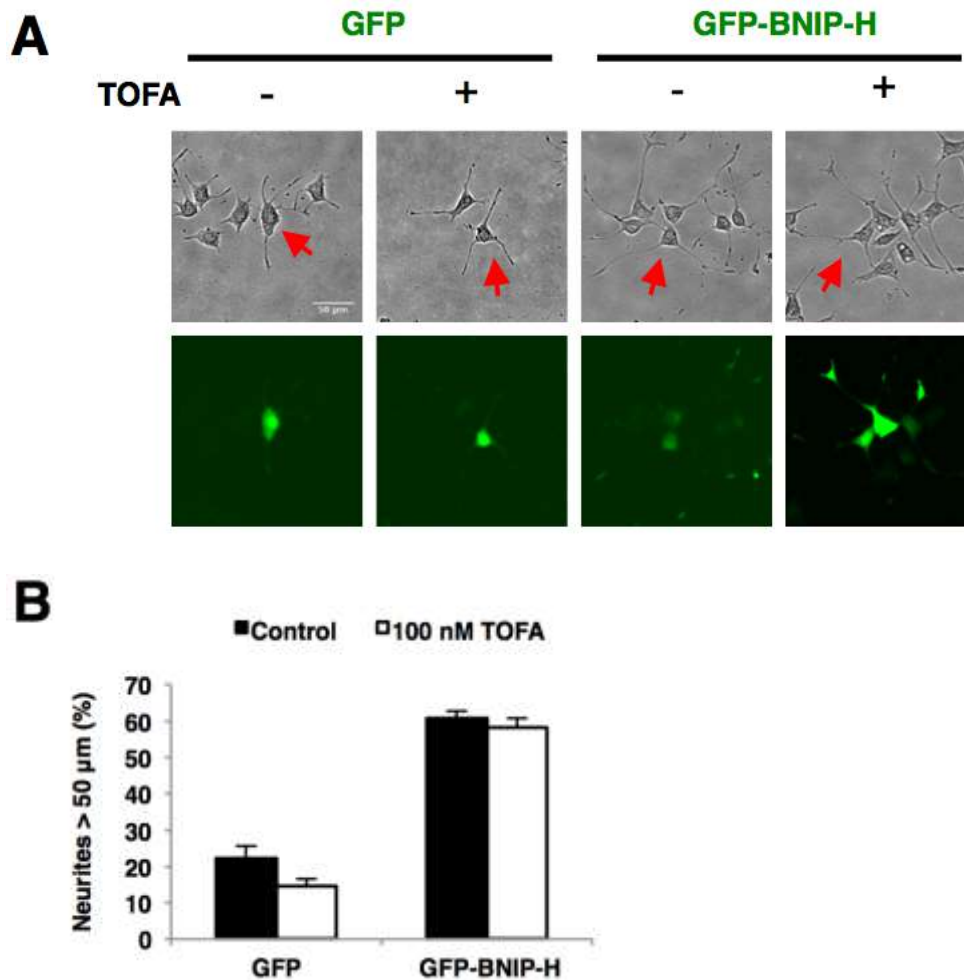


Figure 3-22 BNIP-H-regulated neurite outgrowth is not affected by fatty acid synthesis inhibitor TOFA in PC12 cells.

A. Neurite outgrowth with TOFA treatment. The red arrows indicate the transfected cells. B. Quantification of neurite outgrowth. Percentage (%) of cells with neurites longer than 50 μm is presented. $n = 50-100$ cells/category from three experiments. Scale bar, 50 μm .

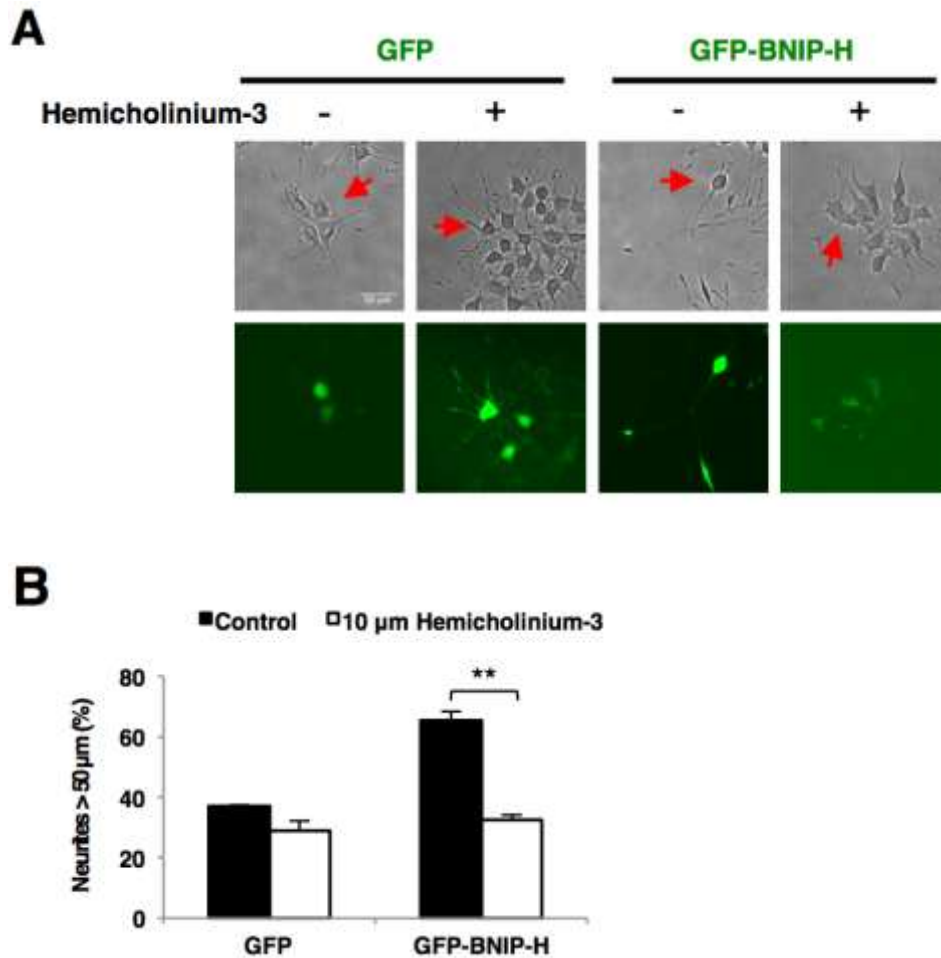


Figure 3-23 BNIP-H-regulated neurite outgrowth is blocked by choline transporter inhibitor hemicholinium-3 in PC12 cells.

A. Neurite outgrowth with hemicholinium-3 treatment. The red arrows indicate the transfected cells. B. Quantification of neurite outgrowth. Percentage (%) of cells with neurites longer than 50 μ m is presented. $n = 50-100$ cells/category from three experiments (** $p < 0.01$). Scale bar, 50 μ m.

3.4 BNIP-H enhances ACh release

3.4.1 BNIP-H and ACL synergistically recruits ChAT at neurite terminal

ChAT combines choline and acetyl-CoA to produce ACh (Nachmansohn and Machado, 1943). Subsequently, ACh is transported into synaptic vesicles by VACHT (Song et al., 1997). Synaptic vesicles filled with ACh are triggered to exocytose neurotransmitters by a transient increase of Ca^{2+} (Jackson and Chapman, 2006)

(Figure 3-24). To investigate whether ChAT could be present in BNIP-H/ACL complex, the interaction among BNIP-H, ACL and ChAT was studied. Remarkably, while overexpression of BNIP-H (Figure 3-25 A) or ACL (Figure 3-25 B) alone did not interact with ChAT, the presence of ACL drastically increased the binding between BNIP-H and ChAT. Similarly, BNIP-H also drastically enhanced the interaction of ACL and ChAT. These results suggested that BNIP-H and ACL might form a complex that synergistically interacts with ChAT. Consequently, immunostaining was performed to study the effect of BNIP-H and ACL on the localization of ChAT in differentiated PC12 cells. The result showed that BNIP-H and ACL facilitated the accumulation of ChAT at the neurite terminals, while BNIP-H or ACL alone had no such effect (Figure 3-26). These data indicated that BNIP-H acts as a functional scaffold to recruit ACh biosynthesis machinery, comprising ACL and ChAT.

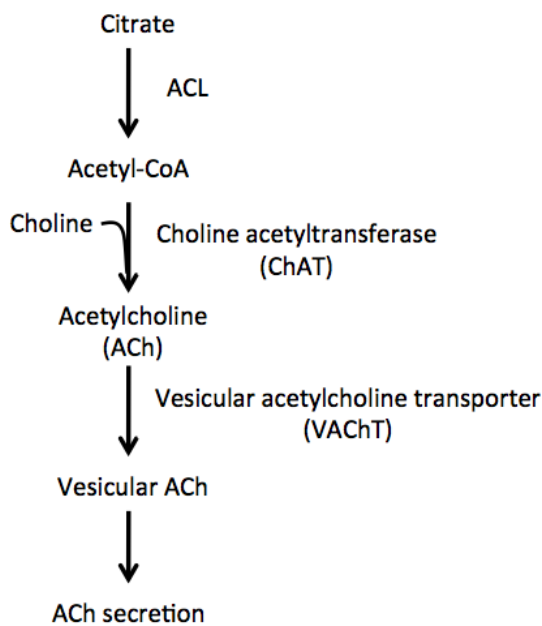


Figure 3-24 Schematic diagram of ACh synthesis and secretion pathway.

At neurite terminals, ACL produces acetyl-CoA and ChAT combines acetyl-CoA and choline to synthesize ACh. Cytosolic ACh is transported into synaptic vesicles by VAChT. And then the synaptic vesicles filled with ACh are exocytosed upon stimulation.

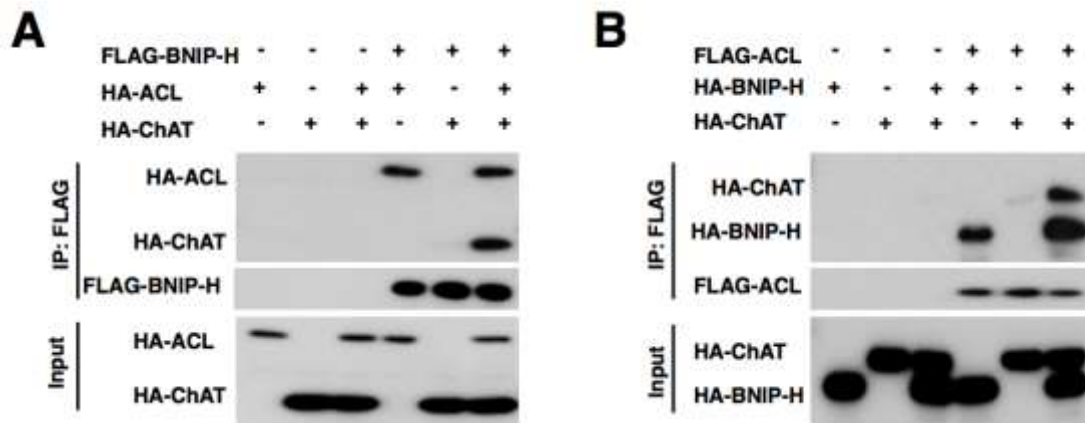
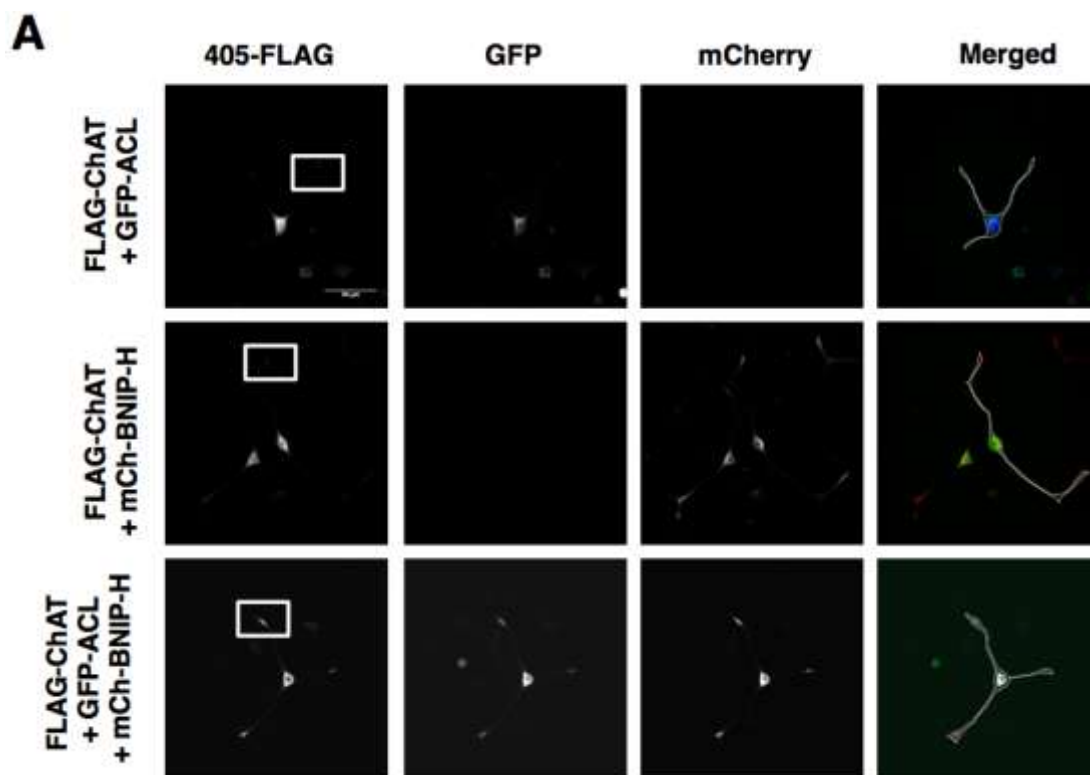


Figure 3-25 Synergistic binding of BNIP-H and ACL with ChAT in 293T cells.

A. The interaction between BNIP-H and ChAT. B. The interaction between ACL and ChAT.



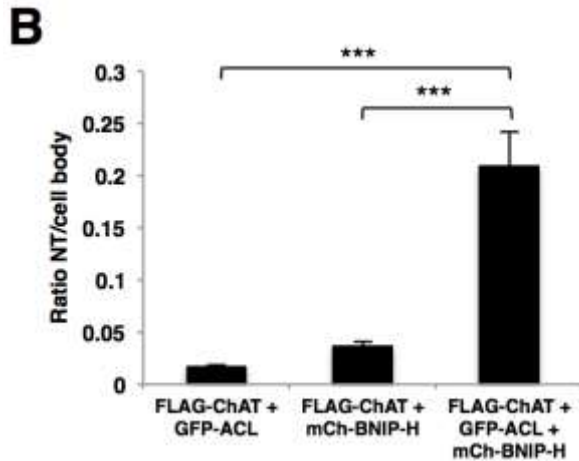


Figure 3-26 BNIP-H and ACL recruit ChAT at PC12 neurite terminal.

A. Localization of ChAT in PC12 cells. Cells were fixed and immunostained with anti-FLAG, followed by fluorophore 405-conjugated secondary antibody. Pictures were taken with confocal microscope. Images are maximum intensity projections of z stacks. B. Quantification of the ratio of FLAG-ChAT fluorescent density between the neurite terminal (white boxes) and cell body. 15 cells for each condition were quantified (** $p < 0.001$). mCh = mCherry. Scale bar, 50 μm .

3.4.2 BNIP-H localizes to synaptic vesicle

Previous studies have shown that BNIP-H is concentrated at presynaptic site of neurons and co-localized with vesicular glutamate transporter (Buschdorf et al., 2006; Hayakawa et al., 2007). My study indicated that BNIP-H could accumulate ACh biosynthesis machinery ACL and ChAT at neurite terminals, implying that BNIP-H might take part in ACh synthesis and release. To further confirm that, the spatial and physical relationship between BNIP-H and VAcHT was investigated. Immunofluorescence study showed that BNIP-H co-localizes with two synaptic vesicle markers, VAcHT and Rab3A at neurite terminals (Figure 3-27). Co-IP study revealed that BNIP-H interacts with VAcHT (Figure 3-28).

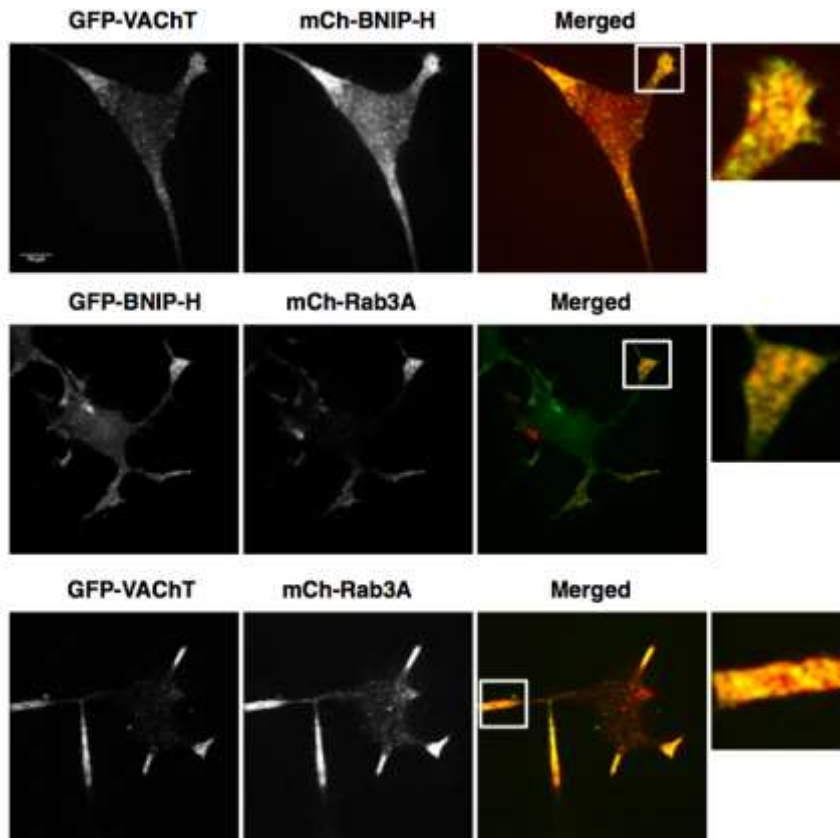


Figure 3-27 BNIP-H localizes at synaptic vesicles of PC12 cells.

Transfected cells were fixed and imaged with confocal microscope. Insets show the magnified view of the boxed area. mCh = mCherry. Scale bar, 10 μ m.

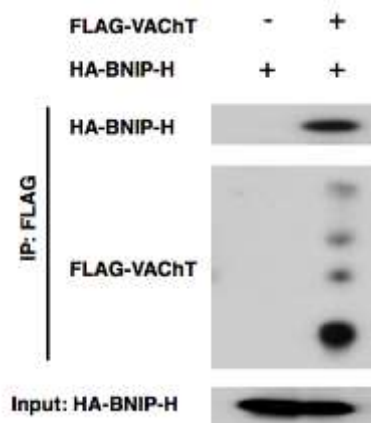


Figure 3-28 BNIP-H interacts with VACHT in 293T cells.

3.4.3 BNIP-H promotes ACh release

The above data demonstrated that BNIP-H accumulates ACh biosynthesis enzymes at neurite terminals and associates with synaptic vesicles filled with ACh, strongly implying that BNIP-H might regulate the ACh release. To test this point, the QqQ LC/MS was employed to quantify ACh secreted by PC12 cells upon NGF stimulation. In the collected cell culture medium, BNIP-H overexpressing cells secreted 40% more ACh than control cells during the 24 h stimulation (Figure 3-29). In contrast, knockdown of BNIP-H reduced ACh secretion by 50% during this period (Figure 3-30 A). As a control, ACL had a similar effect as BNIP-H in both overexpression and knockdown conditions (Figure 3-29 and 3-30 B). These results showed that BNIP-H and ACL synergistically regulate the localization of ChAT and enhance the release of ACh.

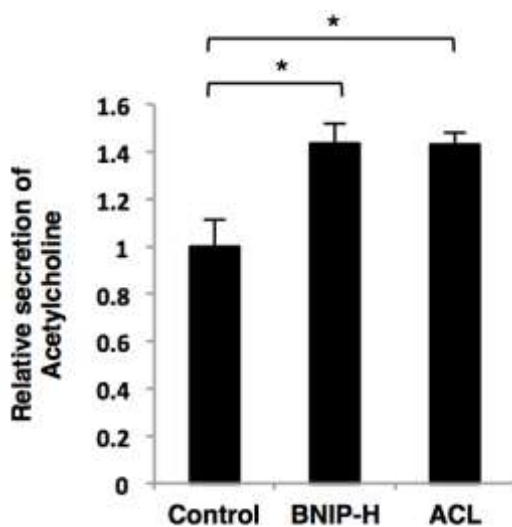


Figure 3-29 BNIP-H and ACL promote ACh release from PC12 cells.

Cells were stimulated with NGF (20 ng/ml; 24h). ACh content in the medium was analyzed by QqQ LC/MS (* $p < 0.05$). $n = 3$.

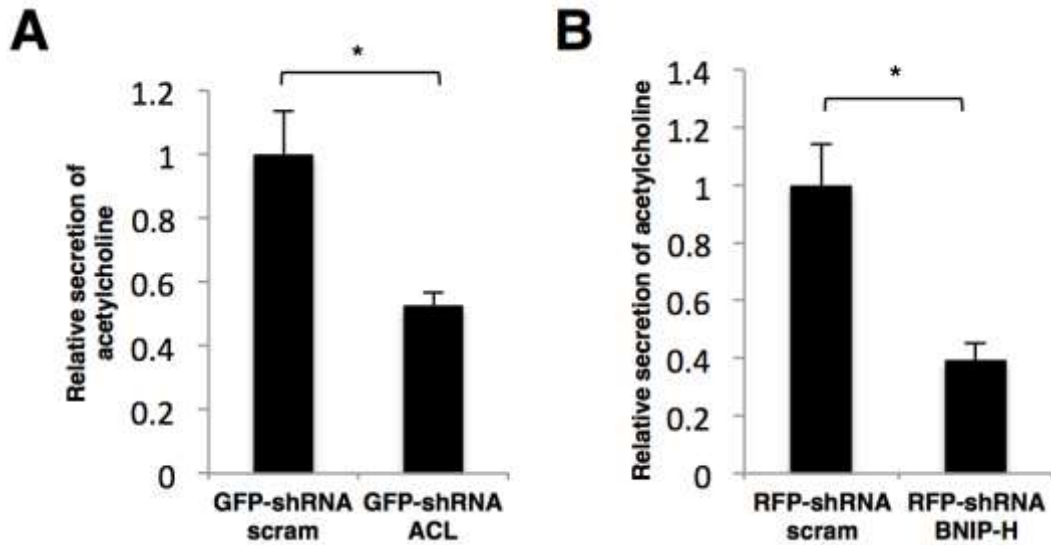


Figure 3-30 Knockdown of BNIP-H or ACL inhibits ACh release from PC12 cells. Cells were stimulated with NGF (100ng/ml; 24 h). ACh content in the medium was analyzed by QqQ LC/MS (* $p < 0.05$). $n = 3$.

3.5 BNIP-H promotes neurite outgrowth through ACh autocrine/paracrine-induced MEK/ERK pathway

3.5.1 BNIP-H promotes neurite outgrowth through ACh secretion

In section 3.3, it has been shown that hemicholinium-3, which inhibits ACh synthesis and subsequent ACh release, blocks BNIP-H-induced neurite outgrowth. And then, BNIP-H has been demonstrated to positively regulate ACh release in section 3.4. Therefore, it was hypothesized that BNIP-H could promote neurite outgrowth through ACh secretion. To verify this, vesamicol, a VAcHT inhibitor that prevents ACh from being packaged into synaptic vesicle was used to block ACh secretion in cholinergic presynaptic terminals. With vesamicol treatment, BNIP-H completely failed to enhance neurite growth (Figure 3-31), indicating that secretion of ACh is necessary for the action of BNIP-H on neurite growth.

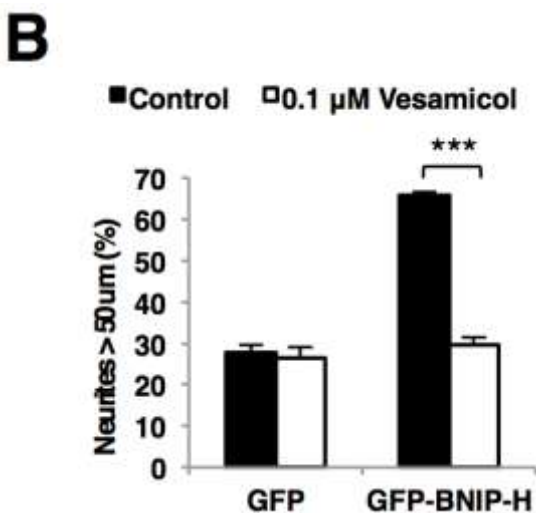
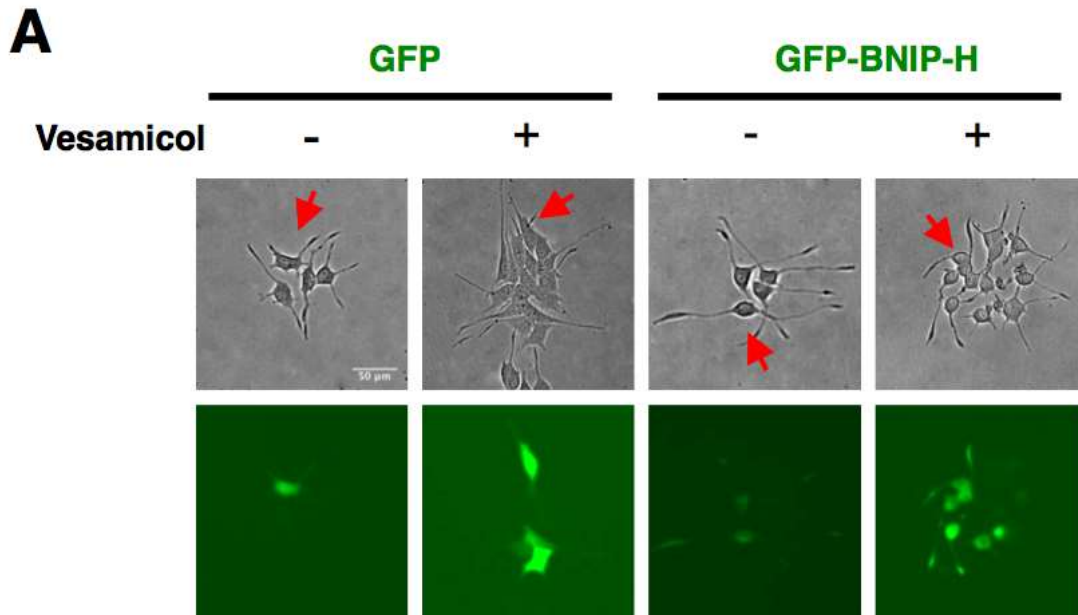


Figure 3-31 BNIP-H-induced neurite outgrowth is blocked by VAcHT inhibitor vesamicol in PC12 cells.

A. Neurite outgrowth with vesamicol treatment. The red arrows indicate the transfected cells. B. Quantification of neurite outgrowth. Percentage (%) of cells with neurites longer than 50 μm is presented. n = 50-100 cells/category from three experiments (***) p < 0.001). Scale bar, 50 μm.

3.5.2 BNIP-H promotes neurite outgrowth through ACh autocrine/paracrine loop

Blockage of neurite outgrowth by vesamicol raised two possibilities: this process is regulated by the exocytosis process or the secreted ACh. To validate the function of

secreted ACh in neurite outgrowth, vesamicol-treated cells were supplied with cholinergic agonist, CCh (Figure 3-32). CCh restored the ability of BNIP-H to promote neurite outgrowth in vesamicol-treated cells in a dose-dependent manner. These data suggested that BNIP-H might promote neurite outgrowth through an ACh feedback loop. This effect was confirmed by the observation that neutralizing ACh with a specific ACh antibody inhibits the neurite extension observed in BNIP-H overexpressing cells (Figure 3-33).

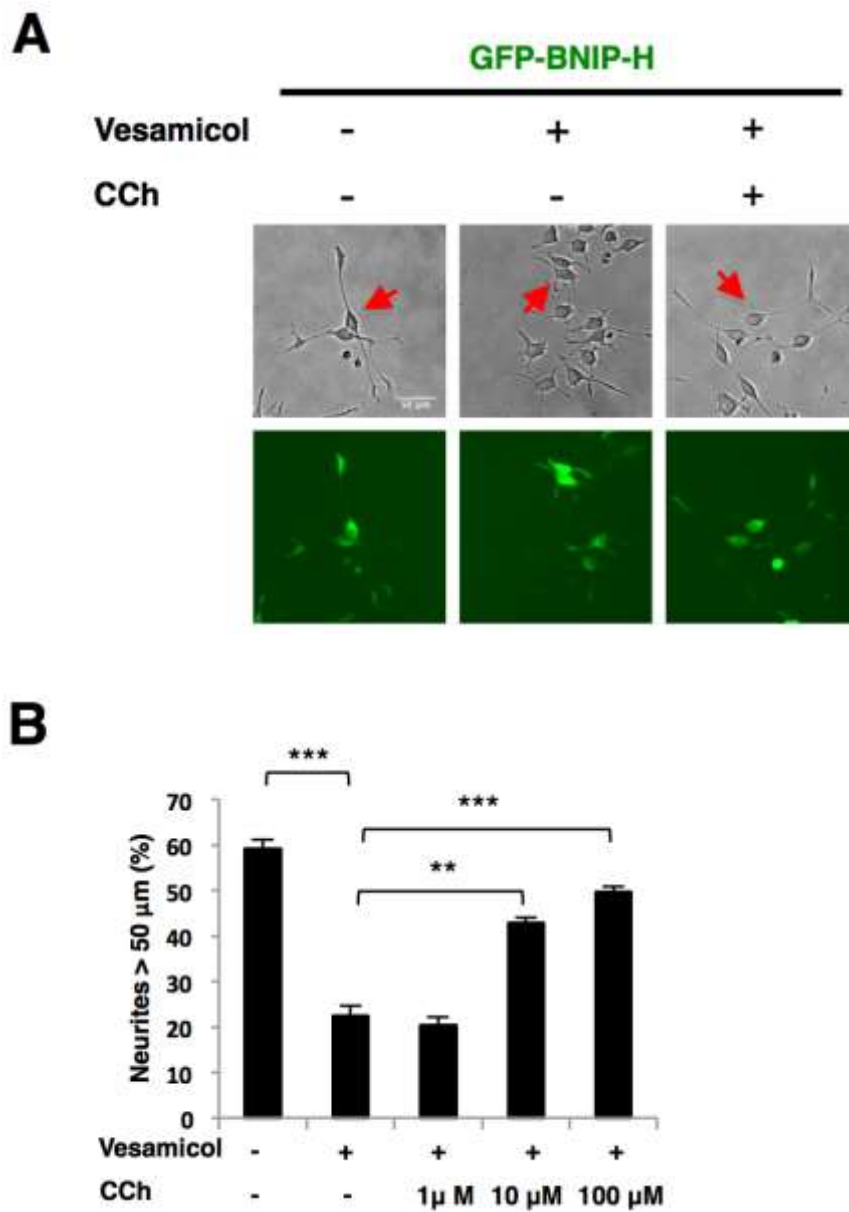


Figure 3-32 CCh rescues vesamicol blockage in neurite outgrowth.

A. Neurite outgrowth with vesamicol and CCh (10 μM) treatment. The red arrows

indicate the transfected cells. B. Quantification of neurite outgrowth. Percentage (%) of cells with neurites longer than 50 μm is presented. $n = 50\text{-}100$ cells/category from three experiments ($***p < 0.001$). Scale bar, 50 μm .

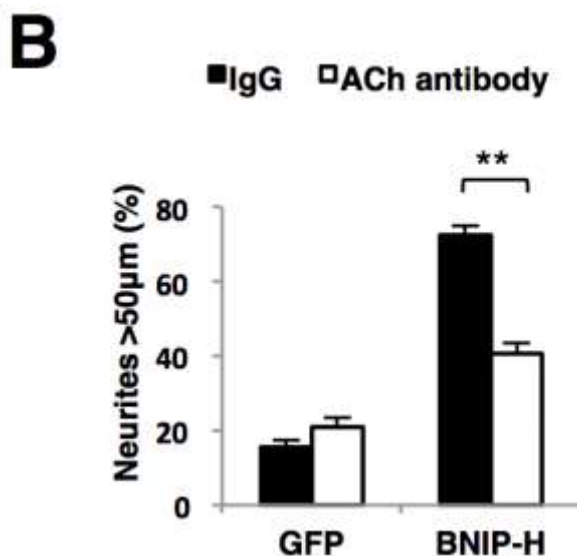
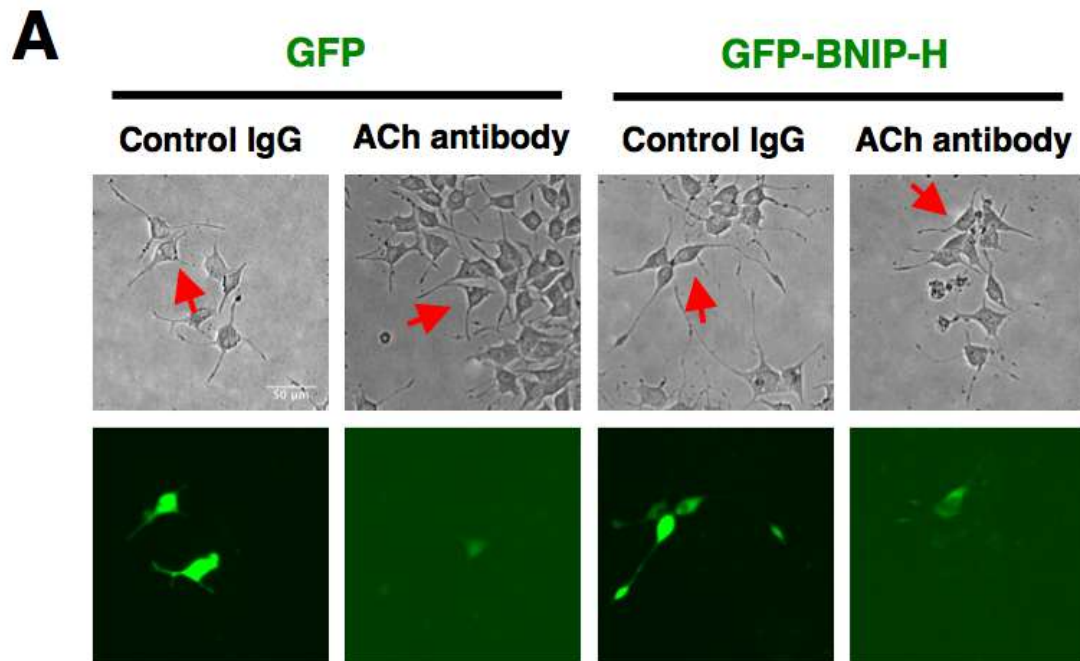


Figure 3-33 BNIP-H's function in PC12 neurite outgrowth is blocked by ACh antibody.

A. Neurite outgrowth with ACh antibody treatment. The red arrows indicate the transfected cells. B. Quantification of neurite outgrowth. Percentage (%) of cells with neurites longer than 50 μm is presented. $n = 50\text{-}100$ cells/category from three experiments ($**p < 0.01$). Scale bar, 50 μm .

It has been reported that supplying ACh into the medium would promote neurite outgrowth of rat Pyramidal hippocampal neurons (VanDeMark et al., 2009). ACh might function similarly in PC12 cells to promote neurite outgrowth. To investigate the effect of ACh on PC12 neurite outgrowth, CCh was used to treat wild type PC12 cells. Supplying CCh to wild type cells enhanced neurite growth under 20 ng/ml NGF stimulation (Figure 3-34), suggesting that CCh could potentiate neurite outgrowth under sub-optimal NGF stimulation. The previous study has shown that BNIP-H enhances ACh release, and potentiates neurite growth through ACh secretion feedback. As the released ACh would diffuse into the medium, the next question was whether enhanced ACh secretion by BNIP-H transfection had any impact on neighbouring untransfected cells. As shown in Figure 3-35, untransfected PC12 cells in BNIP-H transfected wells protruded longer neurites than the control wells, and this induction was also blocked by vesamicol. The enhancement of neurite length is not as potent as BNIP-H transfection (Figure 3-35), but is similar to CCh treatment (Figure 3-34), suggesting that BNIP-H is able to affect the non-transfecting cells through ACh secretion. In addition, BNIP-H knockdown would result in inhibited neurite growth and ACh release. When supplying the knockdown cells with CCh, it rescued the deficiency of neurite outgrowth in a concentration-dependent manner (Figure 3-36), suggesting that the inhibitory effect of BNIP-H knockdown is caused by the defect of ACh release. In summary, these results indicated that BNIP-H enhances neurite outgrowth through an ACh autocrine/paracrine loop.

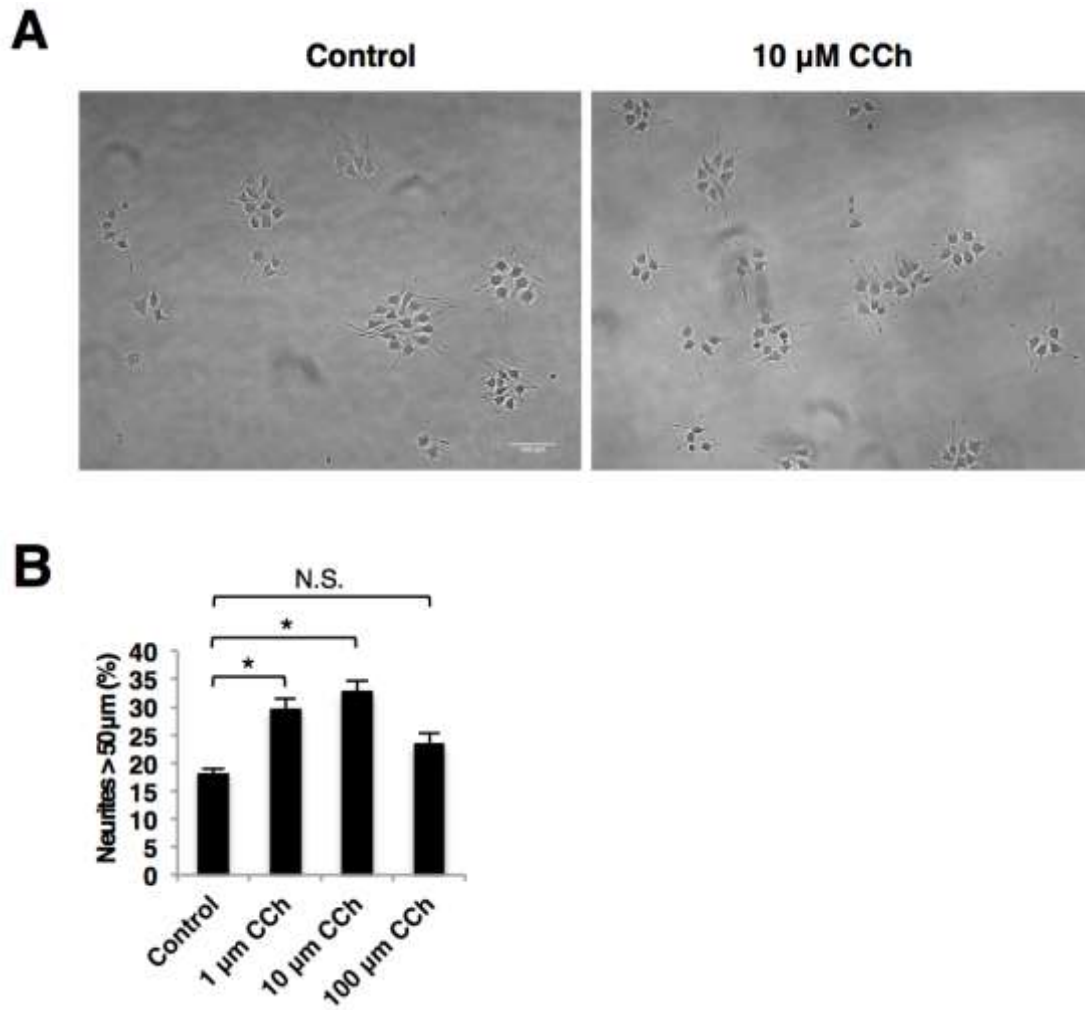


Figure 3-34 The effect of CCh on neurite outgrowth of PC12 cells.

A. Neurite outgrowth with CCh (10 μ M) treatment in the presence of 20 ng/ml NGF.
 B. Quantification of neurite outgrowth. Percentage (%) of cells with neurites longer than 50 μ m is presented. n = 50-100 cells/category from three experiments (*p < 0.05; N.S., not significant). Scale bar, 100 μ m.

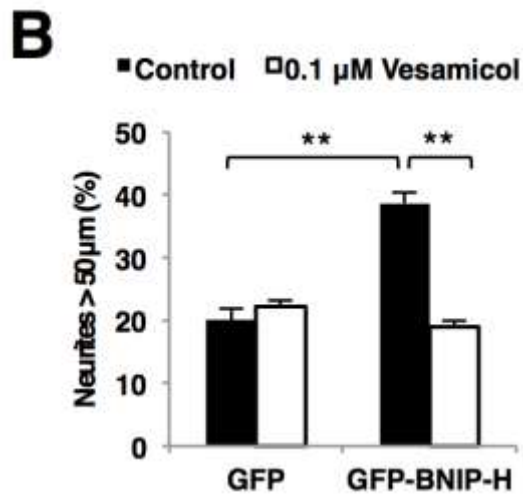
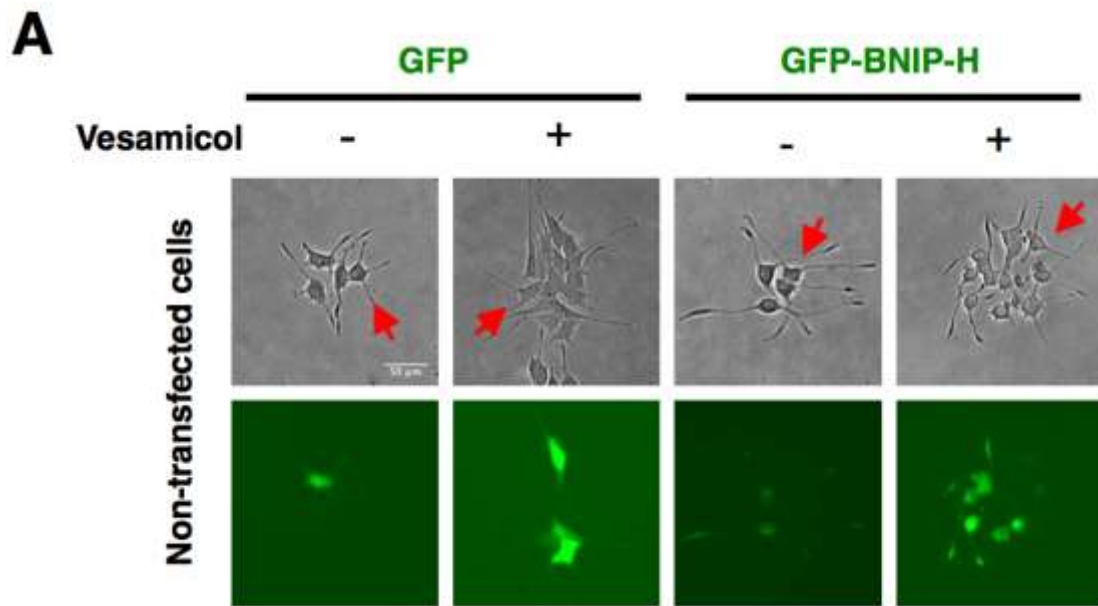


Figure 3-35 BNIP-H-transfected cells promote neurite outgrowth of adjacent wild type cells and this process is blocked by vesamicol.

A. Neurite outgrowth with ACh vesamicol treatment. The red arrows indicate the non-transfected cells. B. Quantification of neurite outgrowth. Percentage (%) of cells with neurites longer than 50 μm is presented. n = 50-100 cells/category from three experiments (**p < 0.01). Scale bar, 50 μm.

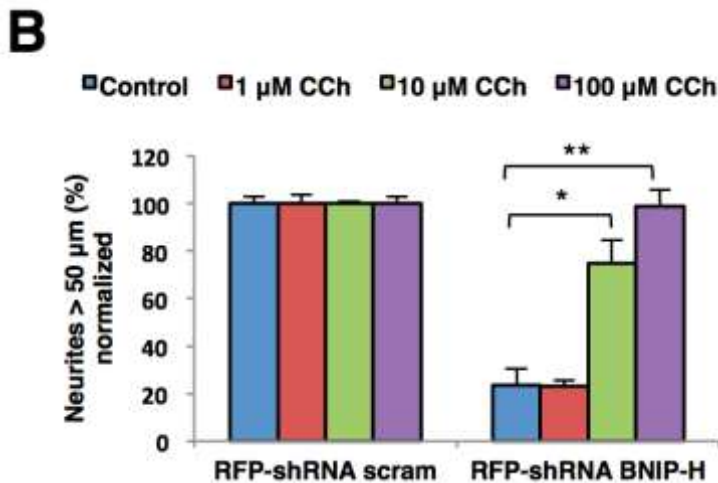
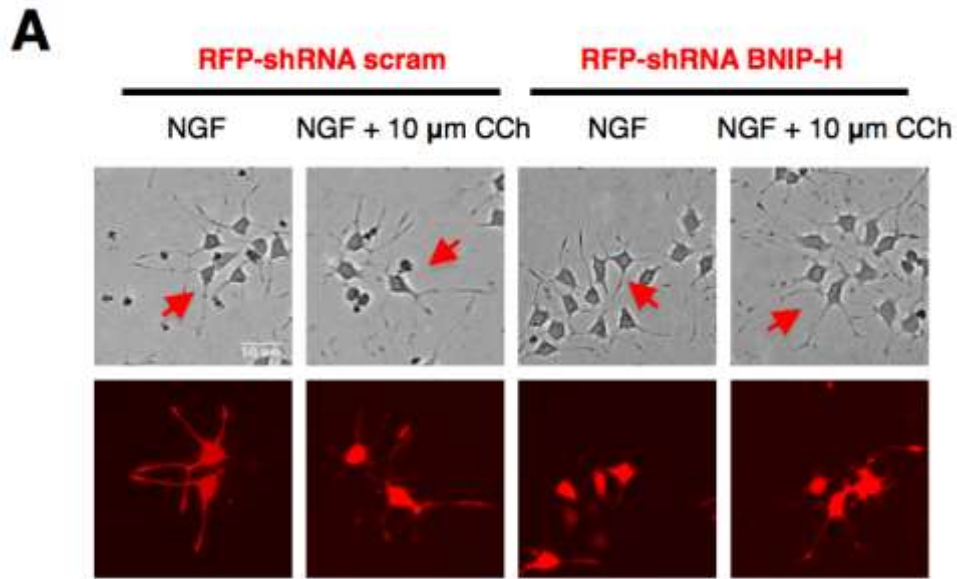


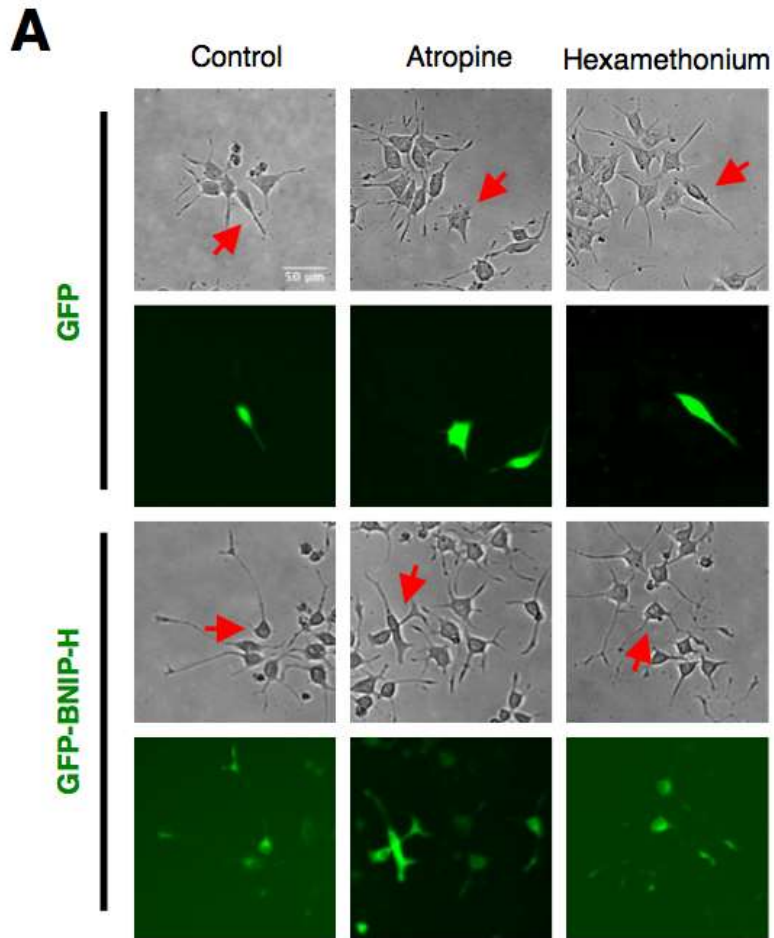
Figure 3-36 CCh rescues the effect of BNIP-H knockdown on neurite outgrowth.

A. Neurite outgrowth with CCh treatment. The red arrows indicate the BNIP-H knockdown cells. B. Quantification of neurite outgrowth. Percentage (%) of cells with neurites longer than 50 μ m is presented. $n = 50-100$ cells/category from three experiments (* $p < 0.05$; ** $p < 0.01$). Scale bar, 50 μ m.

3.5.3 BNIP-H promotes neurite outgrowth through ACh-activated mAChRs and MEK/ERK pathway

Autocrine/paracrine factors must act through their cell surface receptors. ACh has been shown to regulate neurite outgrowth through its muscarinic or nicotinic

receptors (Lipton et al., 1988); Bignami et al., 1997; De Jaco et al., 2002). I next examined which type(s) was important for mediating BNIP-H-induced neurite outgrowth. Using specific inhibitors to these receptors, it was shown that this process was attenuated by muscarinic antagonist atropine, but not by the nicotinic antagonist hexamethonium (Figure 3-37), suggesting that BNIP-H promotes neurite outgrowth through mAChRs.



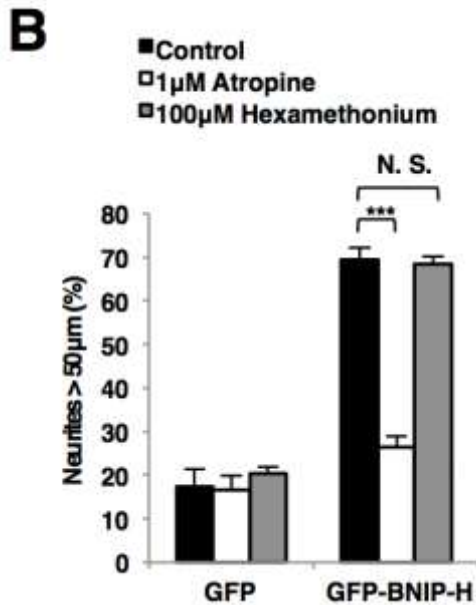


Figure 3-37 BNIP-H-regulated PC12 neurite outgrowth is blocked by muscarinic antagonist atropine, but not by nicotinic antagonist hexamethonium.

A. Neurite outgrowth with atropine or hexamethonium treatment. The red arrows indicate the transfected cells. B. Quantification of neurite outgrowth. Percentage (%) of cells with neurites longer than 50 μm is presented. n = 50-100 cells/category from three experiments (***)p < 0.001; N.S., not significant). Scale bar, 50 μm.

Differentiation of PC12 cells requires ERK, acting downstream of NGF and its tyrosine kinase receptors (Marshall, 1995). It has been known that ACh could activate MAPK pathway through mAChRs (Wess et al., 2007). Consistently, supplementing PC12 cells with ACh triggered robust ERK activation whereas co-treatment with atropine or U0126 completely blocked this effect (Figure 3-38 A). This result suggested that ACh induces ERK activation through mAChRs and MEK. To further determine whether BNIP-H regulates ERK activation through this ACh autocrine/paracrine loop, the ERK activation was examined in PC12 cells overexpressing BNIP-H. As expected, upon NGF stimulation for 40 min, these cells exhibited higher ERK activation than the control, which was blocked by atropine (Figure 3-38 B). These results implied that BNIP-H-induced ACh release could feedback to activate mAChRs and intracellular MAPK pathway.

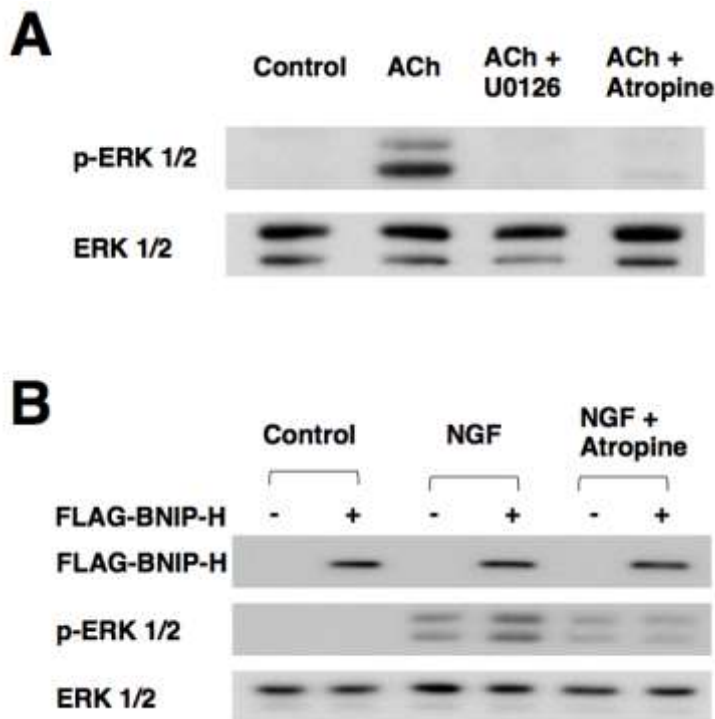
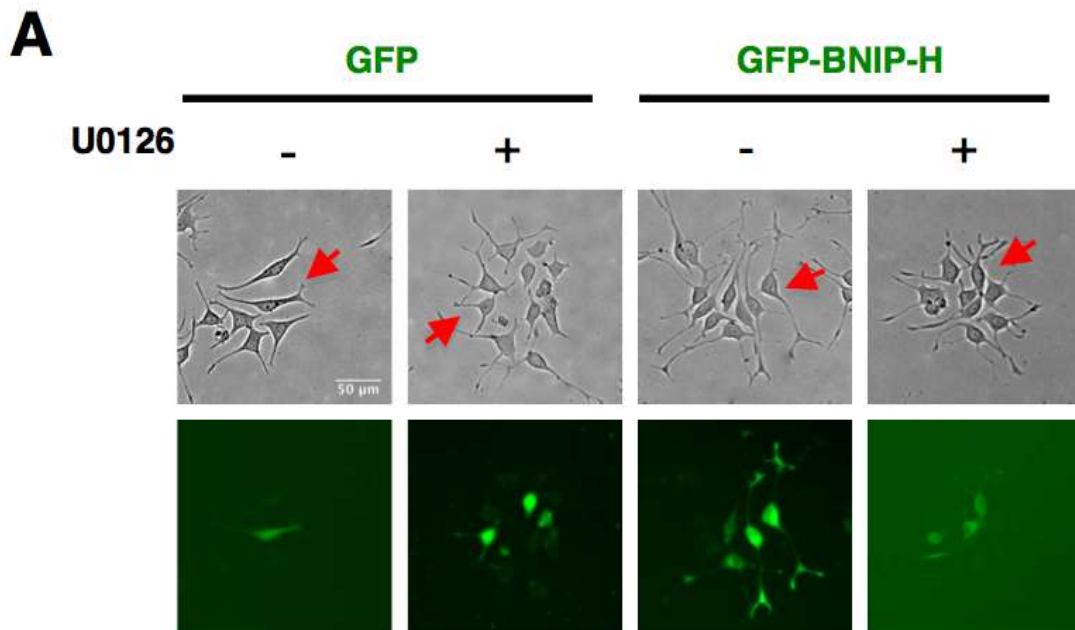


Figure 3-38 BNIP-H enhances ERK activation through ACh release.

A. ACh activates ERK through mAChRs and MEK in PC12 cells. Cells were treated with 10 μ M ACh, 5 μ M U0126 and 1 μ M atropine for 3 min. Total cell lysates were subjected to immunoblotting. B. BNIP-H enhances ERK activation through mAChRs in PC12 cells. Cells were treated with 20 ng/ml NGF and 1 μ M atropine for 40 min. Total cell lysates were subjected to immunoblotting.

To provide further insight to the functional significance of BNIP-H and MAPK signaling mediated by ACh, the function of MAPK pathway was examined on neurite outgrowth. I tested whether inhibition of MAPK pathway would block BNIP-H-enhanced neurite outgrowth. As shown in Figure 3-39, PC12 cells overexpressing BNIP-H showed significantly reduced neurite outgrowth upon inhibiting MEK with U0126, suggesting that MAPK pathway activation is required for BNIP-H to potentiate neurite outgrowth. Conversely, overexpression of a constitutive active MEK2 mutant (MEK2-CA: S222,226D) effectively rescued the deficiency in neurite outgrowth caused by BNIP-H knockdown (Figure 3-40), further confirming that MAPK pathway locates at the downstream of BNIP-H to promote neural outgrowth. The active ERK would translocate into nuclei and activate multiple transcription factors to regulate

gene expression for cell differentiation (Yoon and Seger, 2006). ACh has been shown to induce neurite outgrowth and neuronal differentiation by upregulating gene transcription in neuroblastoma cells (Altin et al., 1991; Berkeley and Levey, 2000; Salani et al., 2009). To test whether BNIP-H could activate gene transcription to regulate neurite growth, I applied transcription inhibitor DRB to BNIP-H transfected cells. As shown in Figure 3-41, DRB effectively blunted the stimulatory effect of BNIP-H in PC12 differentiation, implying that long term genetic reprogramming is crucial for BNIP-H to induce neurite outgrowth. Taken together, these results indicated the role of BNIP-H in controlling neuronal differentiation by integrating ACh and ERK signaling circuitry.



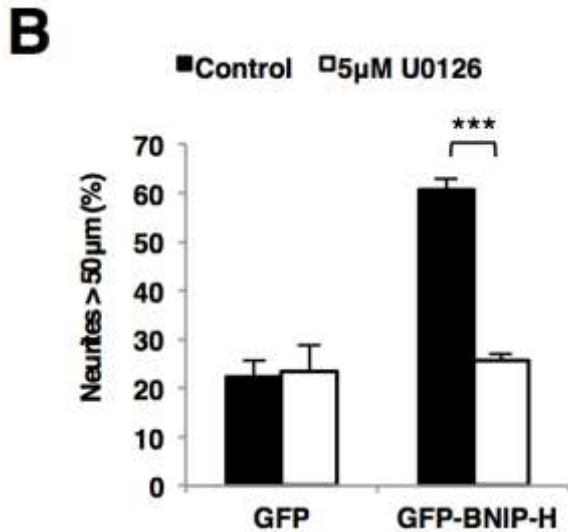
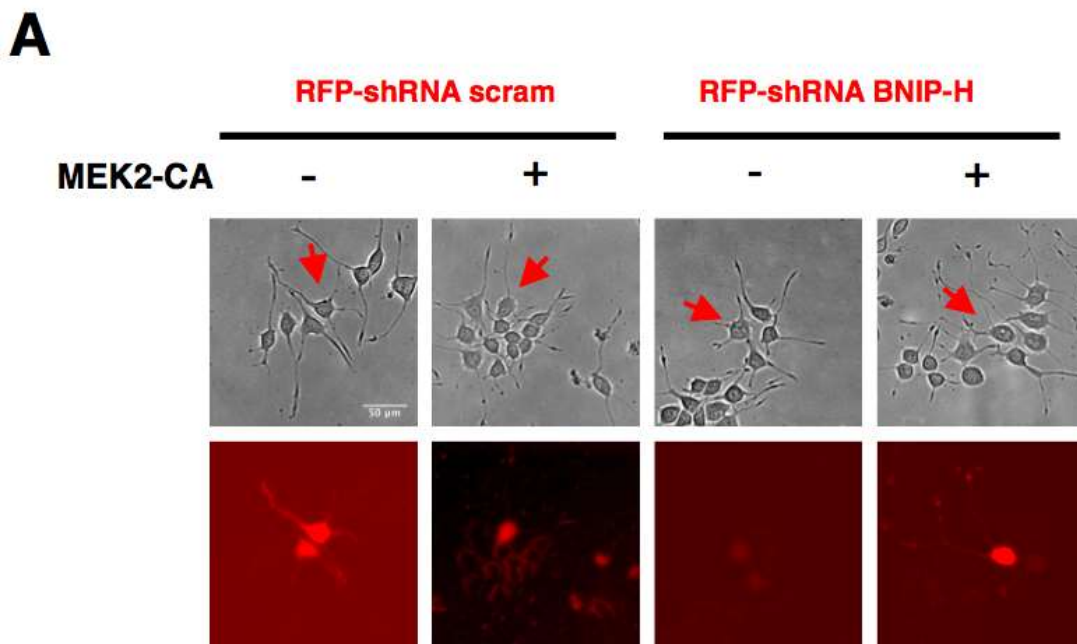


Figure 3-39 BNIP-H-induced PC12 neurite outgrowth is blocked by MEK inhibitor U0126.

A. Neurite outgrowth with U0126 treatment. The red arrows indicate the transfected cells. B. Quantification of neurite outgrowth. Percentage (%) of cells with neurites longer than 50 μm is presented. n = 50-100 cells/category from three experiments (**p < 0.001). Scale bar, 50 μm.



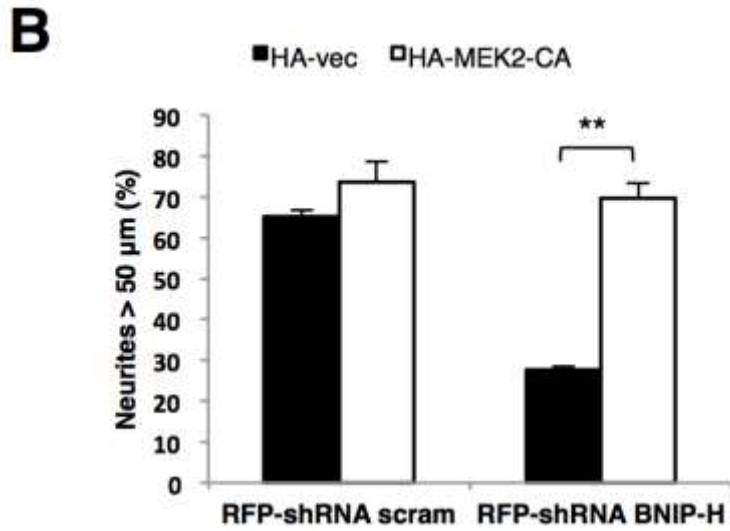
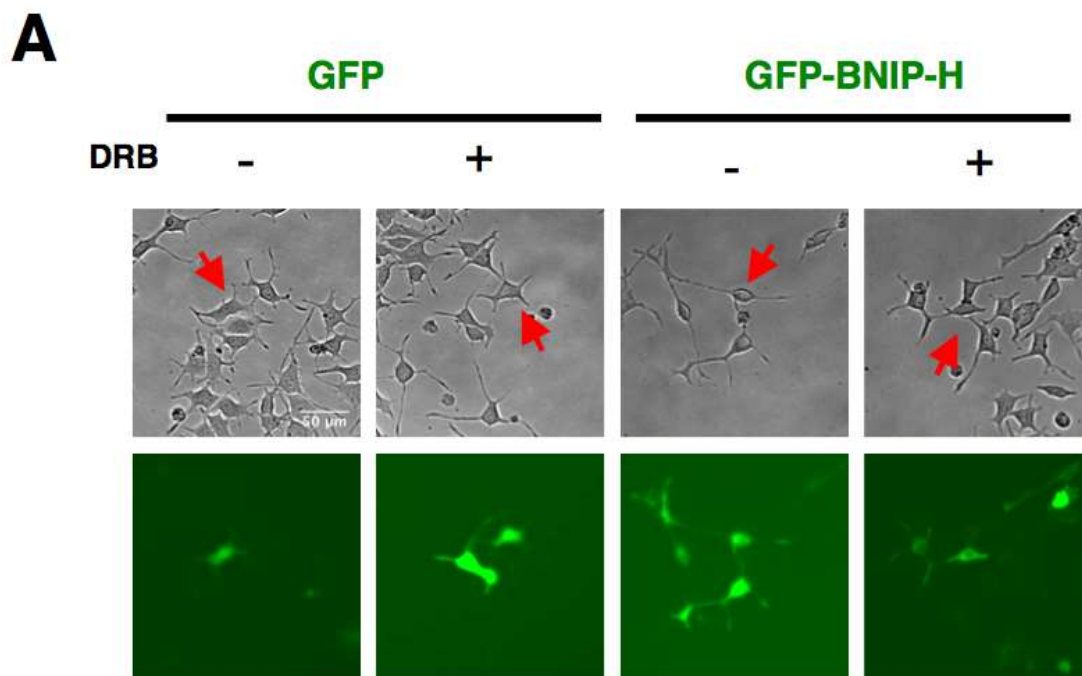


Figure 3-40 Constitutive active MEK rescues effect of BNIP-H knockdown on PC12 neurite outgrowth.

A. Neurite outgrowth with MEK2-CA and shRNA constructs co-transfection. The red arrows indicate the transfected cells. B. Quantification of neurite outgrowth. Percentage (%) of cells with neurites longer than 50 μm is presented. $n = 50\text{-}100$ cells/category from three experiments (** $p < 0.01$). Scale bar, 50 μm .



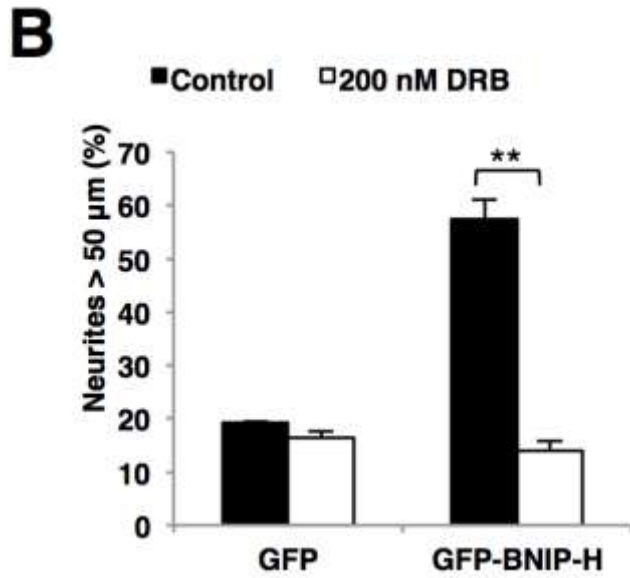


Figure 3-41 BNIP-H-regulated PC12 neurite outgrowth is blocked by transcription inhibitor DRB.

A. Neurite outgrowth with DRB treatment. The red arrows indicate the transfected cells. B. Quantification of neurite outgrowth. Percentage (%) of cells with neurites longer than 50 μm is presented. $n = 50\text{-}100$ cells/category from three experiments (** $p < 0.01$). Scale bar, 50 μm .

4. DISCUSSION

Genetic studies in Cayman ataxia patients and rodent models of ataxia and dystonia point to the importance of BNIP-H/Caytaxin in maintaining the proper functioning of our nervous systems. This thesis provides the first biochemical and molecular evidence that BNIP-H functions as a scaffold protein that links ACL as a cargo on kinesin-1 motor and promotes its trafficking towards neurite terminals. There, BNIP-H and ACL act synergistically to recruit ChAT and modulate the local release of ACh. Consequently, ACh exerts an autocrine/paracrine feedback loop through its mAChRs that activates MEK/ERK signaling and neurite outgrowth. The essential roles of this novel “ACL/BNIP-H/kinesin” complex and their mechanistic action, were confirmed by (i) reciprocal genetic knockdown and functional rescues, (ii) inhibiting the enzymatic activity of ACL, (iii) uncoupling BNIP-H and ACL from kinesin motor, (iv) preventing ACh packaging and secretion, (v) neutralising secreted ACh, (vi) blocking mAChR and (vii) inhibiting MEK/ERK activation. Collectively, these findings underpin the significance of BNIP-H acting both as placemaker and pacemaker in promoting cholinergic signaling and transmission in neurons. These are further discussed below.

4.1 Concerted spatiotemporal regulation of ACh synthesis and release

ACL, as a metabolism enzyme to produce acetyl-CoA, has been found to be concentrated at neurite terminals where the neurotransmitter ACh is synthesized and released (Szutowicz et al., 1982). Several evidences have shown that ACL is required to supply acetyl-CoA for ACh synthesis in nervous system and cell culture (Eissing et al., 2012; Endemann and Brunengraber, 1980; Szutowicz et al., 1983; Szutowicz and Lysiak, 1980a). My results also demonstrated that ACL positively regulates ACh release in PC12 cells (Figure 3-29 and 3-30). However, the mechanism underlying the distribution of this enzyme is unknown. This thesis proposes that ACL is a trafficking cargo of BNIP-H and kinesin-1. Particularly, BNIP-H functions as a scaffold to link ACL to kinesin-1 motor protein. BNIP-H binds with KLC1 through the

“WQ-WED” motif located at the N-terminus of BNIP-H (Figure 3-12). Mutation of this kinesin binding site on BNIP-H fails to transport and accumulate ACL to the neurite terminals (Figure 3-16 and 3-17), and inhibits ACL dynamics and turn over rate at this site (Figure 3-18), suggesting that BNIP-H regulate the transportation and accumulation of ACL to the place producing ACh through the interaction with KLC1. Positive trafficking of metabolism is important for cell survival and function, especially for the highly polarized neuronal cells. It has been shown that deletion of GGA3, which affects the trafficking of metabolism enzyme beta-site APP-cleaving enzyme (BACE), is considered to cause Alzheimer’s disease (Tesco et al., 2007), indicating that defect of protein trafficking might cause nervous system related diseases.

In addition, ChAT is another important metabolism enzyme in producing ACh (Nachmansohn and Machado, 1943). ChAT at neurite terminals would combine acetyl-CoA and choline to generate ACh. It has been reported that ChAT and ACL activities are significantly correlated in the synaptosome of the cholinergic neurons in rat brain (Szutowicz et al., 1983; Szutowicz and Lysiak, 1980a; Szutowicz et al., 1982). However, how functions of ACL and ChAT are coordinated in space and time remains unknown. Using co-IP and immunofluorescence studies, I showed that BNIP-H and ACL synergistically interact with ChAT and promote the recruitment of this enzyme at the neurite terminals (Figure 3-25 and 3-26). Unlike BNIP-H/ACL complex, ChAT has been reported to be transported by kinesin-2 (Sadananda et al., 2012; Tateno et al., 2009). Indeed, BNIP-H, ACL and ChAT never co-trafficked along neurites (data not shown) despite their detection at the terminals. My results therefore suggested that BNIP-H serves as a scaffold that first loads ACL on kinesin-1 and transports it from cell bodies to terminals. There, they recruit ChAT, probably via a different traffic route. Together, they regulate the local production and release of ACh. In the future, it would be interesting to study whether ChAT at the neurite terminals, regulates the disassembly of BNIP-H/ACL from kinesin-1 motor protein, and replaces KLC1 from the ternary complex BNIP-H/ACL/KLC1.

After ACh synthesized, ACh would be loaded into synaptic vesicles by VACHT before secretion (Song et al., 1997). It has been shown that BNIP-H is localized to synaptic vesicles at neurite terminals (Hayakawa et al., 2007). Interestingly, immunofluorescence study demonstrated that BNIP-H co-localizes with Rab3a and VACHT (Figure 3-27), and Co-IP study showed that BNIP-H interacts with VACHT (Figure 3-28). These results further suggested that BNIP-H might partake in ACh packaging in synaptic vesicles and/or subsequent exocytosis of neurotransmitters. BNIP-H overexpression enhances ACh release in differentiating PC12 cells while knockdown of BNIP-H inhibit ACh release (Figure 3-29 and 3-30), suggesting that BNIP-H indeed regulates ACh synthesis and/or secretion. This thesis reveals that BNIP-H not only accumulates ACh synthesis machinery at neurite terminals, but also interacts with VACHT. It needs further investigation to examine that the enhancement of ACh release by BNIP-H is resulted from increase of ACh production, ACh packaging, synaptic vesicle exocytosis, or all the three processes.

4.2 An ACh autocrine/paracrine feedback loop for neurite outgrowth

Neurotransmitters and growth factors both activate various signal transduction pathways, such as PKA, PKC, Ca²⁺, MAPK and so on, to elicit their cellular effects. Utilizing common signaling components provides a mechanism for functional crosstalk between neurotransmitters and growth factors, where signaling crosstalks can be regulated by specific scaffold proteins at different locales and activated at precise timing (Pan et al., 2012). ACh functions through mAChRs to promote neurite growth and neuronal differentiation in hippocampal neuron and neuroblastoma cells (De Jaco et al., 2002; VanDeMark et al., 2009). ACh acts as a growth factor to promote neurite protrusion and potentiates NGF stimulation in M1 receptor stably expressed PC12 cells (Pinkas-Kramarski et al., 1992). Furthermore, activating mAChRs induces MAPK activation and early response genes for neurite growth (Altin et al., 1991; Berkeley and Levey, 2000; Salani et al., 2009). Despite these, little is known about how ACh autocrine/paracrine loop is regulated for neuronal differentiation.

BNIP-H enhances ACh release during differentiation (Figure 3-29). Blockade of ACh release or muscarinic receptors reduces neurite growth in BNIP-H overexpressing cells (Figure 3-31 and 3-37), suggesting that ACh acts as an autocrine/paracrine agent downstream of BNIP-H to potentiate NGF function in neurite extension. However, increasing ACh release by ACL overexpression (Figure 3-29), exposing wild type cells to ACh secreted by BNIP-H overexpressing cells (Figure 3-35), or supplying ACh into the cell culture medium (Figure 3-34) is not as potent as BNIP-H to enhance neurite extension. This raises three possibilities. First, other signaling pathway may be involved in BNIP-H-induced neurite growth, which will be elaborated in the following section. Second, a greater effective concentration of ACh is required locally to elicit its full potency. Third, as ACh enhances neurite growth in M1 receptor stably expressed PC12 cells (Pinkas-Kramarski et al., 1992), it is possible that BNIP-H might regulate transportation of ACh receptors. It will be interested to investigate the effect of BNIP-H on the distribution of two types of ACh receptors on the cell surface.

Besides, my result showed that ACh induces neurite outgrowth of PC12 cells in sub-optimal of NGF stimulation (Figure 3-34). ACh has been found to inhibit neurite outgrowth through nicotinic receptor in a higher dose of NGF stimulation (Nordman and Kabbani, 2012). It should be studied that whether different concentrations of NGF would affect the sensitivity of PC12 cells to ACh for neurite outgrowth.

4.3 The role of BNIP-H in neurite outgrowth

BNIP-H, a neuron specific protein, is transcribed since embryonic day 15 in normal rat's embryos (Xiao and Ledoux, 2005), suggesting that BNIP-H might play an important role in the differentiation of neurons during embryonical development. A linear increase of cerebellar *Atcay* transcript from P1 to P36 is correlated with the maturation of the cerebellar cortex, and the expression peak of BNIP-H at P14 is a time point essential for the development of climbing fiber synapses onto Purkinje cells, supporting possible regulatory role of BNIP-H in neuronal network development. In addition, BNIP-H overexpression in hippocampal neuron results in

enhanced neurite extension while knockdown of BNIP-H reduces neurite length *in vitro* (Aoyama et al., 2009).

The process of differentiation can be divided into two parts: cell morphology change where neurite processes are formed and cellular remodeling including the alteration of genes transcription and translation. Both of the two parts operate in concert in the differentiation of excitable neuronal cells. In PC12 cells, BNIP-H overexpression potentiates neurite outgrowth in sub-optimal concentration of NGF stimulation (Figure 3-1), which is consistent with the hypothesized role of BNIP-H in neuronal differentiation. For the cellular changes, immunofluorescence study showed that BNIP-H overexpressing increases Tuj 1 staining along the neurite (Figure 3-2) and transcription inhibitor DRB blocks BNIP-H-enhanced neurite outgrowth (Figure 3-41), suggesting that BNIP-H regulates gene transcription for neuronal differentiation.

The further mechanistic study indicated that BNIP-H promote neurite outgrowth through ACh autocrine/paracrine loop. However, most of hippocampal neurons are known to be non-cholinergic (Frotscher et al., 1986), implying that BNIP-H might regulate other signaling pathways for the neurite extension of hippocampal neurons. One possible candidate is the glutamatergic signaling as it has been reported that glutamate could promote neurite sprouting of rat hippocampal neurons (Patterson, 1988). Our lab has showed that BNIP-H relocalises glutaminase KGA to neurite terminals and affects glutamate homeostasis (Buschdorf et al., 2006). In the mouse cerebellum, BNIP-H co-localizes with vesicular glutamate transporter 1 (Hayakawa et al., 2007). These suggest that BNIP-H could function in glutamatergic as well as cholinergic signaling. Although BNIP-H inhibits KGA enzyme activity and reduces glutamate synthesis rate, KGA is re-localized to neurite tips from cell body by BNIP-H (Buschdorf et al., 2006). Neurite tips are rich with vesicular glutamate transporters, which load glutamate into vesicle and make glutamate ready to be released (Fremeau et al., 2002). Concentration of KGA in the same small region as vesicular glutamate transporter might enhance glutamate loading efficiency, and therefore

increase glutamate secretion. To determine the final effect of BNIP-H in glutamate neurotransmission, the total amount of secreted glutamate should be investigated in the future. It is also interesting to study whether BNIP-H functions similarly to KGA as to ACL, and even co-regulates glutamatergic and cholinergic signaling in space and time for neuronal functions. Conditional knock-in with specific alleles that are defective in carrying ACL and/or KGA would be instrumental in dissecting their precise functions.

Another possible candidate is the small GTPase. As described previously, BCH domain is a scaffold domain to regulate the activity of Rho small GTPase. BNIP-2, as the earliest identified BCH domain-containing protein and mostly well-studied molecule in BCH family, has been reported to induce membrane protrusion and cell elongation via Cdc42 (Yi et al., 2005). In particular, BNIP-2 regulates Cdc42 activity and p38 MAPK pathway via Cdo receptor to promote neuronal differentiation (Oh et al., 2009). It has also been reported that the BCH domain of BPGAP could induce chronic K-Ras activation and neuronal differentiation (Ravichandran and Low, 2013). In addition, BCH domain of Cdc42GAP also targets to endosomes through interaction with Rab11 and Rab5 (Sirokmany et al., 2006), which are involved in neurite outgrowth as well (Eva et al., 2010; Liu et al., 2007). These evidences imply that BNIP-H might regulate neuronal differentiation through small GTPase.

Besides, although the above data strongly support the role of BNIP-H in neuronal differentiation, no anatomy change of brain was observed in *dt* rats and mutant mice, except for cerebellar hypoplasia in Cayman ataxia patients (Bomar et al., 2003; Lorden et al., 1984). BMCC1, a very large form of BNIP-XL initially identified as a homolog of BNIP-H (Soh and Low, 2008), can also interact with KGA in culture, albeit its function unclear (Boulay et al., 2013). This suggests that perhaps during the development of rodent models, this isoform may compensate for the loss of BNIP-H function *in vivo* and support normal neuronal differentiation. Based on this hypothesis, it should be investigated that whether BMCC1 or other similar BCH

domain containing proteins could rescue neuronal differentiation in the absence of BNIP-H.

4.4 A cholinergic link in ataxia and dystonia

In the animal models of Cayman ataxia, different forms of mutation in the *ATCAY/Atcay* loci have been identified, spontaneously or experimentally induced. These range from missense and splice-site mutations (Cayman ataxia patients and *wobbly* mouse), insertions of B1 element (*jittery* mouse) or IAP elements (*hesitant* mouse and *dt* rat) and dinucleotide deletion (*sidewinder* mouse) (Table 1-1). These would result in various truncated forms of BNIP-H or reduced expression level of wild type protein, leading to a broad spectrum of psychomotor impairment with different levels of severity (Bomar et al., 2003; LeDoux, 2011; Sikora et al., 2012; Xiao and Ledoux, 2005). Of particular interest, the skipping of exon 4 owing to a splice-site transversion in *wobbly* mouse would lead to the loss of the distal “WED” kinesin-binding motif (see <http://mutagenetix.utsouthwestern.edu/>). On the other hand, *jittery* and *sidewinder* mice would express the BNIP-H mutants without its BCH domain which regulates multiple functions (Bomar et al., 2003; Pan and Low, 2012). These results support the requirement of a full-length BNIP-H that undergoes trafficking. In comparison, homozygous knockout of ACL is embryonic lethal, owing to its ubiquitous expression and multiple functions (Beigneux et al., 2004b). In adult mice brain, ACL expression is persistent in the hippocampus, parallel fibers and Purkinje cells. Its expression profile is consistent with the expression of BNIP-H (Beigneux et al., 2004b; Buschdorf et al., 2006), thus supporting their functional convergence in brain.

This thesis uncovers a novel function of BNIP-H in controlling cholinergic signaling with potential insights into the regulation of neuronal maturation, network and transmission. BNIP-H/ACL-induced ACh release promotes the maturation of neurons through its autocrine and paracrine effects. The released ACh could also participate in synaptic cholinergic neurotransmission and modulate synaptic plasticity.

These *in vitro* studies raise a possibility that loss of cholinergic signaling arising from BNIP-H deficiency might account for the ataxia and dystonia phenotypes. Earlier work showed that lesion of cerebellum greatly improves the motor function of *dt* rat, implying that cerebellum is the cause of the dystonic motor syndrome (LeDoux et al., 1995). The *dt* rat exhibits defects in the climbing fiber-Purkinje cell synapse, leading to abnormal bursting firing patterns in the cerebellar nuclei (Lorden et al., 1985). This implies that BNIP-H deficiency is likely to be neurodevelopmental network disorder driven by abnormal cerebellar output (LeDoux, 2005). Purkinje cells adopt a unique anatomical and functional position for processing neuronal information (Apps and Garwicz, 2005) and these cells are the only output signal required for motor coordination (Strick, 1985). Although glutamate is a major neurotransmitter in cerebellum, increasing evidence suggests that Purkinje cells could receive and process ACh signals through the mAChRs to promote their survival (Mount et al., 1994), synaptic plasticity at parallel fiber-Purkinje cell synapse (Rinaldo and Hansel, 2013) and spontaneous excitatory postsynaptic current in Purkinje cells (Takayasu et al., 2003). Besides, these cells may have the capacity to synthesize ACh as evidenced by immunoreactivity for ChAT (Barmack et al., 1992) and VAcHT (Beigneux et al., 2004b). Although it is not clear whether synaptic plasticity deficits directly cause cerebellar ataxia, it has been shown that ataxia is associated with disruption of synaptic plasticity in Purkinje cells (Kashiwabuchi et al., 1995; Shuvaev et al., 2011; Walter et al., 2006). It is tempting to speculate that loss of cholinergic transmission and response in Purkinje cells might cause the deep cerebellar nuclei to become hyperactive, leading to impaired output to the motor system that eventually causes ataxia and dystonia. This work, therefore, warrants a closer examination of the ACL-based cholinergic interaction and response between the Purkinje cells and parallel fibers, under normal versus ataxia/dystonia models.

On the other hand, regional brain glucose utilization is reduced in widespread motor system of the *dt* rat, such as cerebellum, substantia nigra, basal ganglia and so on, indicating that there are widespread abnormalities in *dt* rat (Brown and Lorden,

1989). Cholinergic basal forebrain nuclei are crucial for normal cognition. Degeneration of these neurons is associated with cognition and memory related diseases such as Alzheimer's disease, Down's syndrome and spinocerebellar ataxia type 2 (Hodges, 2006; Whitehouse et al., 1982; Yates et al., 1980). Beyond the cerebellar related phenotypes, Cayman ataxia patients also present certain degree of mental retardation. It remains to be seen if cholinergic basal forebrain neurons are also affected in BNIP-H mutants. In addition, the *dt* rat displays a reduced behavioral response to the dopaminergic blocker, haloperidol, indicating there may be a defect in striatum pathway (McKeon et al., 1984). However, this defect is not caused by an alteration in striatal DA metabolism, as the DA level, DA turnover rate and DA receptor intensity in striatum are not affected in *dt* rat (McKeon et al., 1984). There is a possibility that the insensitivity to haloperidol in *dt* rat may result from deficiency of cholinergic function, as mAChR knockout, application of muscarinic antagonist and reduction of ACh release cause similar phenomena observed in *dt* rat (Fink-Jensen et al., 2011; Gras et al., 2008). Besides, BNIP-H interacts with KGA and affects glutamate hemostasis (Buschdorf et al., 2006), and *dt* rat shows enhanced sensitivity to serotonin agonist (Michela et al., 1990), indicating that multiple neurotransmission systems may be regulated by BNIP-H in nervous system.

4.5 BNIP-H as a kinesin-dependent p(l)acemaker in metabolic and cell signalling

Molecular motors are important for cargo trafficking, especially in highly polarized neurons and are crucial for neurotransmission, differentiation and survival (Gho et al., 1992; Hirokawa et al., 2009). Several neurological disorders, such as Down's syndrome, Alzheimer's disease and Huntington disease, are thought to derive from dysfunction of axonal transportation through kinesins (Gauthier et al., 2004; Lazarov et al., 2005; Lazarov et al., 2007; Rong et al., 2006; Salehi et al., 2006; Salinas et al., 2008). However, more cargos and linkers need to be identified before the complex network of trafficking is fully understood. BNIP-H is a versatile neuro-specific

regulatory scaffold that determines the locale and reactivity of key metabolic enzymes that affect cholinergic neurotransmission in physiological condition. At the molecular level, the presence of putative kinesin-binding sites on other homologs of BNIP-H, such as BNIP-2, BNIP-S, and BMCC1 led us to believe that these evolutionarily conserved BCH domain family proteins could exert their p(l)acemaker functions by conspiring with kinesins (Pan and Low, 2012).

4.6 Conclusion

Taken together, this thesis shows that BNIP-H functions as a scaffold to transport ACL and contributes to acetylcholine secretion, which enhances neurite extension through autocrine/paracrine loop in PC12 cells (Figure 4.1).

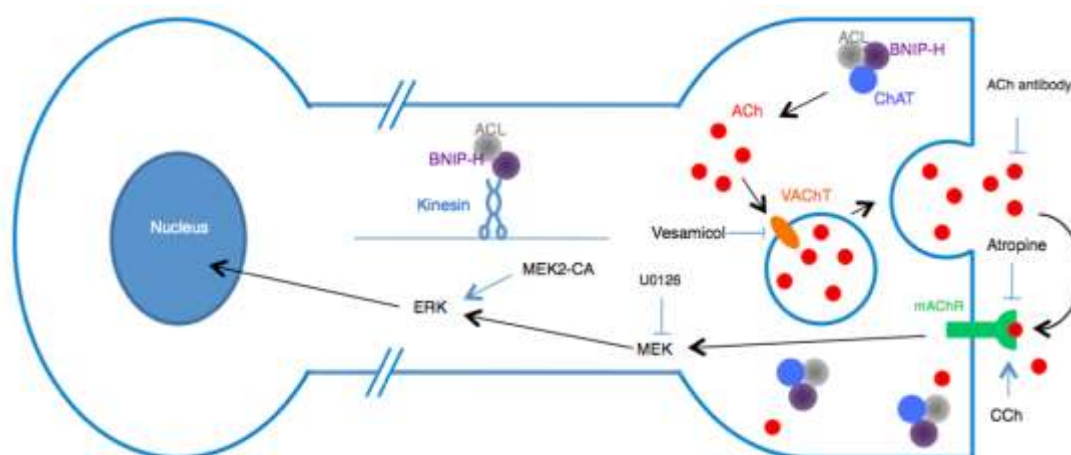


Figure 4-1 Mechanism of BNIP-H action in promoting neurite outgrowth.

BNIP-H transports ACL along the neurite by kinesin motor to neurite terminals and recruits ChAT to synthesize ACh, which is then packaged into synaptic vesicles by VACHT before secretion. Secreted ACh binds to mAChRs and activates intracellular MEK/ERK pathway to promote neurite outgrowth.

In chapter 3.1, I identified ACL as a novel binding partner of BNIP-H, and examined the effect of ACL and BNIP-H on neurite outgrowth of PC12 cells. Proteomics pull down assay showed that ACL was an endogenous binding partner of BNIP-H in PC12 cells and Neuro2a neuroblastoma cells. ACL and BNIP-H co-localized in the granules

along the microtubule and co-trafficked along the neurite. It was also demonstrated that BNIP-H and ACL required each other to promote neurite outgrowth. These results indicated that BNIP-H and ACL might form a complex to regulate neurite outgrowth. It is acknowledged that this study did not examine the interaction of BNIP-H and ACL in brain. Immunohistochemistry study showed that ACL is highly expressed in hippocampus and the granule layer of cerebellum, where BNIP-H is also highly expressed (Beigneux et al., 2004b; Buschdorf et al., 2006), suggesting that ACL and BNIP-H are expressed in the same regions of the brain. Further research is needed to characterize the interaction in brain. In particular, future studies should investigate the binding between ACL and BNIP-H in brain tissue.

In chapter 3.2, I explored how BNIP-H regulated ACL in PC12 cells. It was shown that BNIP-H functioned as a scaffold to link ACL and kinesin motor protein, and facilitated ACL trafficking from the cell body to the neurite terminal. This scaffold function of BNIP-H is in agreement with the result from a previous study (Aoyama et al., 2009), which indicated that BNIP-H acts as a scaffold to link kinesin motor protein and mitochondria. Moreover, our study suggested that BNIP-H also transports other cargos except for mitochondria, as ACL is known not to localize at mitochondria. This investigation may extend our understanding on how motor proteins actively transport the metabolism enzymes in neurons and how scaffold proteins regulate this process. Future study is to identify the organelle where BNIP-H and ACL co-localize.

In chapters 3.3 and 3.4, the downstream signaling pathway of BNIP-H and ACL was examined. The product acetyl-CoA catalyzed by ACL takes part in three main metabolism pathways in cytoplasm, which are fatty acid synthesis, cholesterol synthesis and acetylcholine synthesis. Among the three antagonists against the above three pathways, only the one against acetylcholine synthesis blocked the effect of BNIP-H on neurite outgrowth, indicating that the acetylcholine synthesis pathway may function downstream of BNIP-H. Moreover, it was shown that BNIP-H

up-regulated acetylcholine secretion in PC12 cells. These observations revealed that BNIP-H might play an important role in regulating acetylcholine secretion through transportation of the key enzyme AChE. This study also demonstrated that BNIP-H would regulate cholinergic neurotransmission in brain and BNIP-H deficiency like Cayman ataxia patients might cause acetylcholine secretion defect. This finding might suggest cholinergic agonists as novel therapeutic strategies for Cayman ataxia disease. Hence, the effect of BNIP-H on acetylcholine neurotransmission would be an important issue to be addressed. Firstly, acetylcholine level of cerebellum could be measured in BNIP-H knockout mice. Secondly, the effect of BNIP-H on acetylcholine neurotransmission should be examined in motor neuron-muscle co-cultured system. In addition, it has been reported that BNIP-H could inhibit the enzyme activity of KGA, which is used to produce glutamate in neurons (Buschdorf et al., 2006). Therefore, It will also be crucial to investigate whether BNIP-H regulates glutamate secretion in neurons and how BNIP-H coordinates glutamate and acetylcholine secretion.

In chapter 3.5, the intracellular signaling pathway induced by acetylcholine up-regulation was investigated. It was shown that muscarinic receptor antagonist blocked the neurite outgrowth induced by BNIP-H. Moreover, muscarinic receptor activation by BNIP-H stimulated MAPK pathway and therefore induced neurite outgrowth. These results further suggested that acetylcholine could act as an autocrine factor to promote neurite outgrowth. These observations provided the valuable insight into the role played by BNIP-H in coordinating acetylcholine secretion with neurite outgrowth. Interestingly, it has been shown that acetylcholine and NGF can play a synergic effect on neurite outgrowth in PC12 cells with M1 receptor overexpression (Berkeley and Levey, 2000). It will thus be interesting to determine if BNIP-H modulates acetylcholine receptor distribution on the cell membrane.

4.7 Future perspectives

The work presented here signifies that BNIP-H transports ACL from cell body to neurite terminal and regulates ACh release, and ACh functions through autocrine/paracrine loop to activate MAPK pathway for neuritogenesis. However, several further extensive studies are necessary to understand the neuronal function of BNIP-H (Figure 4-2).

First, it should be examined that whether KGA function similarly as ACL on neurotransmission and neurite outgrowth. KGA has been shown to be translocated by BNIP-H from cell body to neurite terminal (Buschdorf et al., 2006), so the dynamics of KGA along the neurite has to be performed to determine whether BNIP-H also functions as an adaptor for KGA and kinesin and whether BNIP-H co-regulates the trafficking of KGA and ACL. The glutamate release and glutamate effect on neurite outgrowth should be further characterized to provide intriguing insights to BNIP-H function in cellular trafficking and neurotransmission.

Second, other putative binding partners of BNIP-H should be evaluated. As shown in Figure 1-7, BNIP-H contains the motifs to interact with RhoA and Cdc42. And these small GTPase proteins are also important for neurite outgrowth and neurotransmitter release.

Third, the physiological function of BNIP-H should be investigated in a more systematic level. The present findings only provide evidence that BNIP-H might regulate neurite growth and neurotransmission in cell model. ACh is used for the communication between motor neurons and muscle cells. Spinal cord neuron and muscle cell co-culture system should be employed to study the effect of BNIP-H on the cholinergic communication in this system. In addition, conditional knock-in of BNIP-H mutants, which selectively interact with ACL or KGA, or the one present in Cayman ataxia patients and rodent models (Table 1-1), would elucidate the mechanism of Cayman ataxia disease.

Last but not the least, other BCH domain containing proteins should be investigated in neurotransmission and neurite outgrowth. BNIP-H, BMCC1, BNIP-XL and BNIP-2 are highly conserved BCH family proteins, which led us to speculate they might function similarly in nervous system. The neuronal function of BMCC1, BNIP-XL, BNIP-2 and other highly conserved protein in BNIP-H knockdown background would provide strong evidence to show the functional conservation among these proteins.

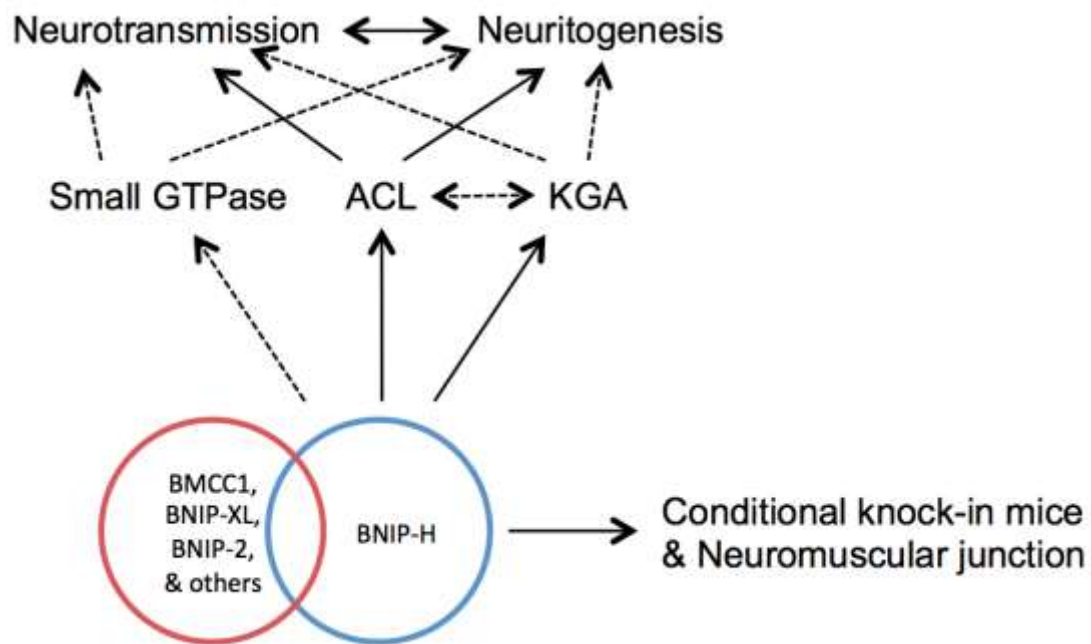


Figure 4-2. Schematic diagram of the future work.

Taken together, this thesis highlights the essential role of the ACL/BNIP-H/kinesin complex that is dynamically (BNIP-H dependent), directionally (kinesin-dependent) and functionally regulated (ACL active) to faithfully regulate cholinergic signaling. Although there is no effective treatment for Cayman ataxia or other cerebellar ataxia, clinical study demonstrates that choline and its derivatives can enhance cholinergic function and improve motor coordination in cerebellar ataxia (Livingstone et al., 1981). We speculate that deficiency in the cholinergic system may cause Cayman ataxia and other related dystonia. The immediate challenge is to determine the subregional flux of ACh, and the cholinergic routing of neurons in the brain. If the

production and release are impaired, rescue of cholinergic function by enhancing ACh synthesis and secretion or treatment with cholinergic agonist, could be potential therapies in ataxia/dystonia disease.

Bibliography

Albuquerque, E.X., Pereira, E.F.R., Alkondon, M., and Rogers, S.W. (2009). Mammalian Nicotinic Acetylcholine Receptors: From Structure to Function. *Physiol Rev* 89, 73-120.

Altin, J.G., Kujubu, D.A., Raffioni, S., Eveleth, D.D., Herschman, H.R., and Bradshaw, R.A. (1991). Differential induction of primary-response (TIS) genes in PC12 pheochromocytoma cells and the unresponsive variant PC12nnr5. *The Journal of biological chemistry* 266, 5401-5406.

Aoyama, T., Hata, S., Nakao, T., Tanigawa, Y., Oka, C., and Kawaichi, M. (2009). Cayman ataxia protein caytaxin is transported by kinesin along neurites through binding to kinesin light chains. *Journal of cell science* 122, 4177-4185.

Apps, R., and Garwicz, M. (2005). Anatomical and physiological foundations of cerebellar information processing. *Nature reviews Neuroscience* 6, 297-311.

Arama, J., Boulay, A.C., Bosc, C., Delphin, C., Loew, D., Rostaing, P., Amigou, E., Ezan, P., Wingertsmann, L., Guillaud, L., *et al.* (2012). Bmcc1s, a novel brain-isoform of Bmcc1, affects cell morphology by regulating MAP6/STOP functions. *PLoS one* 7, e35488.

Barmack, N.H., Baughman, R.W., and Eckenstein, F.P. (1992). Cholinergic Innervation of the Cerebellum of Rat, Rabbit, Cat, and Monkey as Revealed by Choline-Acetyltransferase Activity and Immunohistochemistry. *J Comp Neurol* 317, 233-249.

Beales, M., Lorden, J.F., Walz, E., and Oltmans, G.A. (1990). Quantitative autoradiography reveals selective changes in cerebellar GABA receptors of the rat mutant dystonic. *The Journal of neuroscience : the official journal of the Society for Neuroscience* 10, 1874-1885.

Beigneux, A.P., Kosinski, C., Gavino, B., Horton, J.D., Skarnes, W.C., and Young, S.G. (2004a). ATP-citrate lyase deficiency in the mouse. *Journal of Biological Chemistry* 279, 9557-9564.

Beigneux, A.P., Kosinski, C., Gavino, B., Horton, J.D., Skarnes, W.C., and Young, S.G. (2004b). ATP-citrate lyase deficiency in the mouse. *The Journal of biological chemistry* 279, 9557-9564.

Berglund, E.O., Murai, K.K., Fredette, B., Sekerkova, G., Marturano, B., Weber, L., Mugnaini, E., and Ranscht, B. (1999). Ataxia and abnormal cerebellar microorganization in mice with ablated contactin gene expression. *Neuron* 24, 739-750.

Berkeley, J.L., and Levey, A.I. (2000). Muscarinic activation of mitogen-activated

protein kinase in PC12 cells. *Journal of neurochemistry* 75, 487-493.

Bignami, F., Bevilacqua, P., Biagioni, S., De Jaco, A., Casamenti, F., Felsani, A., and Augusti-Tocco, G. (1997). Cellular acetylcholine content and neuronal differentiation. *Journal of neurochemistry* 69, 1374-1381.

Bomar, J.M., Benke, P.J., Slattery, E.L., Puttagunta, R., Taylor, L.P., Seong, E., Nystuen, A., Chen, W., Albin, R.L., Patel, P.D., *et al.* (2003). Mutations in a novel gene encoding a CRAL-TRIO domain cause human Cayman ataxia and ataxia/dystonia in the jittery mouse. *Nature genetics* 35, 264-269.

Boulay, A.C., Burbassi, S., Lorenzo, H.K., Loew, D., Ezan, P., Giaume, C., and Cohen-Salmon, M. (2013). Bmcc1s interacts with the phosphate-activated glutaminase in the brain. *Biochimie* 95, 799-807.

Bovolenta, P., and Fernaud-Espinosa, I. (2000). Nervous system proteoglycans as modulators of neurite outgrowth. *Prog Neurobiol* 61, 113-132.

Boyd, J.M., Malstrom, S., Subramanian, T., Venkatesh, L.K., Schaeper, U., Elangovan, B., D'Sa-Eipper, C., and Chinnadurai, G. (1994). Adenovirus E1B 19 kDa and Bcl-2 proteins interact with a common set of cellular proteins. *Cell* 79, 341-351.

Bravarenko, N.I., Onufriev, M.V., Stepanichev, M.Y., Ierusalimsky, V.N., Balaban, P.M., and Gulyaeva, N.V. (2006). Caspase-like activity is essential for long-term synaptic plasticity in the terrestrial snail *Helix*. *Eur J Neurosci* 23, 129-140.

Brose, K., Bland, K.S., Wang, K.H., Arnott, D., Henzel, W., Goodman, C.S., Tessier-Lavigne, M., and Kidd, T. (1999). Slit proteins bind Robo receptors and have an evolutionarily conserved role in repulsive axon guidance. *Cell* 96, 795-806.

Brown, A., Yates, P.A., Burrola, P., Ortuno, D., Vaidya, A., Jessell, T.M., Pfaff, S.L., O'Leary, D.D.M., and Lemke, G. (2000). Topographic mapping from the retina to the midbrain is controlled by relative but not absolute levels of EphA receptor signaling. *Cell* 102, 77-88.

Brown, L.L., and Lorden, J.F. (1989). Regional cerebral glucose utilization reveals widespread abnormalities in the motor system of the rat mutant dystonic. *The Journal of neuroscience : the official journal of the Society for Neuroscience* 9, 4033-4041.

Buschdorf, J.P., Chew, L.L., Soh, U.J., Liou, Y.C., and Low, B.C. (2008). Nerve growth factor stimulates interaction of Cayman ataxia protein BNIP-H/Caytaxin with peptidyl-prolyl isomerase Pin1 in differentiating neurons. *PloS one* 3, e2686.

Buschdorf, J.P., Li Chew, L., Zhang, B., Cao, Q., Liang, F.Y., Liou, Y.C., Zhou, Y.T., and Low, B.C. (2006). Brain-specific BNIP-2-homology protein Caytaxin relocalises glutaminase to neurite terminals and reduces glutamate levels. *Journal of cell science* 119, 3337-

3350.

Caulfield, M.P., and Birdsall, N.J.M. (1998). International Union of Pharmacology. XVII. Classification of muscarinic acetylcholine receptors. *Pharmacol Rev* 50, 279-290.

Challacombe, J.F., Snow, D.M., and Letourneau, P.C. (1996). Actin filament bundles are required for microtubule reorientation during growth cone turning to avoid an inhibitory guidance cue. *Journal of cell science* 109, 2031-2040.

Clapp, K.M., Peng, H.M., Jenkins, G.J., Ford, M.J., Morishima, Y., Lau, M., and Osawa, Y. (2012). Ubiquitination of neuronal nitric-oxide synthase in the calmodulin-binding site triggers proteasomal degradation of the protein. *The Journal of biological chemistry* 287, 42601-42610.

Collins, G.G.S. (1972). Gaba-2-Oxoglutarate Transaminase, Glutamate Decarboxylase and Half-Life of Gaba in Different Areas of Rat-Brain. *Biochemical pharmacology* 21, 2849-8.

Crabb, J.W., Gaur, V.P., Garwin, G.G., Marx, S.V., Chapline, C., Johnson, C.M., and Saari, J.C. (1991). Topological and epitope mapping of the cellular retinaldehyde-binding protein from retina. *The Journal of biological chemistry* 266, 16674-16683.

Damon, D.H., Damore, P.A., and Wagner, J.A. (1990). Nerve Growth-Factor and Fibroblast Growth-Factor Regulate Neurite Outgrowth and Gene-Expression in Pc12 Cells Via Both Protein Kinase-C-Independent and Camp-Independent Mechanisms. *Journal of Cell Biology* 110, 1333-1339.

Das, K.P., Freudenrich, T.M., and Mundy, W.R. (2004). Assessment of PC12 cell differentiation and neurite growth: a comparison of morphological and neurochemical measures. *Neurotoxicology and teratology* 26, 397-406.

Davie, J.T., Clark, B.A., and Hausser, M. (2008). The origin of the complex spike in cerebellar Purkinje cells. *The Journal of neuroscience : the official journal of the Society for Neuroscience* 28, 7599-7609.

De Jaco, A., Augusti-Tocco, G., and Biagioni, S. (2002). Muscarinic acetylcholine receptors induce neurite outgrowth and activate the synapsin I gene promoter in neuroblastoma clones. *Neuroscience* 113, 331-338.

de Montigny, C., and Lamarre, Y. (1973). Rhythmic activity induced by harmaline in the olivo-cerebello-bulbar system of the cat. *Brain research* 53, 81-95.

Debant, A., Serra-Pages, C., Seipel, K., O'Brien, S., Tang, M., Park, S.H., and Streuli, M. (1996). The multidomain protein Trio binds the LAR transmembrane tyrosine phosphatase, contains a protein kinase domain, and has separate rac-specific and rho-specific guanine nucleotide exchange factor domains. *Proceedings of the National Academy of Sciences of the United States of America* 93, 5466-5471.

Dodding, M.P., Mitter, R., Humphries, A.C., and Way, M. (2011). A kinesin-1 binding motif in vaccinia virus that is widespread throughout the human genome. *The EMBO journal* 30, 4523-4538.

Dou, C.L., and Levine, J.M. (1994). Inhibition of Neurite Growth by the Ng2 Chondroitin Sulfate Proteoglycan. *Journal of Neuroscience* 14, 7616-7628.

Eglen, R.M., Choppin, A., and Watson, N. (2001). Therapeutic, opportunities from muscarinic receptor research. *Trends Pharmacol Sci* 22, 409-414.

Eissing, A., Fischer, D., Rauch, I., Baumann, A., Schebb, N.H., Karst, U., Rose, K., Klumpp, S., and Kriegstein, J. (2012). Acetylcholine content and viability of cholinergic neurons are influenced by the activity of protein histidine phosphatase. *BMC neuroscience* 13.

Elshourbagy, N.A., Near, J.C., Kmetz, P.J., Sathe, G.M., Southan, C., Strickler, J.E., Gross, M., Young, J.F., Wells, T.N.C., and Groot, P.H.E. (1990). Rat Atp Citrate-Lyase - Molecular-Cloning and Sequence-Analysis of a Full-Length Cdna and Messenger-Rna Abundance as a Function of Diet, Organ, and Age. *Journal of Biological Chemistry* 265, 1430-1435.

Endemann, G., and Brunengraber, H. (1980). The source of acetyl coenzyme A for acetylcholine synthesis in the perfused rat phrenic nerve-hemidiaphragm. *The Journal of biological chemistry* 255, 11091-11093.

Eva, R., Dassie, E., Caswell, P.T., Dick, G., ffrench-Constant, C., Norman, J.C., and Fawcett, J.W. (2010). Rab11 and its effector Rab coupling protein contribute to the trafficking of beta 1 integrins during axon growth in adult dorsal root ganglion neurons and PC12 cells. *The Journal of neuroscience : the official journal of the Society for Neuroscience* 30, 11654-11669.

Fan, F., Williams, H.J., Boyer, J.G., Graham, T.L., Zhao, H., Lehr, R., Qi, H., Schwartz, B., Raushel, F.M., and Meek, T.D. (2012). On the catalytic mechanism of human ATP citrate lyase. *Biochemistry* 51, 5198-5211.

Felder, C.C., Bymaster, F.P., Ward, J., and DeLapp, N. (2000). Therapeutic opportunities for muscarinic receptors in the central nervous system. *Journal of medicinal chemistry* 43, 4333-4353.

Fernando, P., Brunette, S., and Megeney, L.A. (2005). Neural stem cell differentiation is dependent upon endogenous caspase-3 activity. *Faseb Journal* 19, 1671-+.

Fink-Jensen, A., Schmidt, L.S., Dencker, D., Schulein, C., Wess, J., Wortwein, G., and Woldbye, D.P.D. (2011). Antipsychotic-induced catalepsy is attenuated in mice lacking the M-4 muscarinic acetylcholine receptor. *European journal of pharmacology* 656, 39-44.

Freneau, R.T., Jr., Burman, J., Qureshi, T., Tran, C.H., Proctor, J., Johnson, J., Zhang, H., Sulzer, D., Copenhagen, D.R., Storm-Mathisen, J., *et al.* (2002). The identification of vesicular glutamate transporter 3 suggests novel modes of signaling by glutamate. *Proceedings of the National Academy of Sciences of the United States of America* *99*, 14488-14493.

Friedlander, D.R., Milev, P., Karthikeyan, L., Margolis, R.K., Margolis, R.U., and Grumet, M. (1994). Neuronal Chondroitin Sulfate Proteoglycan Neurocan Binds to the Neural Cell-Adhesion Molecules Ng-Cam/L1/Nile and N-Cam, and Inhibits Neuronal Adhesion and Neurite Outgrowth. *Journal of Cell Biology* *125*, 669-680.

Frotscher, M., Schlander, M., and Leranth, C. (1986). Cholinergic neurons in the hippocampus. A combined light- and electron-microscopic immunocytochemical study in the rat. *Cell and tissue research* *246*, 293-301.

Fu, B., Gao, X., Zhang, S.P., Cai, Z., and Shen, J. (2008). Quantification of acetylcholine in microdialysate of subcutaneous tissue by hydrophilic interaction chromatography/tandem mass spectrometry. *Rapid communications in mass spectrometry : RCM* *22*, 1497-1502.

Gauthier, L.R., Charrin, B.C., Borrell-Pages, M., Dompierre, J.P., Rangone, H., Cordelieres, F.P., De Mey, J., MacDonald, M.E., Lessmann, V., Humbert, S., *et al.* (2004). Huntingtin controls neurotrophic support and survival of neurons by enhancing BDNF vesicular transport along microtubules. *Cell* *118*, 127-138.

Geisbrecht, E.R., and Montell, D.J. (2004). A role for Drosophila IAP1-mediated caspase inhibition in Rac-dependent cell migration. *Cell* *118*, 111-125.

Gho, M., Mcdonald, K., Ganetzky, B., and Saxton, W.M. (1992). Effects of Kinesin Mutations on Neuronal Functions. *Science* *258*, 313-316.

Goldberg, D.J., and Burmeister, D.W. (1986). Stages in axon formation: observations of growth of Aplysia axons in culture using video-enhanced contrast-differential interference contrast microscopy. *The Journal of cell biology* *103*, 1921-1931.

Gras, C., Amilhon, B., Lopicard, E.M., Poirel, O., Vinatier, J., Herbin, M., Dumas, S., Tzavara, E.T., Wade, M.R., Nomikos, G.G., *et al.* (2008). The vesicular glutamate transporter VGLUT3 synergizes striatal acetylcholine tone. *Nat Neurosci* *11*, 292-300.

Greene, L.A. (1978). Nerve growth factor prevents the death and stimulates the neuronal differentiation of clonal PC12 pheochromocytoma cells in serum-free medium. *The Journal of cell biology* *78*, 747-755.

Grelle, G., Kostka, S., Otto, A., Kersten, B., Genser, K.F., Muller, E.C., Walter, S., Boddich, A., Stelzl, U., Hanig, C., *et al.* (2006). Identification of VCP/p97, carboxyl terminus of Hsp70-interacting protein (CHIP), and amphiphysin II interaction partners using membrane-based human proteome arrays. *Mol Cell Proteomics* *5*, 234-244.

Gupta, A.B., Wee, L.E., Zhou, Y.T., Hortsch, M., and Low, B.C. (2012). Cross-species analyses identify the BNIP-2 and Cdc42GAP homology (BCH) domain as a distinct functional subclass of the CRAL_TRIO/Sec14 superfamily. *PLoS one* 7, e33863.

Hatzivassiliou, G., Zhao, F.P., Bauer, D.E., Andreadis, C., Shaw, A.N., Dhanak, D., Hingorani, S.R., Tuveson, D.A., and Thompson, C.B. (2005). ATP citrate lyase inhibition can suppress tumor cell growth. *Cancer cell* 8, 311-321.

Hayakawa, Y., Itoh, M., Yamada, A., Mitsuda, T., and Nakagawa, T. (2007). Expression and localization of Cayman ataxia-related protein, Caytaxin, is regulated in a developmental- and spatial-dependent manner. *Brain research* 1129, 100-109.

Hayashi, H., and Kato, T. (1978). Acetyl-Coa Synthesizing Enzyme-Activities in Single Nerve-Cell Bodies of Rabbit. *Journal of neurochemistry* 31, 861-869.

Haydon, P.G., McCobb, D.P., and Kater, S.B. (1987). The regulation of neurite outgrowth, growth cone motility, and electrical synaptogenesis by serotonin. *J Neurobiol* 18, 197-215.

Himanen, J.P., and Nikolov, D.B. (2003). Eph receptors and ephrins. *Int J Biochem Cell B* 35, 130-134.

Hirokawa, N., Noda, Y., Tanaka, Y., and Niwa, S. (2009). Kinesin superfamily motor proteins and intracellular transport. *Nat Rev Mol Cell Bio* 10, 682-696.

Hirokawa, N., and Takemura, R. (2005). Molecular motors and mechanisms of directional transport in neurons. *Nature reviews Neuroscience* 6, 201-214.

Hodges, J.R. (2006). Alzheimer's centennial legacy: origins, landmarks and the current status of knowledge concerning cognitive aspects. *Brain : a journal of neurology* 129, 2811-2822.

Huang, E.J., and Reichardt, L.F. (2001). Neurotrophins: Roles in neuronal development and function. *Annu Rev Neurosci* 24, 677-736.

Itoh, M., Li, S.M., Ohta, K., Yamada, A., Hayakawa-Yano, Y., Ueda, M., Hida, Y., Suzuki, Y., Ohta, E., Mizuno, A., *et al.* (2011). Cayman Ataxia-Related Protein is a Presynapse-Specific Caspase-3 Substrate. *Neurochemical research* 36, 1304-1313.

Jackson, M.B., and Chapman, E.R. (2006). Fusion pores and fusion machines in Ca(2+)-triggered exocytosis. *Annu Rev Bioph Biom* 35, 135-160.

Kang, J.S., Bae, G.U., Yi, M.J., Yang, Y.J., Oh, J.E., Takaesu, G., Zhou, Y.T., Low, B.C., and Krauss, R.S. (2008). A Cdo-Bnip-2-Cdc42 signaling pathway regulates p38 alpha/beta MAPK activity and myogenic differentiation. *Journal of Cell Biology* 182, 497-507.

Kapfhammer, D., Sweet, H.O., Sufalko, D., Warren, S., Johnson, K.R., and Burmeister, M.

(1996). The neurological mouse mutations jittery and hesitant are allelic and map to the region of mouse chromosome 10 homologous to 19p13.3. *Genomics* 35, 533-538.

Kashiwabuchi, N., Ikeda, K., Araki, K., Hirano, T., Shibuki, K., Takayama, C., Inoue, Y., Kutsuwada, T., Yagi, T., Kang, Y., *et al.* (1995). Impairment of motor coordination, Purkinje cell synapse formation, and cerebellar long-term depression in GluR delta 2 mutant mice. *Cell* 81, 245-252.

Keleman, K., and Dickson, B.J. (2001). Short- and long-range repulsion by the *Drosophila* Unc5 netrin receptor. *Neuron* 32, 605-617.

Kim, K.H., Ha, J.H., Chung, S.H., Kim, C.T., Kim, S.K., Hyun, B.H., Sawada, K., Fukui, Y., Park, I.K., Lee, G.J., *et al.* (2003). Glutamate and GABA concentrations in the cerebellum of novel ataxic mutant Pogo mice. *Journal of veterinary science* 4, 209-212.

Kiryushko, D., Berezin, V., and Bock, E. (2004). Regulators of neurite outgrowth: role of cell adhesion molecules. *Annals of the New York Academy of Sciences* 1014, 140-154.

Kravtsova-Ivantsiv, Y., and Ciechanover, A. (2012). Non-canonical ubiquitin-based signals for proteasomal degradation. *Journal of cell science* 125, 539-548.

Kvamme, E., Roberg, B., and Torgner, I.A. (2000). Phosphate-activated glutaminase and mitochondrial glutamine transport in the brain. *Neurochemical research* 25, 1407-1419.

Lamarre, Y., de Montigny, C., Dumont, M., and Weiss, M. (1971). Harmaline-induced rhythmic activity of cerebellar and lower brain stem neurons. *Brain research* 32, 246-250.

Lancaster, C.A., Taylor-Harris, P.M., Self, A.J., Brill, S., van Erp, H.E., and Hall, A. (1994). Characterization of rhoGAP. A GTPase-activating protein for rho-related small GTPases. *The Journal of biological chemistry* 269, 1137-1142.

Lankford, K.L., Demello, F.G., and Klein, W.L. (1988). D1-Type Dopamine-Receptors Inhibit Growth Cone Motility in Cultured Retina Neurons - Evidence That Neurotransmitters Act as Morphogenic Growth-Regulators in the Developing Central Nervous-System. *Proceedings of the National Academy of Sciences of the United States of America* 85, 2839-2843.

Lazarov, O., Morfini, G.A., Lee, E.B., Farah, M.H., Szodorai, A., DeBoer, S.R., Koliatsos, V.E., Kins, S., Lee, V.M., Wong, P.C., *et al.* (2005). Axonal transport, amyloid precursor protein, kinesin-1, and the processing apparatus: revisited. *The Journal of neuroscience : the official journal of the Society for Neuroscience* 25, 2386-2395.

Lazarov, O., Morfini, G.A., Pigino, G., Gadadhar, A., Chen, X., Robinson, J., Ho, H., Brady, S.T., and Sisodia, S.S. (2007). Impairments in fast axonal transport and motor neuron deficits in transgenic mice expressing familial Alzheimer's disease-linked mutant presenilin 1. *The Journal of neuroscience : the official journal of the Society for Neuroscience* *27*, 7011-7020.

LeDoux, M.S. (2011). Animal models of dystonia: Lessons from a mutant rat. *Neurobiol Dis* *42*, 152-161.

LeDoux, M.S., Lorden, J.F., and Meinzen-Derr, J. (1995). Selective elimination of cerebellar output in the genetically dystonic rat. *Brain research* *697*, 91-103.

Lee, M.K., Tuttle, J.B., Rebhun, L.I., Cleveland, D.W., and Frankfurter, A. (1990). The Expression and Posttranslational Modification of a Neuron-Specific Beta-Tubulin Isozyme during Chick Embryogenesis. *Cell Motil Cytoskel* *17*, 118-132.

Lentz, S.I., Knudson, C.M., Korsmeyer, S.J., and Snider, W.D. (1999). Neurotrophins support the development of diverse sensory axon morphologies. *Journal of Neuroscience* *19*, 1038-1048.

Li, Y.S., Milner, P.G., Chauhan, A.K., Watson, M.A., Hoffman, R.M., Kodner, C.M., Milbrandt, J., and Deuel, T.F. (1990). Cloning and expression of a developmentally regulated protein that induces mitogenic and neurite outgrowth activity. *Science* *250*, 1690-1694.

Lipton, S.A., Frosch, M.P., Phillips, M.D., Tauck, D.L., and Aizenman, E. (1988). Nicotinic Antagonists Enhance Process Outgrowth by Rat Retinal Ganglion-Cells in Culture. *Science* *239*, 1293-1296.

Lipton, S.A., and Kater, S.B. (1989). Neurotransmitter Regulation of Neuronal Outgrowth, Plasticity and Survival. *Trends Neurosci* *12*, 265-270.

Liu, J., Lamb, D., Chou, M.M., Liu, Y.J., and Li, G. (2007). Nerve growth factor-mediated neurite outgrowth via regulation of Rab5. *Molecular biology of the cell* *18*, 1375-1384.

Livingstone, I.R., Mastaglia, F.L., Pennington, R.J.T., and Skilbeck, C. (1981). Choline Chloride in the Treatment of Cerebellar and Spinocerebellar Ataxia. *Journal of the neurological sciences* *50*, 161-174.

Lorden, J.F., Lutes, J., Michela, V.L., and Ervin, J. (1992). Abnormal cerebellar output in rats with an inherited movement disorder. *Experimental neurology* *118*, 95-104.

Lorden, J.F., McKeon, T.W., Baker, H.J., Cox, N., and Walkley, S.U. (1984). Characterization of the rat mutant dystonic (dt): a new animal model of dystonia musculorum deformans. *The Journal of neuroscience : the official journal of the Society for Neuroscience* *4*, 1925-1932.

Lorden, J.F., Oltmans, G.A., McKeon, T.W., Lutes, J., and Beales, M. (1985). Decreased cerebellar 3',5'-cyclic guanosine monophosphate levels and insensitivity to harmaline in the genetically dystonic rat (dt). *The Journal of neuroscience : the official journal of the Society for Neuroscience* 5, 2618-2625.

Low, B.C., Lim, Y.P., Lim, J., Wong, E.S., and Guy, G.R. (1999). Tyrosine phosphorylation of the Bcl-2-associated protein BNIP-2 by fibroblast growth factor receptor-1 prevents its binding to Cdc42GAP and Cdc42. *The Journal of biological chemistry* 274, 33123-33130.

Low, B.C., Seow, K.T., and Guy, G.R. (2000a). The BNIP-2 and Cdc42GAP homology domain of BNIP-2 mediates its homophilic association and heterophilic interaction with Cdc42GAP. *The Journal of biological chemistry* 275, 37742-37751.

Low, B.C., Seow, K.T., and Guy, G.R. (2000b). Evidence for a novel Cdc42GAP domain at the carboxyl terminus of BNIP-2. *The Journal of biological chemistry* 275, 14415-14422.

Lua, B.L., and Low, B.C. (2004). BPGAP1 interacts with cortactin and facilitates its translocation to cell periphery for enhanced cell migration. *Molecular biology of the cell* 15, 2873-2883.

Lua, B.L., and Low, B.C. (2005). Activation of EGF receptor endocytosis and ERK1/2 signaling by BPGAP1 requires direct interaction with EEN/endophilin 11 and a functional RhoGAP domain. *Journal of cell science* 118, 2707-2721.

Machida, T., Fujita, T., Ooo, M.L., Ohira, M., Isogai, E., Mihara, M., Hirato, J., Tomotsune, D., Hirata, T., Fujimori, M., *et al.* (2006). Increased expression of proapoptotic BMCC1, a novel gene with the BNIP2 and Cdc42GAP homology (BCH) domain, is associated with favorable prognosis in human neuroblastomas. *Oncogene* 25, 1931-1942.

Mallavarapu, A., and Mitchison, T. (1999). Regulated actin cytoskeleton assembly at filopodium tips controls their extension and retraction. *Journal of Cell Biology* 146, 1097-1106.

Mandelkow, E., and Mandelkow, E.M. (1995). Microtubules and microtubule-associated proteins. *Current opinion in cell biology* 7, 72-81.

Manitt, C., and Kennedy, T.E. (2002). Where the rubber meets the road: netrin expression and function in developing and adult nervous systems. *Prog Brain Res* 137, 425-442.

Mark, M.D., Liu, Y.C., Wong, S.T., Hinds, T.R., and Storm, D.R. (1995). Stimulation of Neurite Outgrowth in Pc12 Cells by Egf and KCl Depolarization - a Ca²⁺-Independent Phenomenon. *Journal of Cell Biology* 130, 701-710.

Marsh, L., and Letourneau, P.C. (1984). Growth of Neurites without Filopodial or Lamellipodial Activity in the Presence of Cytochalasin-B. *Journal of Cell Biology* 99, 2041-2047.

Marshall, C.J. (1995). Specificity of receptor tyrosine kinase signaling: transient versus sustained extracellular signal-regulated kinase activation. *Cell* 80, 179-185.

McKeon, T.W., Lorden, J.F., Oltmans, G.A., Beales, M., and Walkley, S.U. (1984). Decreased catalepsy response to haloperidol in the genetically dystonic (dt) rat. *Brain research* 308, 89-96.

Michela, V.L., Stratton, S.E., and Lorden, J.F. (1990). Enhanced sensitivity to quipazine in the genetically dystonic rat (dt). *Pharmacology, biochemistry, and behavior* 37, 129-133.

Mortimer, D., Fothergill, T., Pujic, Z., Richards, L.J., and Goodhill, G.J. (2008). Growth cone chemotaxis. *Trends Neurosci* 31, 90-98.

Mount, H.T., Dreyfus, C.F., and Black, I.B. (1994). Muscarinic stimulation promotes cultured Purkinje cell survival: a role for acetylcholine in cerebellar development? *Journal of neurochemistry* 63, 2065-2073.

Nachmansohn, D., and Machado, A.L. (1943). The formation of acetylcholine. A new enzyme: "Choline acetylase". *Journal of neurophysiology* 6, 397-403.

Ng, C.E.L., and Tang, B.L. (2002). Nogos and the Nogo-66 receptor: Factors inhibiting CNS neuron regeneration. *Journal of neuroscience research* 67, 559-565.

Nikali, K., Suomalainen, A., Terwilliger, J., Koskinen, T., Weissenbach, J., and Peltonen, L. (1995). Random search for shared chromosomal regions in four affected individuals: the assignment of a new hereditary ataxia locus. *American journal of human genetics* 56, 1088-1095.

Nolo, R., Kaksonen, M., and Rauvala, H. (1996). Developmentally regulated neurite outgrowth response from dorsal root ganglion neurons to heparin-binding growth-associated molecule (HB-GAM) and the expression of HB-GAM in the targets of the developing dorsal root ganglion neurites. *Eur J Neurosci* 8, 1658-1665.

Nordman, J.C., and Kabbani, N. (2012). An interaction between alpha 7 nicotinic receptors and a G-protein pathway complex regulates neurite growth in neural cells. *Journal of cell science* 125, 5502-5513.

Nystuen, A., Benke, P.J., Merren, J., Stone, E.M., and Sheffield, V.C. (1996). A cerebellar ataxia locus identified by DNA pooling to search for linkage disequilibrium in an isolated population from the Cayman Islands. *Human molecular genetics* 5, 525-531.

Oh, J.E., Bae, G.U., Yang, Y.J., Yi, M.J., Lee, H.J., Kim, B.G., Krauss, R.S., and Kang, J.S. (2009). Cdo promotes neuronal differentiation via activation of the p38 mitogen-activated protein kinase pathway. *Faseb Journal* 23, 2088-2099.

Oltmans, G.A., Beales, M., Lorden, J.F., and Gordon, J.H. (1984). Alterations in cerebellar glutamic acid decarboxylase (GAD) activity in a genetic model of torsion dystonia (rat). *Experimental neurology* 85, 216-222.

Pan, C.Q., Liou, Y.C., and Low, B.C. (2010). Active Mek2 as a regulatory scaffold that promotes Pin1 binding to BPGAP1 to suppress BPGAP1-induced acute Erk activation and cell migration. *Journal of cell science* 123, 903-916.

Pan, C.Q., and Low, B.C. (2012). Functional plasticity of the BNIP-2 and Cdc42GAP Homology (BCH) domain in cell signaling and cell dynamics. *FEBS letters* 586, 2674-2691.

Pan, C.Q., Sudol, M., Sheetz, M., and Low, B.C. (2012). Modularity and functional plasticity of scaffold proteins as p(l)acemakers in cell signaling. *Cellular signalling* 24, 2143-2165.

Panagabko, C., Morley, S., Hernandez, M., Cassolato, P., Gordon, H., Parsons, R., Manor, D., and Atkinson, J. (2003). Ligand specificity in the CRAL-TRIO protein family. *Biochemistry* 42, 6467-6474.

Patterson, P.H. (1988). On the Importance of Being Inhibited, or Saying No to Growth Cones. *Neuron* 1, 263-267.

Perrone-Bizzozero, N.I., Cansino, V.V., and Kohn, D.T. (1993). Posttranscriptional regulation of GAP-43 gene expression in PC12 cells through protein kinase C-dependent stabilization of the mRNA. *The Journal of cell biology* 120, 1263-1270.

Phillips, S.E., Sha, B.D., Topalof, L., Xie, Z.G., Alb, J.G., Klenchin, V.A., Swigart, P., Cockcroft, S., Martin, T.F.J., Luo, M., *et al.* (1999). Yeast Sec14p deficient in phosphatidylinositol transfer activity is functional in vivo. *Mol Cell* 4, 187-197.

Pinkas-Kramarski, R., Stein, R., Lindenboim, L., and Sokolovsky, M. (1992). Growth factor-like effects mediated by muscarinic receptors in PC12M1 cells. *Journal of neurochemistry* 59, 2158-2166.

Polinsky, R.J., Holmes, K.V., Brown, R.T., and Weise, V. (1989). Csf Acetylcholinesterase Levels Are Reduced in Multiple System Atrophy with Autonomic Failure. *Neurology* 39, 40-44.

Rauvala, H. (1989). An 18-Kd Heparin-Binding Protein of Developing Brain That Is Distinct from Fibroblast Growth-Factors. *Embo Journal* 8, 2933-2941.

Ravichandran, A., and Low, B.C. (2013). SmgGDS antagonizes BPGAP1-induced

Ras/ERK activation and neuritogenesis in PC12 cell differentiation. *Molecular biology of the cell* 24, 145-156.

Reisine, T.D., Azari, J., Johnson, P.C., Barbeau, A., Huxtable, R., and Yamamura, H.I. (1979). Brain neurotransmitter receptors in Friedreich's ataxia. *Can J Neurol Sci* 6, 259-262.

Richardson, P.M., McGuinness, U.M., and Aguayo, A.J. (1980). Axons from Cns Neurons Regenerate into Pns Grafts. *Nature* 284, 264-265.

Riehl, R., Johnson, K., Bradley, R., Grunwald, G.B., Cornel, E., Lilienbaum, A., and Holt, C.E. (1996). Cadherin function is required for axon outgrowth in retinal ganglion cells in vivo. *Neuron* 17, 837-848.

Rinaldo, L., and Hansel, C. (2013). Muscarinic acetylcholine receptor activation blocks long-term potentiation at cerebellar parallel fiber-Purkinje cell synapses via cannabinoid signaling. *Proceedings of the National Academy of Sciences of the United States of America*.

Rong, J., McGuire, J.R., Fang, Z.H., Sheng, G., Shin, J.Y., Li, S.H., and Li, X.J. (2006). Regulation of intracellular trafficking of huntingtin-associated protein-1 is critical for TrkA protein levels and neurite outgrowth. *The Journal of neuroscience : the official journal of the Society for Neuroscience* 26, 6019-6030.

Sadananda, A., Hamid, R., Doodhi, H., Ghosal, D., Girotra, M., Jana, S.C., and Ray, K. (2012). Interaction with a kinesin-2 tail propels choline acetyltransferase flow towards synapse. *Traffic* 13, 979-991.

Salani, M., Anelli, T., Tocco, G.A., Lucarini, E., Mozzetta, C., Poiana, G., Tata, A.M., and Biagioni, S. (2009). Acetylcholine-induced neuronal differentiation: muscarinic receptor activation regulates EGR-1 and REST expression in neuroblastoma cells. *Journal of neurochemistry* 108, 821-834.

Salehi, A., Delcroix, J.D., Belichenko, P.V., Zhan, K., Wu, C., Valletta, J.S., Takimoto-Kimura, R., Kleschevnikov, A.M., Sambamurti, K., Chung, P.P., *et al.* (2006). Increased App expression in a mouse model of Down's syndrome disrupts NGF transport and causes cholinergic neuron degeneration. *Neuron* 51, 29-42.

Salinas, S., Bilsland, L.G., and Schiavo, G. (2008). Molecular landmarks along the axonal route: axonal transport in health and disease. *Current opinion in cell biology* 20, 445-453.

Schmahmann, J.D. (2004). Disorders of the cerebellum: ataxia, dysmetria of thought, and the cerebellar cognitive affective syndrome. *The Journal of neuropsychiatry and clinical neurosciences* 16, 367-378.

Scott, G.B., Bowles, P.A., Wilson, E.B., Meade, J.L., Low, B.C., Davison, A., Blair, G.E.,

and Cook, G.P. (2010). Identification of the BCL2/adenovirus E1B-19K protein-interacting protein 2 (BNIP-2) as a granzyme B target during human natural killer cell-mediated killing. *Biochemical Journal* 431, 423-431.

Seidman, C., Struhl, K., Sheen, J., and Jessen, T. (2001). Introduction of plasmid DNA into cells. *Current protocols in molecular biology* / edited by Frederick M Ausubel [et al] *Chapter 1*.

Shang, X., Zhou, Y.T., and Low, B.C. (2003). Concerted regulation of cell dynamics by BNIP-2 and Cdc42GAP Homology/Sec14p-like, Proline-rich, and GTPase-activating protein domains of a novel Rho GTPase-activating protein, BPGAP1. *Journal of Biological Chemistry* 278, 45903-45914.

Sheffield, V.C., Weber, J.L., Buetow, K.H., Murray, J.C., Even, D.A., Wiles, K., Gastier, J.M., Pulido, J.C., Yandava, C., Sunden, S.L., *et al.* (1995). A collection of tri- and tetranucleotide repeat markers used to generate high quality, high resolution human genome-wide linkage maps. *Human molecular genetics* 4, 1837-1844.

Shuvaev, A.N., Horiuchi, H., Seki, T., Goenawan, H., Irie, T., Iizuka, A., Sakai, N., and Hirai, H. (2011). Mutant PKC γ in spinocerebellar ataxia type 14 disrupts synapse elimination and long-term depression in Purkinje cells in vivo. *The Journal of neuroscience : the official journal of the Society for Neuroscience* 31, 14324-14334.

Sikora, K.M., Nosavanh, L.M., Kantheti, P., Burmeister, M., and Hortsch, M. (2012). Expression of Caytaxin Protein in Cayman Ataxia Mouse Models Correlates with Phenotype Severity. *PloS one* 7.

Silver, A. (1963). A Histochemical Investigation of Cholinesterases at Neuromuscular Junctions in Mammalian and Avian Muscle. *J Physiol-London* 169, 386-&.

Singh, M., Richards, E.G., Mukherjee, A., and Srere, P.A. (1976). Structure of Atp Citrate Lyase from Rat-Liver - Physicochemical Studies and Proteolytic Modification. *Journal of Biological Chemistry* 251, 5242-5250.

Sirokmany, G., Szidonya, L., Kaldi, K., Gaborik, Z., Ligeti, E., and Geiszt, M. (2006). Sec14 homology domain targets p50RhoGAP to endosomes and provides a link between Rab and Rho GTPases. *The Journal of biological chemistry* 281, 6096-6105.

Sofroniew, M.V., Howe, C.L., and Mobley, W.C. (2001). Nerve growth factor signaling, neuroprotection, and neural repair. *Annu Rev Neurosci* 24, 1217-1281.

Soh, U.J.K., and Low, B.C. (2008). BNIP2 extra long inhibits RhoA and cellular transformation by Lbc RhoGEF via its BCH domain. *Journal of cell science* 121, 1739-1749.

Song, H.J., Ming, G.L., Fon, E., Bellocchio, E., Edwards, R.H., and Poo, M.M. (1997). Expression of a putative vesicular acetylcholine transporter facilitates quantal

transmitter packaging. *Neuron* 18, 815-826.

Song, H.J., and Poo, M.M. (2001). The cell biology of neuronal navigation. *Nat Cell Biol* 3, E81-E88.

Sperry, R.W. (1963). Chemoaffinity in the Orderly Growth of Nerve Fiber Patterns and Connections. *Proceedings of the National Academy of Sciences of the United States of America* 50, 703-710.

Spinazzi, M., Angelini, C., and Patrini, C. (2010). Subacute sensory ataxia and optic neuropathy with thiamine deficiency. *Nature reviews Neurology* 6, 288-293.

Srere, P.A. (1959). The citrate cleavage enzyme. I. Distribution and purification. *The Journal of biological chemistry* 234, 2544-2547.

Srere, P.A. (1961). Citrate Cleavage Enzyme .2. Stoichiometry Substrate Specificity and Its Use for Coenzyme a Assay. *Journal of Biological Chemistry* 236, 50-&.

Sterri, S.H., and Fonnum, F. (1980). Acetyl-Coa Synthesizing Enzymes in Cholinergic Nerve-Terminals. *Journal of neurochemistry* 35, 249-254.

Strick, P.L. (1985). The cerebellum: the cerebellum and neural control. *Science* 229, 547.

Szczur, K., Xu, H., Atkinson, S., Zheng, Y., and Filippi, M.D. (2006). Rho GTPase CDC42 regulates directionality and random movement via distinct MAPK pathways in neutrophils. *Blood* 108, 4205-4213.

Szutowicz, A., Harris, N.F., Srere, P.A., and Crawford, I.L. (1983). ATP-citrate lyase and other enzymes of acetyl-CoA metabolism in fractions of small and large synaptosomes from rat brain hippocampus and cerebellum. *Journal of neurochemistry* 41, 1502-1505.

Szutowicz, A., and Lysiak, W. (1980a). Regional and subcellular distribution of ATP-citrate lyase and other enzymes of acetyl-CoA metabolism in rat brain. *Journal of neurochemistry* 35, 775-785.

Szutowicz, A., and Lysiak, W. (1980b). Regional and Subcellular-Distribution of Atp-Citrate Lyase and Other Enzymes of Acetyl-Coa Metabolism in Rat-Brain. *Journal of neurochemistry* 35, 775-785.

Szutowicz, A., and Srere, P.A. (1983). Purification and Some Properties of Atp-Citrate Lyase from Rat-Brain. *Archives of biochemistry and biophysics* 221, 168-174.

Szutowicz, A., Stepien, M., Bielarczyk, H., Kabata, J., and Lysiak, W. (1982). ATP citrate lyase in cholinergic nerve endings. *Neurochemical research* 7, 799-810.

Takayasu, Y., Iino, M., Furuya, N., and Ozawa, S. (2003). Muscarine-induced increase

in frequency of spontaneous EPSCs in Purkinje cells in the vestibulo-cerebellum of the rat. *The Journal of neuroscience : the official journal of the Society for Neuroscience* 23, 6200-6208.

Taly, A., Corringer, P.J., Guedin, D., Lestage, P., and Changeux, J.P. (2009). Nicotinic receptors: allosteric transitions and therapeutic targets in the nervous system. *Nat Rev Drug Discov* 8, 733-750.

Tang, B.L. (2003). Inhibitors of neuronal regeneration: mediators and signaling mechanisms. *Neurochem Int* 42, 189-203.

Tateno, M., Kato, S., Sakurai, T., Nukina, N., Takahashi, R., and Araki, T. (2009). Mutant SOD1 impairs axonal transport of choline acetyltransferase and acetylcholine release by sequestering KAP3. *Human molecular genetics* 18, 942-955.

Tesco, G., Koh, Y.H., Kang, E.L., Cameron, A.N., Das, S., Sena-Esteves, M., Hiltunen, M., Yang, S.H., Zhong, Z., Shen, Y., *et al.* (2007). Depletion of GGA3 stabilizes BACE and enhances beta-secretase activity. *Neuron* 54, 721-737.

Thurtell, M.J., and Leigh, R.J. (2011). Nystagmus and saccadic intrusions. *Handbook of clinical neurology* 102, 333-378.

Valencia, C.A., Cotten, S.W., and Liu, R.H. (2007). Cleavage of BNIP-2 and BNIP-XL by caspases. *Biochemical and biophysical research communications* 364, 495-501.

VanDeMark, K.L., Guizzetti, M., Giordano, G., and Costa, L.G. (2009). The activation of M1 muscarinic receptor signaling induces neuronal differentiation in pyramidal hippocampal neurons. *The Journal of pharmacology and experimental therapeutics* 329, 532-542.

Walter, J.T., Alvina, K., Womack, M.D., Chevez, C., and Khodakhah, K. (2006). Decreases in the precision of Purkinje cell pacemaking cause cerebellar dysfunction and ataxia. *Nat Neurosci* 9, 389-397.

Wang, L., Yang, L., Filippi, M.D., Williams, D.A., and Zheng, Y. (2006). Genetic deletion of Cdc42GAP reveals a role of Cdc42 in erythropoiesis and hematopoietic stem/progenitor cell survival, adhesion, and engraftment. *Blood* 107, 98-105.

Wanker, E.E., Rovira, C., Scherzinger, E., Hasenbank, R., Walter, S., Tait, D., Colicelli, J., and Lehrach, H. (1997). HIP-I: a huntingtin interacting protein isolated by the yeast two-hybrid system. *Human molecular genetics* 6, 487-495.

Weiss, E.R., Maness, P., and Lauder, J.M. (1998). Why do neurotransmitters act like growth factors? Perspectives on developmental neurobiology 5, 323-335.

Wellen, K.E., Hatzivassiliou, G., Sachdeva, U.M., Bui, T.V., Cross, J.R., and Thompson, C.B. (2009). ATP-Citrate Lyase Links Cellular Metabolism to Histone Acetylation.

Science 324, 1076-1080.

Wess, J. (1996). Molecular biology of muscarinic acetylcholine receptors. *Crit Rev Neurobiol* 10, 69-99.

Wess, J., Eglén, R.M., and Gautam, D. (2007). Muscarinic acetylcholine receptors: mutant mice provide new insights for drug development. *Nat Rev Drug Discov* 6, 721-733.

Whitehouse, P.J., Price, D.L., Struble, R.G., Clark, A.W., Coyle, J.T., and Delon, M.R. (1982). Alzheimer's disease and senile dementia: loss of neurons in the basal forebrain. *Science* 215, 1237-1239.

Xiao, J., Gong, S., and Ledoux, M.S. (2007). Caytaxin deficiency disrupts signaling pathways in cerebellar cortex. *Neuroscience* 144, 439-461.

Xiao, J., and Ledoux, M.S. (2005). Caytaxin deficiency causes generalized dystonia in rats. *Brain research Molecular brain research* 141, 181-192.

Yamashita, T., Higuchi, H., and Tohyama, M. (2002). The p75 receptor transduces the signal from myelin-associated glycoprotein to Rho. *Journal of Cell Biology* 157, 565-570.

Yang, M., Wang, C., Zhu, X., Tang, S., Shi, L., Cao, X., and Chen, T. (2011). E3 ubiquitin ligase CHIP facilitates Toll-like receptor signaling by recruiting and polyubiquitinating Src and atypical PKC{zeta}. *The Journal of experimental medicine* 208, 2099-2112.

Yates, C.M., Simpson, J., Maloney, A.F., Gordon, A., and Reid, A.H. (1980). Alzheimer-like cholinergic deficiency in Down syndrome. *Lancet* 2, 979.

Yi, T.Z., Guy, G.R., and Low, B.C. (2005). BNIP-2 induces cell elongation and membrane protrusions by interacting with Cdc42 via a unique Cdc42-binding motif within its B-INIP-2 and Cdc42GAP homology domain. *Experimental cell research* 303, 263-274.

Yoon, S., and Seger, R. (2006). The extracellular signal-regulated kinase: Multiple substrates regulate diverse cellular functions. *Growth Factors* 24, 21-44.

Zagris, N. (2001). Extracellular matrix in development of the early embryo. *Micron* 32, 427-438.

Zheng, J.Q., Felder, M., Connor, J.A., and Poo, M.M. (1994). Turning of Nerve Growth Cones Induced by Neurotransmitters. *Nature* 368, 140-144.

Zhou, Y.T., Chew, L.L., Lin, S.C., and Low, B.C. (2010). The BNIP-2 and Cdc42GAP Homology (BCH) Domain of p50RhoGAP/Cdc42GAP Sequesters RhoA from Inactivation by the Adjacent GTPase-activating Protein Domain. *Molecular biology of*

the cell 21, 3232-3246.

Zhou, Y.T., Guy, G.R., and Low, B.C. (2006). BNIP-Salpha induces cell rounding and apoptosis by displacing p50RhoGAP and facilitating RhoA activation via its unique motifs in the BNIP-2 and Cdc42GAP homology domain. *Oncogene* 25, 2393-2408.

Zhou, Y.T., Soh, U.J.K., Shang, X., Guy, G.R., and Low, B.C. (2002). The BNIP-2 and Cdc42GAP homology/Sec14p-like domain of BNIP-S alpha is a novel apoptosis-inducing sequence. *Journal of Biological Chemistry* 277, 7483-7492.